



Original research

Blocking hepatocarcinogenesis by a cytochrome P450 family member with female-preferential expression

Fubo Ji,^{1,2} Jianjuan Zhang,^{1,2} Niya Liu,^{1,2} Yuanzhuo Gu,¹ Yan Zhang,^{1,2} Peipei Huang,^{1,2} Nachuan Zhang,^{1,2} Shengda Lin,¹ Ran Pan,³ Zhuoxian Meng,³ Xin-Hua Feng,^{1,2,4} Stephanie Roessler ,⁵ Xin Zheng,⁶ Junfang Ji ^{1,2}

► Additional supplemental material is published online only. To view, please visit the journal online (<http://dx.doi.org/10.1136/gutjnl-2021-326050>).

¹The MOE Key Laboratory of Biosystems Homeostasis & Protection, Zhejiang Provincial Key Laboratory for Cancer Molecular Cell Biology, Life Sciences Institute, Zhejiang University, Hangzhou, Zhejiang, China

²Cancer Center, Zhejiang University, Hangzhou, Zhejiang, China

³Department of Pathology and Pathophysiology, Zhejiang Provincial Key Laboratory of Pancreatic Disease, the First Affiliated Hospital, Zhejiang University School of Medicine, Hangzhou, Zhejiang, China

⁴Innovation Center for Cell Signaling Network, Zhejiang University, Hangzhou, Zhejiang, China

⁵Institute of Pathology, Heidelberg University Hospital, Heidelberg, Germany

⁶Taoharmony Biotech L.L.C, Hangzhou, Zhejiang, China

Correspondence to

Dr Junfang Ji, Life Sciences Institute, Zhejiang University, Hangzhou 310058, Zhejiang Province, China; junfangji@zju.edu.cn

Received 4 September 2021
Accepted 21 December 2021



© Author(s) (or their employer(s)) 2022. No commercial re-use. See rights and permissions. Published by BMJ.

To cite: Ji F, Zhang J, Liu N, et al. *Gut* Epub ahead of print: [please include Day Month Year]. doi:10.1136/gutjnl-2021-326050

ABSTRACT

Objects The incidence of hepatocellular carcinoma (HCC) shows an obvious male dominance in rodents and humans. We aimed to identify the key autosomal liver-specific sex-related genes and investigate their roles in hepatocarcinogenesis.

Design Two HCC cohorts (n=551) with available transcriptome and metabolome data were used. Class comparisons of omics data and ingenuity pathway analysis were performed to explore sex-related molecules and their associated functions. Functional assays were employed to investigate roles of the key candidates, including cellular assays, molecular assays and multiple orthotopic HCC mouse models.

Results A global comparison of multiple omics data revealed 861 sex-related molecules in non-tumour liver tissues between female and male HCC patients, which denoted a significant suppression of cancer-related diseases and functions in female liver than male. A member of cytochrome P450 family, CYP39A1, was one of the top liver-specific candidates with significantly higher levels in female vs male liver. In HCC tumours, CYP39A1 expression was dramatically reduced in over 90% HCC patients. Exogenous CYP39A1 significantly blocked tumour formation in both female and male mice and partially reduced the sex disparity of hepatocarcinogenesis. The HCC suppressor role of CYP39A1 did not rely on its known P450 enzyme activity but its C-terminal region, by which CYP39A1 impeded the transcriptional activation activity of c-Myc, leading to a significant inhibition of hepatocarcinogenesis.

Conclusions The liver-specific CYP39A1 with female-preferential expression was a strong suppressor of HCC development. Strategies to up-regulate CYP39A1 might be promising methods for HCC treatment in both women and men in future.

INTRODUCTION

Sex differences in incidence and mortality of many cancers are evident world widely, often with a much higher rate in men than in women. Hepatocellular carcinoma (HCC) is one of the most malignant solid tumours with obvious sex disparity (online supplemental figure S1A).¹ HCC incidence rates are two to five times higher among men than women in different areas.^{2,3} In various HCC animal models, male mice also tend to develop more tumours than females.⁴⁻⁷

Significance of this study

What is already known on this subject?

- Sex difference is evident in incidence and mortality of hepatocellular carcinoma (HCC), with a much higher rate in men than in women. Sex hormones and sex chromosome genes were reported to affect the HCC incidence in rodents.

What are the new findings?

- We globally identified sex-related molecules in liver, which demonstrated a significant suppression of cancer-related functions in women compared with men. With a focus on autosomal liver-specific candidate genes, we discovered that CYP39A1, with female-preferential expression, was a strong suppressor of HCC development.

How might it impact on clinical practice in the foreseeable future?

- Strategies to upregulate CYP39A1 might be promising methods for HCC treatment as well as prevention in both women and men, without influences on sex hormones and with the limited side effects on other organs.

Research to investigate mechanisms of the low HCC incidence in women is mainly focused on sex hormones and sex chromosome genes. It is known that estrogens prevent, and androgens promote liver cancer. Androgen receptor (AR) promotes hepatitis B virus (HBV)-induced hepatocarcinogenesis through modulation of HBV RNA transcription.⁸ Oestrogen receptor (ER) inhibits HBV replication,⁹ and oestrogen inhibits IL-6, a cytokine that mediates chronic liver inflammation.¹⁰ ER-dependent prevention and AR-mediated promotion of HCC also depend on Foxa1/2 and the onset of carcinogen exposure.¹¹ Meanwhile, some X-inactivation genes also contribute to the sexual dimorphic feature of HCC. DDX3 and LncRNA FTX escape the X-inactivation and inhibit HCC proliferation as well as metastasis.^{12,13} TSPY and TSPX are a pair of homologue genes located on the Y and X chromosome, respectively. TSPY promotes cell proliferation but TSPX retards cell cycle.¹⁴ We and other researchers also showed that women had higher expression of miR-26s (on autosomes) than men in non-tumour

liver tissue, and miR-26s play significant tumour suppressor roles in hepatocarcinogenesis.^{15 16}

Sex differences in hepatic expression are observed for numerous genes. Majority of these genes locate on the autosomes and their function in hepatocarcinogenesis remains unclear.^{17 18} A paradox is also noticed that oestrogen and X-inactivation genes prevent HCC cell growth but promote the growth of hepatoma and ER-positive breast cancer cells.^{6 19 20} Therefore, we aimed to globally identify the sex-related molecules in liver and explore their functional roles in hepatic carcinogenesis with a focus on autosomal liver-specific candidate genes. These autosomal sex-related liver-specific genes might assist in discovering HCC treatment and prevention methods with the limited influences on sex hormones and the limited side effects on other organs.

MATERIALS AND METHODS

Datasets and cell lines

Datasets from two independent HCC cohorts were used. Cohort 1 included 184 HCC patients. In this cohort, miRNA microarray data (GSE6857, <https://www.ncbi.nlm.nih.gov/geo/query/acc.cgi?acc=GSE6857>),²¹ mRNA microarray data (GSE14520, <https://www.ncbi.nlm.nih.gov/geo/query/acc.cgi?acc=GSE14520>)²² and metabolomics profiling in paired tumour and non-tumour samples were used.²³ Cohort 2 included 367 HCC patients. MiRNA and mRNA sequencing data from 367 tumour tissues and 50 non-tumour liver tissues were used (The Cancer Genome Atlas, <https://portal.gdc.cancer.gov>).²⁴ Clinical characteristics of HCC patients from two cohorts were summarised in online supplemental table S1. Briefly, Cohort 1 is an Asian patient cohort and most of cases are HBV positive. Cohort 2 whereas has a diverse population in terms of ethnicity (Caucasian n=165, Asian n=155, African American n=16, and others n=31) and HCC aetiology (HBV n=71, hepatitis C virus (HCV) n=31, alcoholic liver disease n=70, non-alcoholic fatty liver disease n=10, and others). Huh7, Huh1, HLF, HLE and 293 T cells were routinely cultured in our lab.^{25 26}

Lentivirus and adeno associated viruses packaging

Constructs pCDH-CMV-MCS-EF1 α -copGFP (SBI Biosciences) and pCDH-CMV-CYP39A1-3xflag-EF1 α -copGFP were used for lentivirus packaging with plasmids psPAX2 and pMD2.G (Addgene) in 293 T cells. Constructs adeno associated virus (AAV)-TBG-GFP, AAV-TBG-CYP39A1, AAV-shCtrl and AAV-shCYP39A1 were used for AAV packaging with plasmids pHelper (Delta F6 helper) and RepCap (AAV8 serotype packaging plasmid) in 293 T cells. The AAV particles was further purified by iodixanol gradient ultracentrifugation and concentrated by Centrifugal filter (Millipore).

The rest of Materials and Methods were included in online supplemental file.

RESULTS

The female-preferential expression of sex-related molecules in liver associates with tumour suppression

To globally identify sex-related molecules in liver, we compared transcriptome and metabolome data of non-tumour liver tissues between female and male patients from HCC Cohort 1 (n=184) (figure 1A). In this cohort, we have previously identified six sex-related miRNAs.¹⁵ With the similar method including a sex-balanced case set (consisting of all 20 women and two groups of men with 20 patients each shown in online supplemental table S2), class comparison revealed that 808 genes were differentially

expressed in both comparisons, that is, women versus two groups of men (figure 1B, online supplemental table S3). Metabolome comparison revealed 47 metabolites with differential levels between 5 women and 25 men (figure 1B, online supplemental table S3).

The chromosome location of these 808 sex-related genes and 6 miRNAs were uniformly distributed with no noticeable specific assembling on sex chromosomes (figure 1C). In 22 patients with both transcriptome and metabolome data, the expression of all 861 sex-related molecules in non-tumour liver tissues were able to distinctly classify women and men via hierarchical analysis. Consistent data were obtained in all patients of cohort 1 and cohort 2 using the expression levels of 808 sex-related genes and 6 miRNAs (figure 1D, online supplemental figure S1B–D).

Ingenuity pathway analysis (IPA) was performed using the expression ratios of all 861 sex-related molecules between female vs male non-tumour livers. ESR1 was identified as the most significantly activated upstream regulators as expected (online supplemental table S4). Moreover, six out of the top eight identified associated networks were related to cancer and developmental disorder (online supplemental table S5). In the analysis of associated diseases and functions, the categories of cancer, cellular growth and developmental disorder etc were suppressed in women vs men (figure 1E, online supplemental table S6). Among a total of 56 cancer-related diseases and functions (p<0.001), 52 showed reduced activities in women and liver cancer was one of the most suppressed activities (figure 1F). Together, the female-preferential expression of these sex-related molecules was related to the suppressive features of tumour development.

CYP39A1 is a unique female preferentially expressed, liver-specific and tumour-related gene

Among these sex-related genes, 18 were liver specific (figure 2A), which were expressed four times higher in liver than the average level in 60 other tissues (<https://www.proteinatlas.org/>). They are all autosomal genes. Sixteen showed the female-preferential expression, among which ten genes were significantly downregulated in tumours compared with non-tumours from 176 HCC patients (p<0.001, ie, CYP39A1, ETFDH, LEPR, PZP, CYP3A7, AGTR1, TF, FETUB, SUCLG2, COLEC10) (figure 2A). LEPR and PZP were shown to have HCC tumour suppressor roles.^{27 28} Low levels of ETFDH and COLEC10 in HCC were related to poor prognosis of HCC patients.^{29 30} These autosomal liver-specific genes with female-preferential expression thus likely presented the potential HCC-prevention roles. Among them, CYP39A1 was selected as our key candidate for further study since it presented the most significant downregulation in HCC tumours (figure 2A). It was expressed 12.6 times lower in HCC tumour than non-tumour livers in cohort 1 and 16.5 times lower in cohort 2 (figure 2B). In both cohorts, its downregulation occurred in 93.8% and 96.0% of HCC patients, respectively. Consistently, CYP39A1 level was lower in seven HCC cell lines compared with normal adult livers (figure 2C). Its protein sequence was also highly conserved among different species (online supplemental figure S2A) while its role in cancer development remained unknown.

The liver-specific female-preferential expression of CYP39A1 was further confirmed. Among 20 human normal organs, human liver exhibited the highest expression level of CYP39A1 (figure 2D). In NCBI RNA sequencing data of human and mouse organs, CYP39A1 also showed the highest expression in adult liver (figure 2D, online supplemental figure S2B). In human

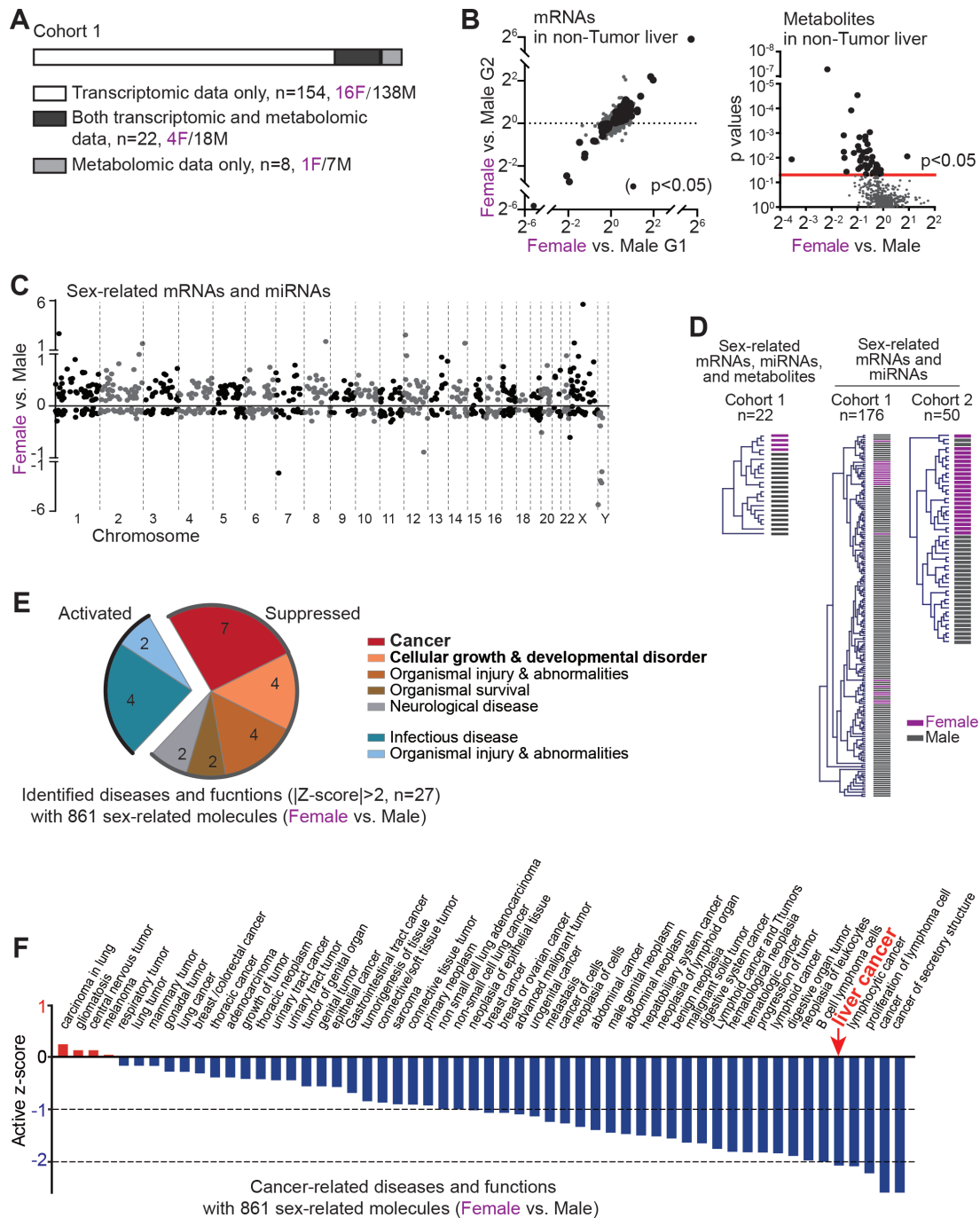


Figure 1 The sex-related molecules in non-tumour livers associate with cancer-related diseases and functions. (A) Available profiling data in cohort 1. (B) Sex-related genes and metabolites. Genes and metabolites were compared between female and male in their non-tumour tissues. (C) The chromosome location of 808 sex-related genes and 6 miRNAs. (D) Hierarchical clustering analysis with all sex-related molecules in cohorts 1 and 2. (E, F) The identified diseases and functions (E) and cancer-related diseases and functions (F) with all sex-related molecules via IPA. The log₂ expression ratios of all sex-related molecules between female versus male non-tumour livers were used for analysis. Any functions with $p < 0.001$ (Fisher's exact test) and $|z\text{-score}| \geq 2$ were considered as significant enrichment. F, female; G1, group 1; G2, group 2; IPA, ingenuity pathway analysis; M, male.

non-tumour livers, CYP39A1 expressed 1.2 times higher in female than male of cohort 1 and 1.4 times higher in cohort 2 (figure 2E). In C57BL/6 mouse, CYP39A1 expression level was reduced from newborn to 6 weeks but remained stable afterwards. From 6 weeks, CYP39A1 exhibited a female-preferential expression in liver and remained on average 3.2 ± 0.5 times higher in female mice than male (figure 2F). Comparable data were noticed in FVB mouse liver (figure 2F). More significantly, the female-preferential expression of CYP39A1 in liver was still

preserved after castration, exhibiting a 2.0-fold higher level in female mice than male mice (figure 2G).

Previous studies have reported several CYP members with sex-biased expression.^{17,18,31} We thus analysed all 57 CYP family members on their sex-related and tumour-related expression in both HCC cohorts. As shown in online supplemental figure S2C, CYP39A1 was the only CYP with a significantly high level in female liver in both cohorts. CYP17A1, CYP3A43 and CYP2A6 expressed higher levels while CYP11A1 and CYP11B2 exhibited

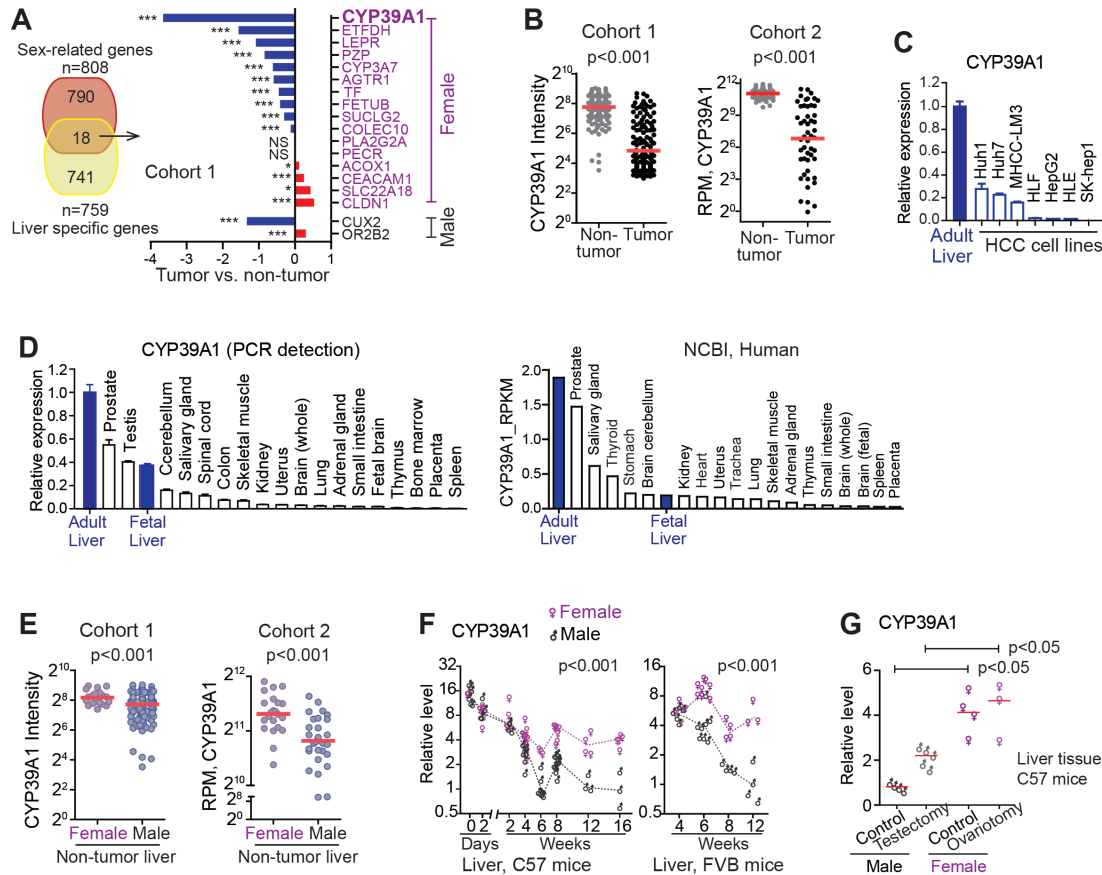


Figure 2 CYP39A1 is a unique female differentially expressed, liver-specific and tumour-related gene. (A) Venn diagram analysis of sex-related molecules and liver-specific genes. The differential expression of liver-specific sex-related molecules was shown in cohort 1 between tumour and non-tumour tissues. * $P < 0.05$, ** $P < 0.001$. NS, not significant. (B) CYP39A1 levels in tumour and non-tumours of HCC cohorts 1–2. (C) CYP39A1 expression in HCC cell lines and adult liver tissue was measured by qRT-PCR. (D) CYP39A1 expression in 20 human normal organs by RT-PCR and RNA sequencing. (E) CYP39A1 levels in female and male non-tumour liver tissues in cohorts 1–2. (F) CYP39A1 levels in normal liver tissues from C57BL/6 mice and FVB/N mice. Three to eight mice were used of each sex at each time point. (G) CYP39A1 levels in female and male normal liver tissues in C57BL/6 mice with and without gonadectomy. (A, B, E, G) Student's t-test was used. (F) Two-way ANOVA was performed. ANOVA, analysis of variance; HCC, hepatocellular carcinoma; RPKM, reads per kilobase of transcript per million mapped reads; RPM, reads per million mapped reads.

lower levels in female liver than male liver in both cohorts, but $p < 0.05$ was only reached in one cohort. The female-preferential expression of CYP17A1 was validated in C57BL/6 mouse livers (online supplemental figure S2D), while the expression of CYP11A1 and CYP11B2 was undetectable in mouse liver and there were no homolog genes of human CYP3A43 and CYP2A6 in mice. In HCC cell lines, CYP17A1 expression presented a higher level in Huh7 but lower levels in the other six HCC cell lines compared with its level in normal adult liver (online supplemental figure S2E). In HCC patients, its expression level was upregulated in tumour compared with non-tumour tissues (online supplemental figure S2F). Taken together, CYP39A1 is a unique CYP gene with female-preferential expression in liver and with a significantly reduced level in over 90% HCC tumours.

CYP39A1 inhibits HCC malignancy features in vitro and blocks orthotopic HCC formation in vivo

In four HCC cell lines (Huh7, HLF, Huh1 and HLE), overexpressed CYP39A1 significantly suppressed cell proliferation and colony formation (figure 3A,B, online supplemental figure S3A,B). CYP39A1 knockdown in Huh7 significantly promoted cell proliferation and colony formation (figure 3C, online supplemental figure S3C). In addition, overexpressed CYP39A1 slightly promoted while CYP39A1 knockdown inhibited cell

apoptosis (online supplemental figures S3D,E). Tumourigenicity assays further revealed that CYP39A1 knockdown significantly accelerated the tumour onset time and increased the rate of tumour occurrence as well as tumour size (figure 3D). These findings indicated a robust tumour suppressor role of CYP39A1 in HCC cells.

The diethylnitrosamine (DEN) and carbon tetrachloride (CCL_4)-induced orthotopic HCC mouse model shows sex disparity of male dominance in hepatocarcinogenesis.³² We then further tested CYP39A1 roles as a tumour suppressor as well as its contribution to HCC sex disparity in this model. Human CYP39A1 AAV virus (AAV.CYP39A1) and mouse CYP39A1 shRNA AAV virus (AAV.shCYP39A1) were used. As shown in figure 3E,F, male mice formed more tumours in liver than female mice consistently. In both female and male mice, overexpression of CYP39A1 with AAV.CYP39A1 significantly reduced while knockdown of mouse CYP39A1 with AAV.shCYP39A1 significantly increased the number of formed tumour nodules and the tumour sizes (figure 3E,F, online supplemental figure S3E,G). Meanwhile, tumour numbers and tumour sizes were similar between male mice with AAV.CYP39A1 and female control mice, as well as between female mice with AAV.shCYP39A1 and male control mice. These results indicated that CYP39A1 significantly inhibited HCC development and partially diminished the sex disparity of HCC formation.

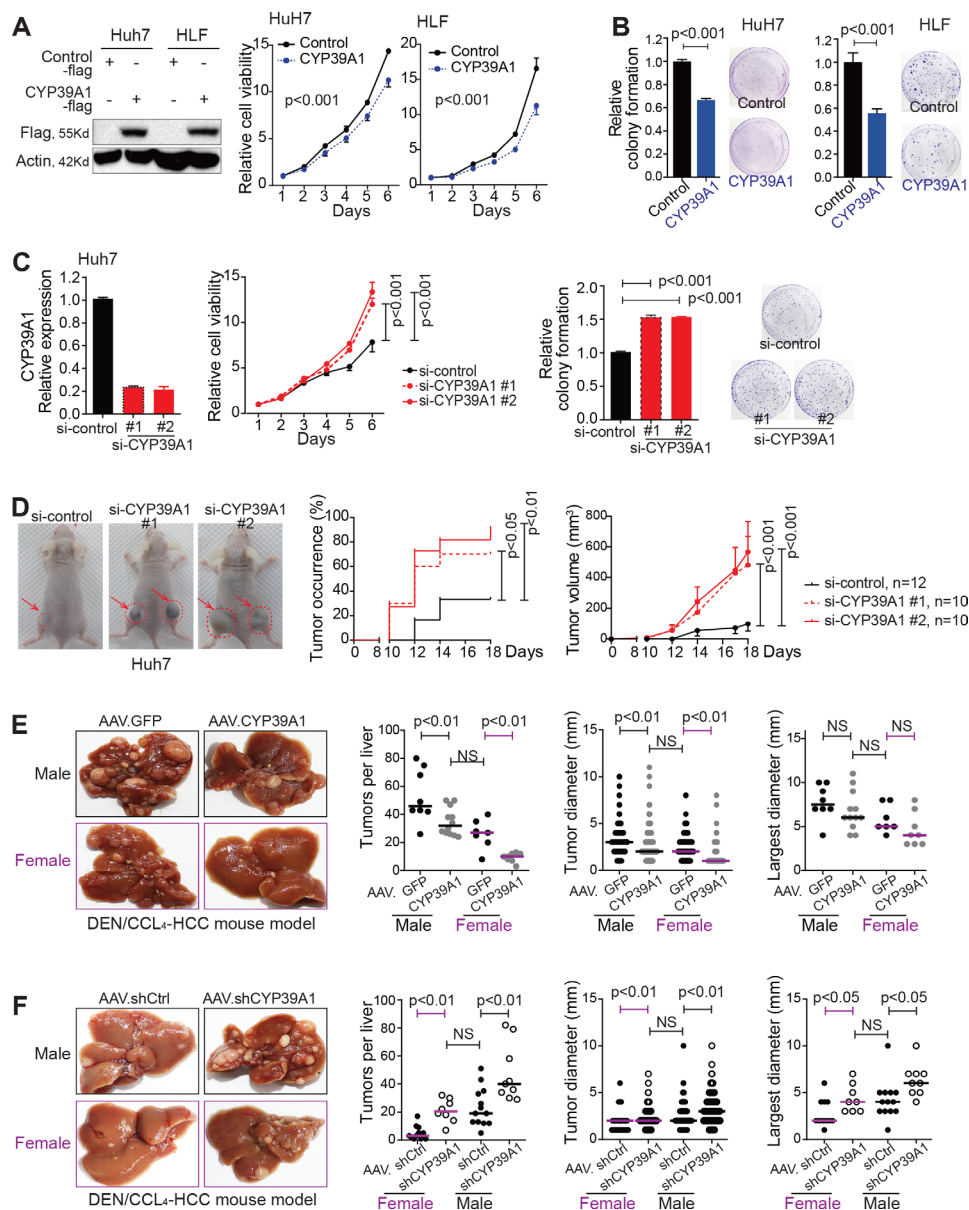


Figure 3 CYP39A1 inhibits HCC cell proliferation and colony formation in vitro, and tumourigenicity in vivo. (A, B) Cell viability (A) and colony formation (B) were examined in Huh7 and HLF cells transfected with control-Flag and CYP39A1-Flag. (C) Cell viability and colony formation were examined in Huh7 cells being transfected with control siRNAs and CYP39A1 siRNAs. (D) Tumourigenicity assay using Huh7 cells in male BALB/c nude mice and two injection sites per mouse. Representative images are shown for the tumours of nude mice derived from Huh7 cells being transfected with control siRNAs and CYP39A1 siRNAs. Tumour occurrence rate and tumour volume were compared. (E) Representative images of HCC formation from DEN+CCl₄-induced HCC mouse model with AAV.GFP (male, n=8; female, n=7) or AAV.CYP39A1 (male, n=12; female, n=8). Tumour numbers per liver and tumour sizes were quantified and compared. (F) Representative images of HCC formation from DEN+CCl₄-induced HCC mouse model with AAV.shCtrl (male, n=13; female, n=11) or AAV.shCYP39A1 (male, n=9; female, n=8). Tumour numbers per liver and tumour sizes were quantified and compared. (A, C, D) Two-way ANOVA was used. (B, C, E, F) Student's t-test was used. NS, not significant. AAV, adeno-associated virus; ANOVA, analysis of variance; CCl₄, carbon tetrachloride; HCC, hepatocellular carcinoma.

CYP39A1 suppresses the c-myc signalling and c-myc-induced HCC formation

As a CYP enzyme, CYP39A1 is involved in bile acid metabolism via converting 24s-hydroxycholesterol (24s-HC) to 7 α -24s-dihydroxycholesterol (7 α -24s-diHC), whereas CYP39A1 K329Q variant loses such an enzyme activity^{33,34} (online supplemental figure S4A). However, overexpressed CYP39A1-K329Q reduced the colony formation, similarly with wild-type CYP39A1 (online supplemental figure S4B). The CYP39A1 substrate (24s-HC) did not promote but significantly inhibited cell malignant features shown by reduced cell viability and colony formation in a dose dependent manner (online supplemental figure S4C,D).

7 α -24s-diHC, the product, did not seem to significantly suppress HCC cell malignant feature either (online supplemental figure S4E,F). Therefore, the tumour suppressor role of CYP39A1 is less likely due to its enzyme catalytic activity of metabolising 24s-HC, but other potential mechanisms.

To identify the key down-stream targets of CYP39A1 in blocking hepatocarcinogenesis, we analysed the common regulators of CYP39A1 surrogates in HCC. A total of 911 CYP39A1 surrogates were identified in Cohort 1 (p < 0.001, figure 4A), yielding to 62 potential regulators with |z-score| > 2 via IPA analysis (figure 4B). The most significant common regulators (p < 10⁻¹⁰, |z-score| > 3) included five HCC-related transcription factors

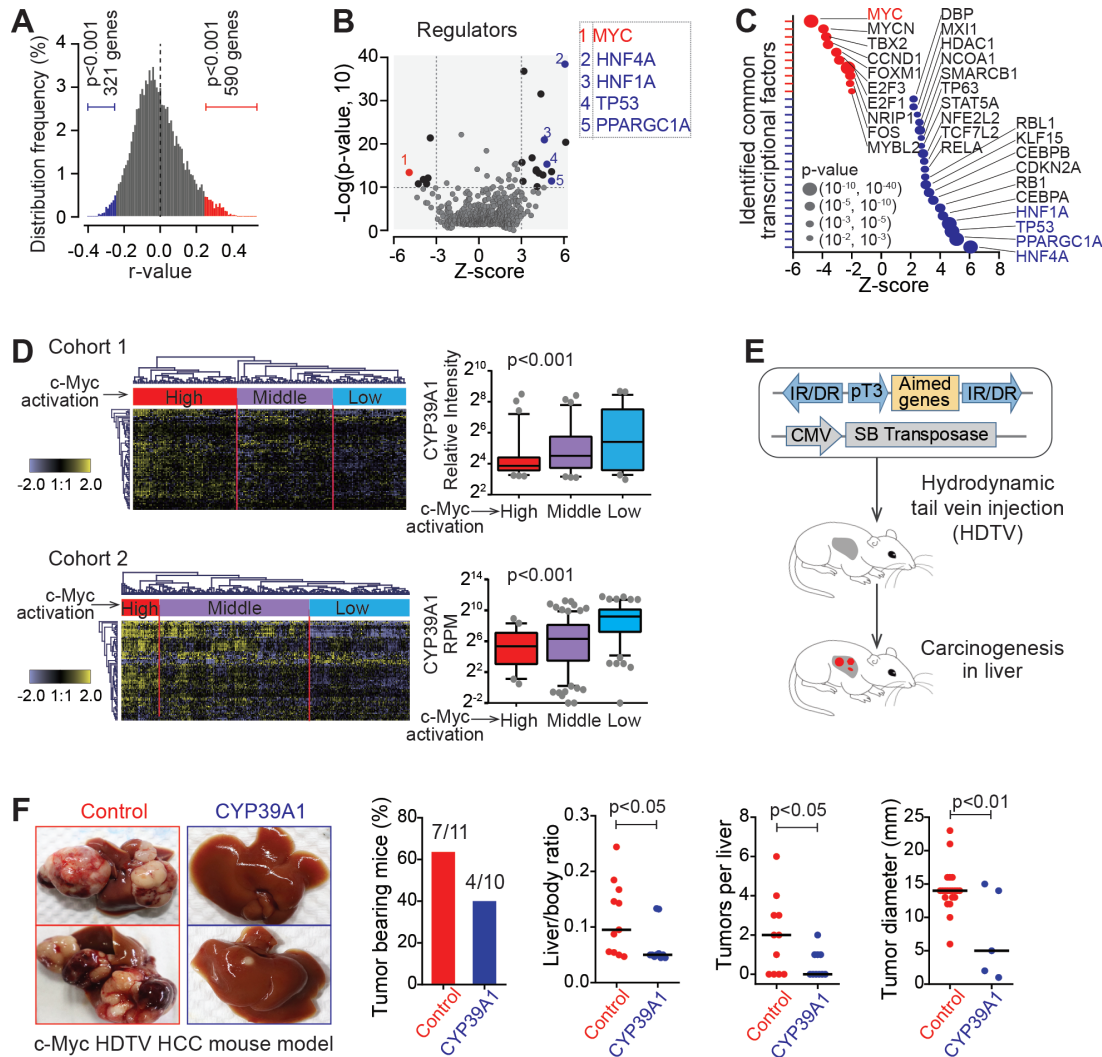


Figure 4 Reduced level of CYP39A1 associates with the activated c-myc pathway. (A) The distribution of genes correlated with CYP39A1 according to their r-values. (B) Common regulators of CYP39A1 surrogates were identified via ipa. (C) Transcriptional factors with $p < 0.01$ and $|z\text{-score}| > 2$ among the common regulators from (B). (D) HCC patients in cohorts 1 and 2 were clustered into three groups by 76 important c-myc target genes. CYP39A1 expression was compared among three groups with different c-myc activation status. One-way ANOVA was used. (E) Overall flow of hydrodynamic tail vein injection HCC mouse model. (F) Representative tumour images of c-myc HDTV HCC mouse model at 8.5 weeks after injection. Tumour bearing animals, ratio of liver vs body, tumours per liver and diameter were quantified and compared between two groups including 11 and 10 female mice for the control group and CYP39A1 group, respectively. Unpaired t-test was used. ANOVA, analysis of variance; HCC, hepatocellular carcinoma.

(TFs), which were the suppressed oncogenic TF MYC (c-Myc) and four activated TFs with tumour suppressor roles (HNF4A, HNF1A, TP53 and PPARGC1A) (figure 4B,C, online supplemental table S7). Among all identified TFs with $p < 0.01$ and $|z\text{-score}| > 2$, many oncogenic TFs were suppressed (such as c-Myc, MYCN, CCND1, ROXM1 and E2Fs) and TFs with tumour suppressor roles were largely activated (such as HNF4A, TP53, RB1, CDKN2A and CEBPA) (figure 4C), further indicating the tumour suppressor role of CYP39A1. c-Myc was the top one identified oncogenic TF of CYP39A1 surrogates. When HCC patients were classified into high, middle and low c-Myc activation groups with the well-established c-Myc target genes, CYP39A1 showed the highest level in the low c-Myc activation group and the lowest level in the high c-Myc activation group in both cohorts (figure 4D). These data highlighted a potential key role of oncogenic c-Myc pathway in CYP39A1-mediated tumour suppression. This possibility was then validated via the c-Myc driven hydrodynamic tail vein injection (HDTV) HCC mouse model (figure 4E). Specifically, CYP39A1 significantly

suppressed c-Myc-induced tumour formation (figure 4F). In this model, 63.6% of mice (7 out of 11) developed liver tumours in the c-Myc control group, while only 40.0% mice (4 out of 10) developed tumours in the group of c-Myc and CYP39A1. Moreover, CYP39A1 also significantly reduced c-Myc-mediated tumour burden, shown by decreased liver/body ratios, tumour numbers and sizes (figure 4F). Histologically, the tumours exhibited similar features in both groups (data not shown). c-Myc/Mcl1 HDTV model was further used to allow for 100% tumour formation in the control group. In this model, CYP39A1 also remarkably inhibited c-Myc-induced tumour formation and tumour burden (figure 5A). At 5.5 weeks postinjection, all eight mice in the c-Myc/Mcl1 control group developed palpable abdominal masses caused by massive tumour formation, while only 1 out of 8 mice in c-Myc/Mcl1/CYP39A1 group showed palpable abdominal mass. From this time point on, two mice per week were sacrificed in the c-Myc/Mcl1/CYP39A1 group to collect tumour incidence data. As shown in figure 5A, CYP39A1 significantly retarded and blocked hepatocarcinogenesis. Even at

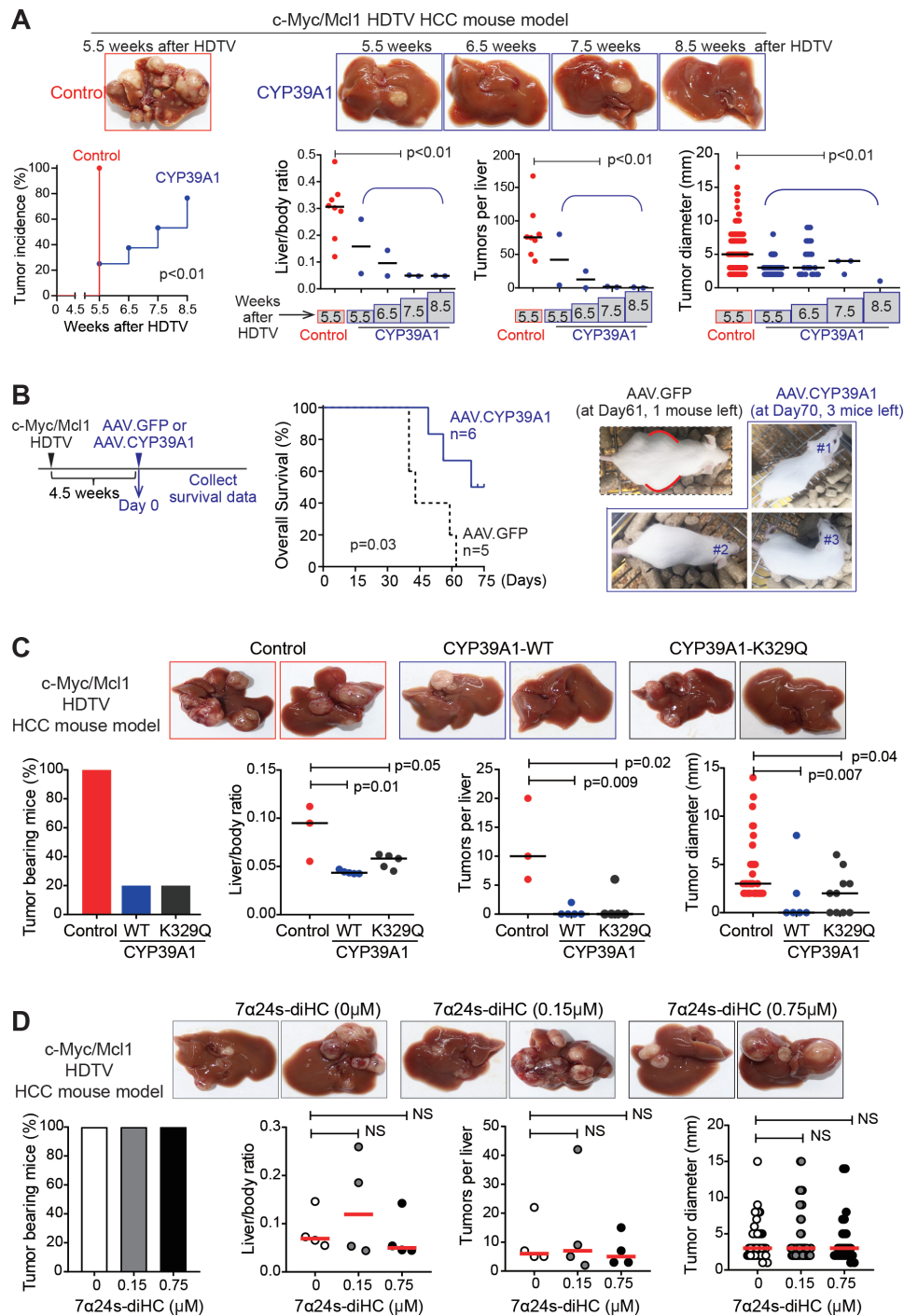


Figure 5 CYP39A1 inhibits c-myc-induced HCC initiation and progression. (A) c-Myc/Mcl1 HDTV HCC mouse model was used with or without CYP39A1. Representative tumour images were shown. Tumour incidence rate, ratios of liver versus body, tumours per liver and diameter were quantified between two groups (eight mice per group). (B) The relationship of mouse survival with AAV.CYP39A1 in c-Myc/Mcl1 HDTV HCC mouse model. Representative images were shown, and the palpable abdominal mass was labelled with red curve. Log-rank test was performed. (C) c-Myc/Mcl1 HCC mouse model was used with CYP39A1-WT or CYP39A1-K329Q (control group, n=3; WT group, n=5; K329Q group, n=5). (D) c-Myc/Mcl1 HCC mouse model was used with different dose of 7α24s-diHC (4 mice per group). (C, D) Representative tumour images were shown. Tumour-bearing animals, ratio of liver versus body, tumours per liver and diameter were quantified and compared. Unpaired t-test was used. Female mice were used for (A–D). AAV, adeno-associated virus; HCC, hepatocellular carcinoma; HDTV, hydrodynamic tail vein; NS, not significant.

8.5 weeks post oncogene injection, there was still one mouse without hepatocarcinogenesis and the other one bearing a single 1 mm tumour nodule.

AAV.CYP39A1 also significantly blocked tumour development and reduced tumour burden in c-Myc/Mcl1 HDTV HCC mouse model (figure 5B). AAV particles were delivered at 4.5 weeks after oncogene injection. Significantly, AAV.

CYP39A1 prolonged mouse medium survival from 6 weeks to >10 weeks. At 10 weeks after virus delivery, all mice died with palpable abdominal mass in AAV.GFP control group, while three out of six mice in AAV.CYP39A1 group were still alive and showed no suspectable abdominal mass. Meanwhile, CYP39A1 suppressing c-Myc-induced HCC formation did not seem to be attributed to its enzyme catalytic activity of converting 24s-HC.

CYP39A1-K329Q notably inhibited c-Myc-mediated tumour formation, similar to wild-type CYP39A1 (figure 5C). Neither 7 α 24s-diHC nor 24s-HC altered c-Myc-induced hepatocarcinogenesis (figure 5D, online supplemental figure S4G). In addition, AAV.CYP39A1 did not seem to alter sex hormones in mice as expected (online supplemental figure S5). Together, these data highlighted the specific new role of CYP39A1 in impeding c-Myc oncogenic pathway and c-Myc-mediated hepatocarcinogenesis.

CYP39A1 suppresses c-myc transcriptional activity

In HCC cells, CYP39A1 did not inhibit c-Myc expression or its protein stability, affect c-Myc cellular location, or interact with c-Myc (online supplemental figure S6A–D). However, CYP39A1 significantly reduced the c-Myc-mediated E-box-dependent luciferase activity in a dose-dependent manner (figure 6A). Nine representative c-Myc target genes were further examined (figure 6B, online supplemental figure S6E). Consistently, overexpressed CYP39A1 reduced the mRNA levels of these nine c-Myc targets in both Huh7 and HLF cells (figure 6C). Comparable data were also obtained in liver tissues of DEN/CCL₄-induced HCC mouse model with AAV.CYP39A1 or AAV.shCYP39A1 (online supplemental figure S6F). Since CYP39A1-K329Q inhibited c-Myc activity in luciferase reporter assays while either 24s-HC or 7 α 24s-diHC did not (figure 6D), CYP39A1 suppressing c-Myc activity was less likely due to its enzyme catalytic activity of metabolising 24s-HC. c-Myc IP/MS revealed that CYP39A1 largely reduced the number of proteins interacting with c-Myc (figure 6E, CYP39A1 vs control, 218 vs 429). Among them, 83 and 11 c-Myc interacting proteins were evidenced in high-throughput screening data (deposited in UniProt) and in affinity capture assay (in literatures), respectively (figure 6F, online supplemental table S8). Their total number and abundance were also largely reduced in CYP39A1 overexpression group and the interaction of Hsp90 with c-Myc was most noticeably reduced by CYP39A1 (figure 6F). Many c-Myc interacting proteins mediate c-Myc transcriptional regulatory activities via interacting with c-Myc N-terminal transcription activation domain (TAD, amino acids 1–143).^{35–37} Hsp90 was also reported to increase c-Myc transcriptional activation ability.^{38,39} Therefore, CYP39A1 likely inhibited c-Myc transactivating activity housed in its TAD via impeding the interactions between c-Myc and its interacting proteins.

The impeded interaction between Hsp90 and c-Myc by CYP39A1 was first confirmed in both Huh7 and HLF cells (online supplemental figure S7A). Hsp90 increased the c-Myc luciferase reporter activity, which was also significantly reduced by CYP39A1 (online supplemental figure S7B,C). Consistent data were observed in vivo that Hsp90 promoted c-Myc-induced tumour formation while CYP39A1 remarkably abolished the c-Myc and Hsp90-induced tumour formation and tumour burden (online supplemental figure S7D).

To further test whether CYP39A1 interfered with c-Myc transcriptional activation ability, the whole length c-Myc TAD and its multiple truncations were then constructed and fused to yeast Gal4 DNA-binding domain. Using Gal4-Myc fusion proteins and a Gal4 luciferase reporter, we found that CYP39A1 significantly suppressed the TAD activity of c-Myc (figure 6G). Such an inhibition remained even when either of the conserved Myc box 1 (MBI) and 2 (MBII) of c-Myc or both were deleted (figure 6G). Therefore, CYP39A1 broadly impeded c-Myc transcriptional activation capability of the different c-Myc TAD segments, partially via influencing the interactions between c-Myc and its interacting proteins, such as Hsp90.

The C-terminal domain of CYP39A1 is essential for suppressing c-myc transcriptional activity

As expected, the suppressed c-Myc transcriptional activation activity by CYP39A1 was not dependent on the CYP39A1 enzyme catalytic activity of metabolising 24s-HC (figure 6H). To explore the functional domain of CYP39A1, multiple CYP39A1 truncations were constructed based on the predicted protein domain information (figure 7A). CYP39A1 presents a relative weak sequence consensus with other 56 CYP450 family members but is highly conserved among different species (online supplemental figure S8A, S2A). The 1–23aa region of CYP39A1 served as a signal peptide (SP) since CYP39A1 protein did not express when its 2–21aa was removed or when HA tag was inserted to its SP N-terminal (figure 7A, online supplemental figure S8B). Among these truncations, CYP39A1 ^{Δ 2–145} maintained but CYP39A1 ^{Δ 291–469} and CYP39A1 ^{Δ 369–469} lost the ability of inhibiting c-Myc luciferase reporter activity (figure 7B). Consistently, CYP39A1 ^{Δ 369–469} did not inhibit c-Myc transcriptional activation activity either (figure 7C). IP/MS assay showed that CYP39A1 ^{Δ 369–469} rescued the reduced number of c-Myc interacting proteins by CYP39A1^{WT} and Hsp90 was also one of the most significant one (figure 7D,E, online supplemental table S9). IP assay in both Huh7 and HLF cells further evidenced that CYP39A1^{WT} did but CYP39A1 ^{Δ 369–469} did not inhibit the interaction of Hsp90 and c-Myc (figure 7F). These results indicated that the C-terminal 369–469aa of CYP39A1 was important for its role in suppressing c-Myc transcriptional activity.

Consistent data were obtained in vivo (figure 7G). In c-Myc/Mcl1 HDTV mouse model, CYP39A1 ^{Δ 369–469} could not suppress c-Myc-induced tumour formation or tumour burden at all, which however were significantly suppressed by CYP39A1^{WT}. As a control, tumours from CYP39A1 ^{Δ 369–469} group expressed the truncated CYP39A1 (figure 7H). Interestingly, tumours from CYP39A1^{WT} group did not exhibit CYP39A1 expression. In this case, hepatocytes forming tumours in CYP39A1^{WT} group were potentially those cells abandoning CYP39A1, further implying the important role of CYP39A1 in suppressing hepatocarcinogenesis. Based on the protein structure prediction, we have also constructed three additional truncations of CYP39A1 at its C-terminal (Δ 369–404, Δ 405–434, Δ 435–469) to further locate the functional domain of CYP39A1. However, deleting any of these three fragments did not affect CYP39A1's role in suppressing hepatocarcinogenesis (data not shown), indicating the functional domain of CYP39A1 potentially formed via 3D spatial folding of its 369–469aa region. Together, female preferentially expressed CYP39A1 significantly inhibited hepatocarcinogenesis via its C-terminal 369–469aa region.

DISCUSSION

Many risk factors of HCC susceptibility have been well investigated, including chronic infection with HBV or HCV, heavy alcohol consumption, diabetes and obesity, exposure to aflatoxin B1. However, male sex as an HCC risk factor has not yet been well studied. Previous studies showed that the oestrogen pathway prevented but the androgen pathway promoted liver carcinogenesis. Some X-chromosome-located or Y-chromosome-located genes and sex hormone-related pathways were also involved in hepatocarcinogenesis.^{11,13,14} However, oestrogen may promote hepatoma formation as well as cancer progression in other organs such as ER-positive breast cancer and bladder cancer.^{19,20,40} Moreover, it is not feasible to use estrogen-related supplements as a prevention strategy against HCC. Hence, we aimed to identify sex-related liver-specific genes on autosomes as

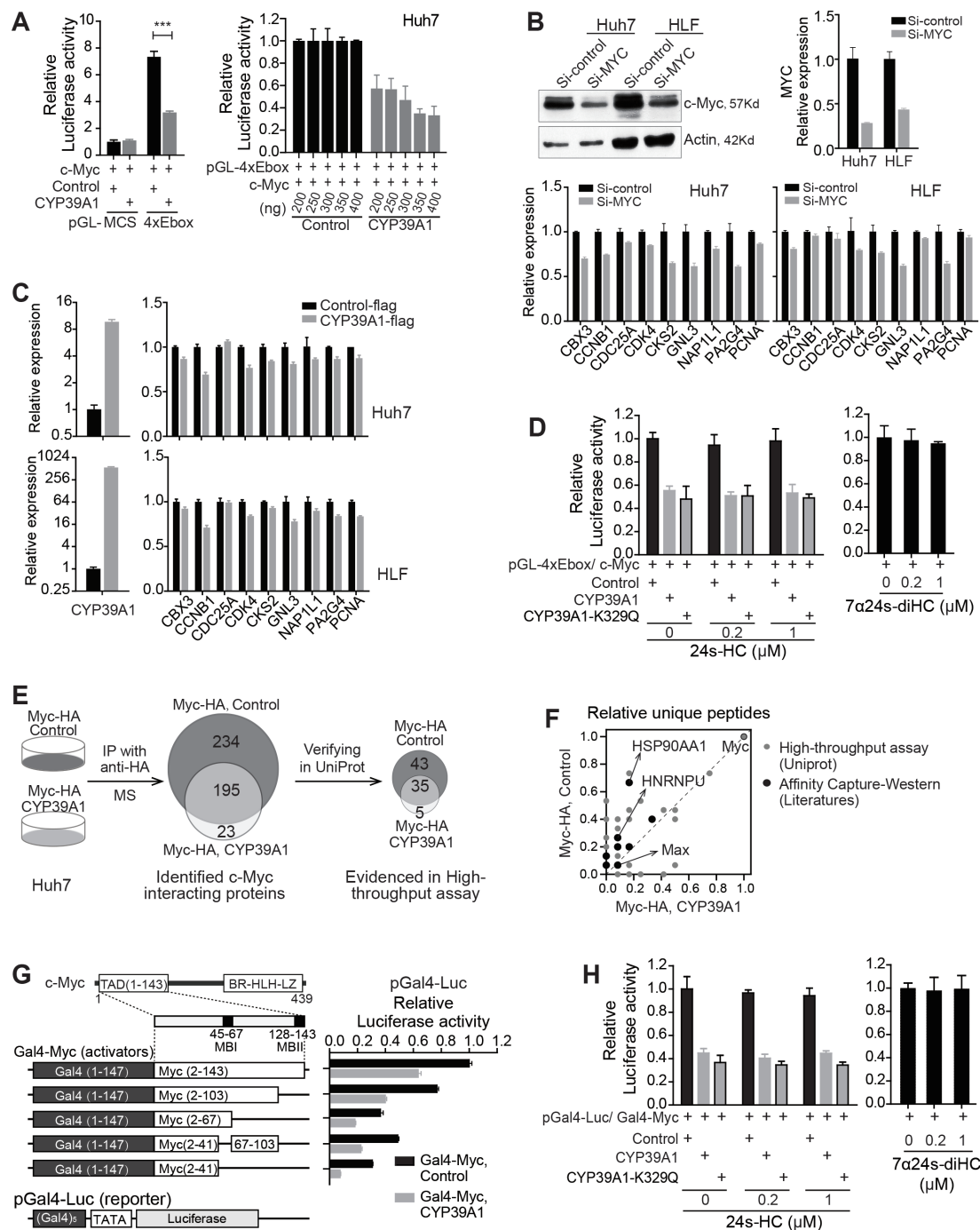


Figure 6 CYP39A1 inhibits c-myc transcriptional activation ability. (A) Promoter luciferase reporter assay with pGL-4xE-box. Huh7 cells were cotransfected with indicated amount of pGL-4xE-box, c-myc and CYP39A1 together with pRL-CMV as a control. Relative luciferase activities were measured 24 HS after transfection. Unpaired t-test was used. ***, $p < 0.001$ from Student's t-test. (B) Huh7 and HLF cells were transiently transfected with control siRNA or c-myc siRNAs. The expression of c-myc was detected by Western blot analysis and qRT-PCR. Nine classical c-myc targeted genes were examined via qRT-PCR. (C) Expression levels of CYP39A1 and nine c-myc targets in Huh7 and HLF cells with overexpressed CYP39A1. (D) pGL-4xE-box luciferase reporter activity in Huh7 cells transfected with c-myc, c-myc with CYP39A1 and c-myc with CYP39A1-K329Q. Cells were exposed to 24s-HC or 7 α 24s-diHC at the indicated concentration. (E) Myc interacting proteins were identified by IP/MS in Huh7 cells transfected with c-myc only and Huh7 cotransfected with CYP39A1 and c-myc. The IP/MS data were further overlapped with Myc-interacting proteins from UniProt database. (F) Scatter plot of unique peptides for proteins being identified by both Myc-IP/MS and Myc-interacting proteins from UniProt and Literatures. (G) Promoter luciferase reporter assay with pGal4-Luc (reporter) and Gal4-Myc fusion proteins. relative luciferase activities were measured 24 HS after transfection. (H) pGal4-Luc reporter activity in Huh7 cells transfected with c-myc, c-myc with CYP39A1 and c-myc with CYP39A1-K329Q. Cells were exposed to 24s-HC or 7 α 24s-diHC at the indicated concentration. IP/MS, immunoprecipitation/ mass spectrometry.

key regulators in hepatocarcinogenesis, with the hope of discovering potentially feasible HCC prevention methods.

Using multiomics data, we globally identified sex-related molecules in non-tumour livers of HCC patients. These molecules

were evenly distributed across chromosomes and could successfully classify HCC patients to women and men subgroups. Their expression ratios of female vs male were largely associated with suppression of cancer-related diseases and functions. Thus, the

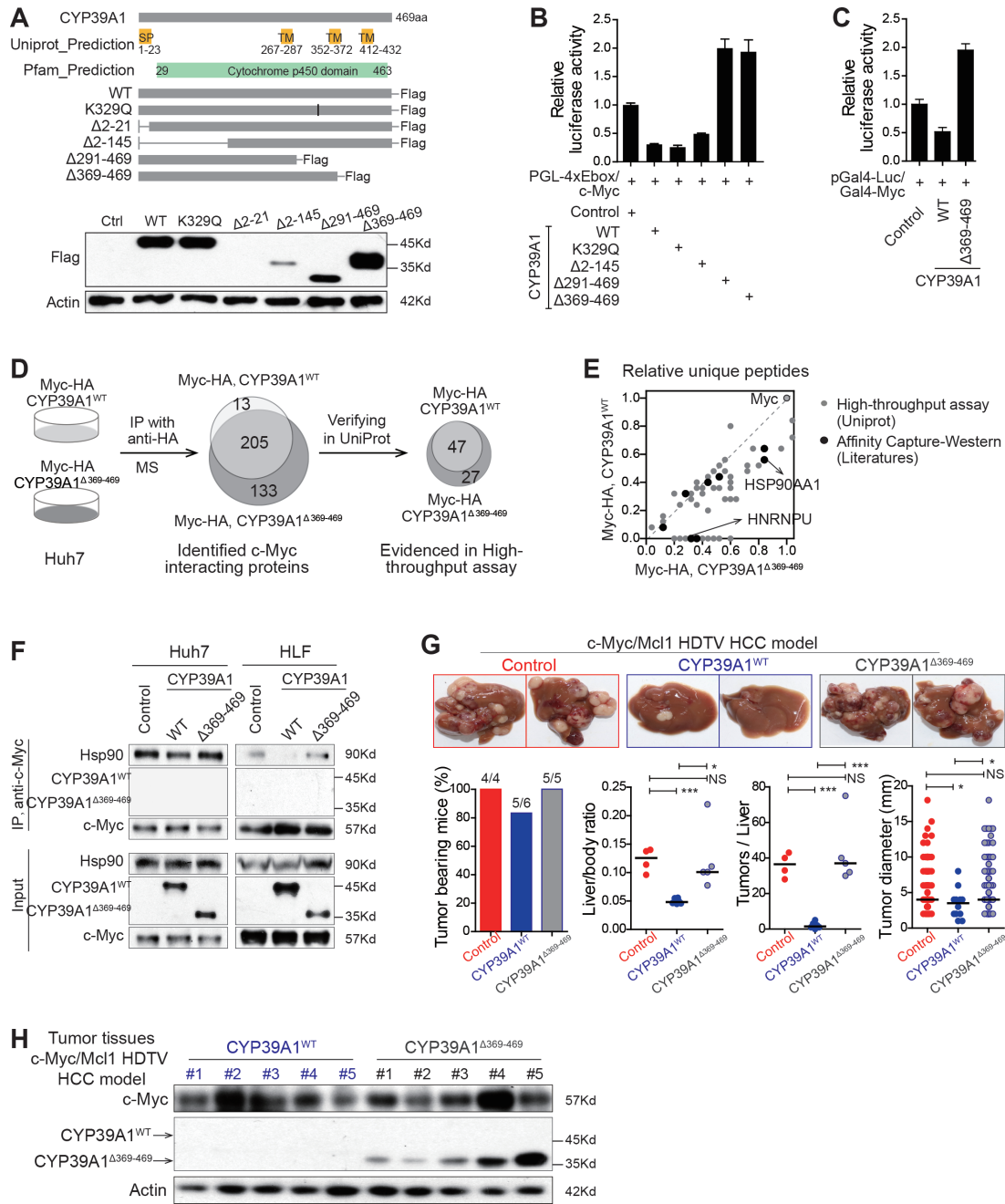


Figure 7 The C-terminal 369-469aa of CYP39A1 is essential for suppressing c-myc transcriptional activity. (A) The predicted functional domains of CYP39A1 and the designed truncations of CYP39A1. The expression of these truncations was detected by Western blot. (B) pGL-4xE-box luciferase activity in Huh7 cells transfected with c-myc control and c-myc with different CYP39A1 truncations. Relative luciferase activities were measured 24 HS after transfection. (C) pGal4-Luc luciferase activity in Huh7 transfected with Gal4-Myc control, Gal4-Myc with CYP39A1^{WT}, and Gal4-Myc with CYP39A1^{Δ369-469}. (D) c-myc interacting proteins were identified by IP/MS in Huh7 cells cotransfected with c-myc and CYP39A1^{WT} or CYP39A1^{Δ369-469}. The IP/MS data were further overlapped with Myc-interacting proteins from UniProt. (E) Scatter plot of unique peptides for proteins being identified by both c-myc-IP/MS and c-Myc-interacting proteins from UniProt or Literatures. (F) Co-IP between Hsp90 and c-myc in Huh7 and HLF cells with over-expression of CYP39A1^{WT} or CYP39A1^{Δ369-469}. (G) c-Myc/Mcl1 HCC mouse model was used with control (n=4), CYP39A1^{WT} (n=6) or CYP39A1^{Δ369-469} (n=5). Female mice were used, and representative tumour images were shown. Tumour-bearing animals, ratio of liver versus body, tumours per liver and diameter were quantified and compared. Unpaired t-test was used. NS, not significant. ***P<0.001. *p<0.05. (H) c-myc, CYP39A1^{WT} and CYP39A1^{Δ369-469} protein levels in tumour tissues from c-Myc/Mcl1/CYP39A1^{WT} HDTV mice and c-Myc/Mcl1/CYP39A1^{Δ369-469} mice. HCC, hepatocellular carcinoma; IP/MS, immunoprecipitation/ mass spectrum.

molecular environment in female liver was potentially protective in HCC development. CYP39A1, a gene at Chr.6p, was one of the identified liver specific genes with female-preferential expression. It exhibited a robust role in suppressing hepatocarcinogenesis in multiple orthotopic HCC mouse models, and

its expression was significantly downregulated in over 90% of human HCCs. The mechanisms for CYP39A1 against hepatocarcinogenesis could be attenuating the c-Myc pathway but not via its known cytochrome p450 function of metabolising 24s-HC. Meanwhile, CYP39A1 did not seem to alter sex hormones in

either female or male mice. Thus, female preferentially expressed CYP39A1 hosts the potential of preventing HCC development in patients carrying HCC risk factors.

In the cytochrome P450 superfamily of enzymes, CYP39A1 was the first member being discovered to possess the ability of dramatically inhibiting hepatocarcinogenesis. The expression of many members of CYP family was downregulated in HCCs (online supplemental figure S8C in both cohorts), but currently, it remains less discovered whether and how they functioned in hepatocarcinogenesis. The reduced expression of some CYPs in HCCs were reported to associate with poor prognosis of HCC such as CYP1A2 and CYP2C19.^{41,42} However, some CYP family members were found to promote HCC development via its P450 enzymatic function, that is, CYP2E1 metabolising hepatic procarcinogen DEN⁴³ and CYP2J2 metabolising 4-epoxyeicosatrienoic acid.⁴⁴ In addition, CYP3A5 suppressed HCC migration and invasion via inhibiting mTORC2/AKT signalling.⁴⁵ Here, we found that CYP39A1 significantly inhibited hepatic carcinogenesis via suppressing c-Myc signalling by its C-terminal region, but not its catalytic activity of converting 24s-HC. Thus, it appears to be interesting and important to revisit the society of CYP family and evaluate their roles in hepatocarcinogenesis thoroughly.

CYP39A1 suppressed c-Myc-mediated signalling activation through interfering c-Myc transcriptional activation activity. Such an interfering was not dependent on the CYP39A1 enzyme catalytic activity of converting 24s-HC, but the 101 amino acids of CYP39A1's C-terminal region (369aa-469aa). However, further short truncations of CYP39A1 in this region, that is, Δ369–404, Δ405–434 and Δ435–469, did not alter CYP39A1's role in suppressing hepatocarcinogenesis. Thus, the functional domain of CYP39A1 in this region was likely formed via 3D spatial folding. It is also possible that CYP39A1 has new enzymatic function beyond metabolising 24s-HC, which was important for its tumour suppressor role. Future research on decoding CYP39A1 protein structure is urgently needed, which will certainly offer additional clues on mechanisms of CYP39A1 in suppressing c-Myc signalling.

In addition, c-Myc upregulation preferentially occurred in male mice at early stage in hepatocarcinogenesis.⁴⁶ Many HCC mouse models consistently presented a significant sex disparity while c-Myc transgenic HCC mouse model showed an inconsistent result. Dr Thorgeirsson's group showed a higher HCC rate in male mice compared with female mice at 20 months,⁴⁷ whereas one study also reported that no sex difference of liver tumour development in mice with constitutive hepatic c-Myc expression, which were housed in a Helicobacter-free barrier facility.⁴⁸ We noticed that there was no sex disparity of HCC occurrence in c-Myc HDTV HCC mouse model. Subsequent investigations on whether and how CYP39A1 and c-Myc together with microbiota contribute to sex disparity of HCC development might shed lights on this contradictory phenotype of sex disparity in c-Myc-related HCCs and improve our understanding on HCC sex disparity.

In summary, CYP39A1 was a liver-specific female-preferentially expressed gene and significantly suppressed tumour formation in multiple orthotopic HCC mouse models. Mechanistically, CYP39A1 inhibited c-Myc-mediated transcriptional activation of down-stream signals through weakening interactions of c-Myc with its interacting proteins including Hsp90. CYP39A1 may guard women from HCC development, contributing to HCC sex disparity.

Acknowledgements We thank Dr Xin Chen for pT3-EF1α-cMyc, pT3-EF1α-myr-AKT, NRasV12/pT2-CAGGS, pT3-EF1α-MCL1, and pCMV/SB plasmids, Dr Hai Song for pcDNA3.0-3XHA plasmid, Dr Xin Wang for his critical comments and sharing metabolomic profiling data of Cohort 1, Dr Sheng Wang for CYP39A1 protein structure prediction. The authors thank our core facility at Life Sciences Institute for their support on FACS analysis.

Contributors Conception and design: FJ and JJ; Acquisition of data: FJ, JZ, NZ, YG, YZ, PH, NZ and JJ; Analysis and interpretation of data: FJ and JJ; Methodology, resources and materials: FJ, JZ, NL, SL, RP, ZM, X-HF and XZ; Writing and/or revision of the manuscript: FJ, JZ, NL, YG, SR, XZ and JJ; Study supervision and guarantor: JJ.

Funding This work was supported by National Natural Science Foundation of China (No. 81874054 and 81672905) (JJ), National Key R&D Program of China (2018YFA0800504) (JJ), Zhejiang Basic Public Welfare Research Programme (LZ20H160003) (JJ), the Fundamental Research Funds for the Central Universities in China (JJ).

Competing interests None declared.

Patient consent for publication Not applicable.

Provenance and peer review Not commissioned; externally peer reviewed.

Data availability statement Data are available in a public, open access repository. Data may be obtained from a third party and are not publicly available. All data relevant to the study are included in the article or uploaded as online supplemental information. The miRNA profiling data of cohort 1 were available at GEO datasets of NCBI (GSE6857, <https://www.ncbi.nlm.nih.gov/geo/query/acc.cgi?acc=GSE6857>). The mRNA profiling data of cohort 1 were available at GEO datasets (GSE14520, <https://www.ncbi.nlm.nih.gov/geo/query/acc.cgi?acc=GSE14520>). The miRNA and mRNA sequencing data of cohort 2 were available at the Cancer Genome Atlas (TCGA) portal (<https://portal.gdc.cancer.gov>). The metabolomic profiling data of cohort 1 were obtained from Dr Xin W Wang (<https://www.ncbi.nlm.nih.gov/pmc/articles/PMC3633738/>).

Supplemental material This content has been supplied by the author(s). It has not been vetted by BMJ Publishing Group Limited (BMJ) and may not have been peer-reviewed. Any opinions or recommendations discussed are solely those of the author(s) and are not endorsed by BMJ. BMJ disclaims all liability and responsibility arising from any reliance placed on the content. Where the content includes any translated material, BMJ does not warrant the accuracy and reliability of the translations (including but not limited to local regulations, clinical guidelines, terminology, drug names and drug dosages), and is not responsible for any error and/or omissions arising from translation and adaptation or otherwise.

ORCID iDs

Stephanie Roessler <http://orcid.org/0000-0002-5333-5942>
Junfang Ji <http://orcid.org/0000-0002-3071-6494>

REFERENCES

- Siegel RL, Miller KD, Jemal A. Cancer statistics, 2019. *CA Cancer J Clin* 2019;69:7–34.
- Kulik L, El-Serag HB. Epidemiology and management of hepatocellular carcinoma. *Gastroenterology* 2019;156:477–91.
- El-Serag HB. Epidemiology of viral hepatitis and hepatocellular carcinoma. *Gastroenterology* 2012;142:1264–73.
- Ghebranion N, Sell S, injury HB. Hepatitis B injury, male gender, aflatoxin, and p53 expression each contribute to hepatocarcinogenesis in transgenic mice. *Hepatology* 1998;27:383–91.
- Nakatani T, Roy G, Fujimoto N, et al. Sex hormone dependency of diethylnitrosamine-induced liver tumors in mice and chemoprevention by leuprorelin. *Jpn J Cancer Res* 2001;92:249–56.
- Naugler WE, Sakurai T, Kim S, et al. Gender disparity in liver cancer due to sex differences in MyD88-dependent IL-6 production. *Science* 2007;317:121–4.
- Rogers AB, Theve EJ, Feng Y, et al. Hepatocellular carcinoma associated with liver-gender disruption in male mice. *Cancer Res* 2007;67:11536–46.
- Wu M-H, Ma W-L, Hsu C-L, et al. Androgen receptor promotes hepatitis B virus-induced hepatocarcinogenesis through modulation of hepatitis B virus RNA transcription. *Sci Transl Med* 2010;2:32ra35.
- Liu W-C, Liu QY. Molecular mechanisms of gender disparity in hepatitis B virus-associated hepatocellular carcinoma. *WJG* 2014;20:6252–61.
- Shi L, Feng Y, Lin H, et al. Role of estrogen in hepatocellular carcinoma: is inflammation the key? *J Transl Med* 2014;12:93.
- Li Z, Tuteja G, Schug J, et al. Foxa1 and Foxa2 are essential for sexual dimorphism in liver cancer. *Cell* 2012;148:72–83.
- Chang P-C, Chi C-W, Chau G-Y, et al. Ddx3, a DEAD box RNA helicase, is deregulated in hepatitis virus-associated hepatocellular carcinoma and is involved in cell growth control. *Oncogene* 2006;25:1991–2003.
- Liu F, Yuan J-H, Huang J-F, et al. Long noncoding RNA FTX inhibits hepatocellular carcinoma proliferation and metastasis by binding MCM2 and miR-374a. *Oncogene* 2016;35:5422–34.

- 14 Kido T, Lo RC-lam, Li Y, *et al.* The potential contributions of a Y-located protooncogene and its X homologue in sexual dimorphisms in hepatocellular carcinoma. *Hum Pathol* 2014;45:1847–58.
- 15 Ji J, Shi J, Budhu A, *et al.* MicroRNA expression, survival, and response to interferon in liver cancer. *N Engl J Med* 2009;361:1437–47.
- 16 Kota J, Chivukula RR, O'Donnell KA, *et al.* Therapeutic microRNA delivery suppresses tumorigenesis in a murine liver cancer model. *Cell* 2009;137:1005–17.
- 17 Clodfelter KH, Holloway MG, Hodor P, *et al.* Sex-dependent liver gene expression is extensive and largely dependent upon signal transducer and activator of transcription 5b (Stat5b): STAT5b-dependent activation of male genes and repression of female genes revealed by microarray analysis. *Mol Endocrinol* 2006;20:1333–51.
- 18 Naqvi S, Godfrey AK, Hughes JF, *et al.* Conservation, acquisition, and functional impact of sex-biased gene expression in mammals. *Science* 2019;365.
- 19 Botlagunta M, Vesuna F, Mironchik Y, *et al.* Oncogenic role of DDX3 in breast cancer biogenesis. *Oncogene* 2008;27:3912–22.
- 20 Hollingsworth AB, Lerner MR, Lightfoot SA, *et al.* Prevention of DMBA-induced rat mammary carcinomas comparing leuprolide, oophorectomy, and tamoxifen. *Breast Cancer Res Treat* 1998;47:63–70.
- 21 Budhu A, Jia H-L, Forgues M, *et al.* Identification of metastasis-related microRNAs in hepatocellular carcinoma. *Hepatology* 2008;47:897–907.
- 22 Roessler S, Jia H-L, Budhu A, *et al.* A unique metastasis gene signature enables prediction of tumor relapse in early-stage hepatocellular carcinoma patients. *Cancer Res* 2010;70:10202–12.
- 23 Budhu A, Roessler S, Zhao X, *et al.* Integrated metabolite and gene expression profiles identify lipid biomarkers associated with progression of hepatocellular carcinoma and patient outcomes. *Gastroenterology* 2013;144:1066–75.
- 24 Cancer Genome Atlas Research Network. Electronic address: wheeler@bcm.edu, Cancer Genome Atlas Research Network. Comprehensive and integrative genomic characterization of hepatocellular carcinoma. *Cell* 2017;169:1327–1341.e23.
- 25 Gu Y, Wei X, Sun Y, *et al.* miR-192-5p silencing by genetic aberrations is a key event in hepatocellular carcinomas with cancer stem cell features. *Cancer Res* 2019;79:941–53.
- 26 Wei X, Zhao L, Ren R, *et al.* Mir-125B loss activated HIF1 α /pAKT loop, leading to transarterial chemoembolization resistance in hepatocellular carcinoma. *Hepatology* 2021;73:1381–98.
- 27 Ikeda A, Shimizu T, Matsumoto Y, *et al.* Leptin receptor somatic mutations are frequent in HCV-infected cirrhotic liver and associated with hepatocellular carcinoma. *Gastroenterology* 2014;146:222–32.
- 28 Wu M, Lan H, Ye Z, *et al.* Hypermethylation of the PZP gene is associated with hepatocellular carcinoma cell proliferation, invasion and migration. *FEBS Open Bio* 2021;11:826–32.
- 29 Zhang B, Wu H. Decreased expression of *COLEC10* predicts poor overall survival in patients with hepatocellular carcinoma. *Cancer Manag Res* 2018;10:2369–75.
- 30 Wu Y, Zhang X, Shen R, *et al.* Expression and significance of ETFDH in hepatocellular carcinoma. *Pathol Res Pract* 2019;215:152702.
- 31 Baik M, Yu JH, Hennighausen L. Growth hormone-STAT5 regulation of growth, hepatocellular carcinoma, and liver metabolism. *Ann N Y Acad Sci* 2011;1229:29–37.
- 32 Romualdo GR, Prata GB, da Silva TC, *et al.* Fibrosis-associated hepatocarcinogenesis revisited: establishing standard medium-term chemically-induced male and female models. *PLoS One* 2018;13:e0203879.
- 33 Stiles AR, Kozlitina J, Thompson BM, *et al.* Genetic, anatomic, and clinical determinants of human serum sterol and vitamin D levels. *Proc Natl Acad Sci U S A* 2014;111:E4006–14.
- 34 Genetics of Exfoliation Syndrome Partnership, Li Z, Wang Z, *et al.* Association of rare CYP39A1 variants with exfoliation syndrome involving the anterior chamber of the eye. *JAMA* 2021;325:753–64.
- 35 Fladvad M, Zhou K, Moshref A, *et al.* N and C-terminal sub-regions in the c-myc transactivation region and their joint role in creating versatility in folding and binding. *J Mol Biol* 2005;346:175–89.
- 36 Liu X, Tesfai J, Evrard YA, *et al.* C-Myc transformation domain recruits the human STAGA complex and requires TRRAP and GCN5 acetylase activity for transcription activation. *J Biol Chem* 2003;278:20405–12.
- 37 Kato GJ, Barrett J, Villa-Garcia M, *et al.* An amino-terminal c-myc domain required for neoplastic transformation activates transcription. *Mol Cell Biol* 1990;10:5914–20.
- 38 Calderwood SK, Khaleque MA, Sawyer DB, *et al.* Heat shock proteins in cancer: chaperones of tumorigenesis. *Trends Biochem Sci* 2006;31:164–72.
- 39 Carystinos GD, Kandouz M, Alaoui-Jamali MA, *et al.* Unexpected induction of the human connexin 43 promoter by the Ras signaling pathway is mediated by a novel putative promoter sequence. *Mol Pharmacol* 2003;63:821–31.
- 40 Lucca I, Fajkovic H, Klatt T. Sex steroids and gender differences in nonmuscle invasive bladder cancer. *Curr Opin Urol* 2014;24:500–5.
- 41 Tanaka S, Mogushi K, Yasen M, *et al.* Oxidative stress pathways in noncancerous human liver tissue to predict hepatocellular carcinoma recurrence: a prospective, multicenter study. *Hepatology* 2011;54:1273–81.
- 42 Ashida R, Okamura Y, Ohshima K, *et al.* The down-regulation of the CYP2C19 gene is associated with aggressive tumor potential and the poorer recurrence-free survival of hepatocellular carcinoma. *Oncotarget* 2018;9:22058–68.
- 43 Kang JS, Wanibuchi H, Morimura K, *et al.* Role of CYP2E1 in diethylnitrosamine-induced hepatocarcinogenesis in vivo. *Cancer Res* 2007;67:11141–6.
- 44 Zhang D, Lou J, Zhang X, *et al.* Hyperhomocysteinemia results from and promotes hepatocellular carcinoma via CYP450 metabolism by CYP2J2 DNA methylation. *Oncotarget* 2017;8:15377–92.
- 45 Jiang F, Chen L, Yang Y-C, *et al.* Cyp3A5 functions as a tumor suppressor in hepatocellular carcinoma by regulating mTORC2/Akt signaling. *Cancer Res* 2015;75:1470–81.
- 46 Luo M, Yang F, Huang S-xin, *et al.* Two-Stage model of chemically induced hepatocellular carcinoma in mouse. *Oncol Res* 2013;20:517–28.
- 47 Santoni-Rugiu E, Nagy P, Jensen MR, *et al.* Evolution of neoplastic development in the liver of transgenic mice co-expressing c-myc and transforming growth factor- α . *Am J Pathol* 1996;149:407–28.
- 48 Hartwell HJ, Petrosky KY, Fox JG, *et al.* Prolactin prevents hepatocellular carcinoma by restricting innate immune activation of c-myc in mice. *Proc Natl Acad Sci U S A* 2014;111:11455–60.

*Supplementary File***Blockings Hepatocarcinogenesis by A Cytochrome P450 Family Member with Female-preferential expression****Supplementary Materials and Methods-----Page s1-5****Supplementary Figures (n=8)-----Page s6-15****Supplementary Tables (n=11)-----Page s16-43****Supplementary Materials and Methods****Plasmids and siRNAs**

Vectors pT3-EF1 α -cMyc, pT3-EF1 α -myr-AKT, NRasV12/pT2-CAGGS, and pT3-EF1 α -MCL1, and pCMV/Sleeping Beauty transposase (pCMV/SB) were constructed as previously described^{1, 2}. Plasmids p3Xflag-CMV-14-CYP39A1, p3Xflag-CMV-14-CYP39A1 $\Delta^{369-469}$, p3Xflag-CMV-14-CYP39A1 Δ^{2-21} , p3Xflag-CMV-14-CYP39A1 Δ^{2-145} , p3Xflag-CMV-14-CYP39A1 $\Delta^{291-469}$, pBiFC-VC155-HA-CYP39A1, p3Xflag-CMV-14-HSP90AA1, pCDH-CMV-CYP39A1-3xflag-EF1 α -copGFP, pEGFP-attL-HSP90AA1, AAV-TBG-CYP39A1 and pCDNA3.0-MYC-3x HA were generated via amplifying whole length of CYP39A1, CYP39A1 truncations, HSP90AA1 and MYC cDNA fragments through RT-PCR and inserting them into the corresponding restrict enzyme sites. p3Xflag-CMV-14-CYP39A1-K329Q were derived from p3Xflag-CMV-14-CYP39A1. pGL-4xEbox was constructed by synthesizing four ligated canonical c-Myc binding enhancer box (E-box) and inserting it into XhoI/HindIII sites of pGL4.20. Gal4-Myc (2-143aa), Gal4-Myc (2-103aa), Gal4-Myc (2-67aa), Gal4-Myc (2-41,67-103aa), and Gal4-Myc (2-41aa) were generated via recombining Gal4 DNA binding domain (2-147aa) and the corresponding c-Myc fragments with the ClonExpress MultiS One Step Cloning Kit (Vazyme). AAV-shCYP39A1 were constructed via synthesizing shCYP39A1 and inserting it into BamHI/XbaI sites of AAV-shCtrl. Vectors of multiple pT3-EF1 α -CYP39A1s and pT3-EF1 α -HSP90AA1 were generated via recombining CYP39A1, CYP39A1 truncations, CYP39A1 mutants, and HSP90AA1 entry clones with a destination vector pT3-EF1 α -attR-ccdb vector using the Gateway LRTM ClonaseTM II Enzyme mix (Thermo Fisher Scientific). MYC and CYP39A1 siRNAs and negative control siRNA were purchased (Ribo, Guangzhou). Lipofectamine 3000 (Invitrogen) reagent was used for transfections of plasmids and siRNAs. All information of constructs and sequences are listed in Table S10.

Luciferase assay

pGL-4xE-box was transfected together with pRL-CMV containing Renilla luciferase and pT3-EF1 α -Myc. Gal4-Luc was transfected together with pRL-CMV containing Renilla luciferase and the indicated Gal4-Myc plasmids. Other plasmids were also co-transfected including pT3-EF1 α -CT, pT3-EF1 α -CYP39A1, pT3-EF1 α -CYP39A1-K329Q, pT3-EF1 α -CYP39A1 truncations, or p3x flag-CMV-14-HSP90AA1 to investigate the regulatory function of CYP39A1 and Hsp90. Twenty-four hours after transfection, firefly and renilla luciferase activities were measured using Dual-Luciferase Reporter Assay.

Immunoprecipitation (IP) and IP/Mass spectrum (IP/MS)

For IP assay, cells were lysed in IP buffer. The supernatants were incubated at 4°C for overnight with anti-Flag-M2 magnetic beads (Sigma, Cat# M8823), Pierce™ anti-HA magnetic beads (Thermo Scientific, Cat# 88836) or protein A/G beads (Thermo Scientific, Cat#88802) with the presence of indicated antibodies. Then, the immunoprecipitated proteins were subjected to immunoblotting.

For IP/MS assay, the cell supernatants were incubated at 4°C for overnight with pierce™ anti-HA magnetic beads. Proteins were boiled off the beads in 1% SDS loading buffer. The immunoprecipitated proteins were running with SDS-PAGE gel for 0.8-1cm and the gel was stained by coomassie blue. The stained gel was sliced out, destained, and used for mass spectrometry analysis in our institute.

Mouse study

The mouse study was approved by the Experimental Animal Committee of Zhejiang University. All animal experiments met the Animal Welfare Guidelines. C57BL/6 mice and BALB/c nude mice were purchased from Shanghai SLAC Laboratory Animal Co.Ltd. FVB/N mice were from Beijing Vital River Laboratory Animal Technology. All mice were housed in Zhejiang University Laboratory Animal Center in laminar-flow cabinets under specific pathogen-free conditions at room temperature with a 24-hour night-day cycle.

Liver tissues were collected from C57BL/6 mice at their ages of 0 and 2 days as well as 2, 4, 6, 8, 12, and 16 weeks. FVB/N liver tissues were collected at their ages of 4, 6, 8 and 12 weeks. For testosterone and estradiol deprivation assays, gonadectomy or sham surgery were performed at 7-week-old mice. Eight weeks after castration, the liver tissues were collected and CYP39A1 mRNA level were examined. For xenograft tumorigenicity assay, 1×10^6 HuH7 cells suspended in 100 μ l of PBS and Matrigel (1:1) were injected subcutaneously to flank regions of BALB/c nude mice.

For DEN and CCL₄ induced orthotopic HCC tumorigenicity assay, DEN (20mg/kg) was given to WT C57BL/6 mice at age p12 by intraperitoneal injection, followed by CCL₄ (1ml/kg)

intraperitoneal injection weekly starting at the 5th week for the indicated times. In this model, 1×10^{11} genomic particles AAV.GFP, AAV.CYP39A1, AAV.shCtrl, or AAV.shCYP39A1 were tail vein injected at 6.5 week.

For oncogene-induced orthotopic HCC tumorigenicity assay, a sleeping beauty (SB) transposon system and six-week-old wild-type FVB/N mice was used. Hydrodynamic injection was performed as described. Briefly, pT3-EF1 α -Myc, or the combination of pT3-EF1 α -Myc/ pT3-EF1 α -Mcl1 along with pCMV/SB was introduced to induce HCC formation through hydrodynamic tail vein injection¹⁻³. pT3-EF1 α -CYP39A1, pT3-EF1 α -CYP39A1-K329Q, pT3-EF1 α -CYP39A1 Δ ³⁶⁹⁻⁴⁶⁹, and pT3-EF1 α -HSP90AA1 was used to test their function in regulating HCC formation. For each injection, the combined plasmids were diluted in 2 ml saline (0.9% NaCl), filtered through a 0.22 μ m filter, and injected into the lateral tail vein of mice in 5 to 7 seconds. The detail plasmid combination and amount are listed in Table S11.

For 7 α 24s-diHC and 24s-HC treatment assay, both 7 α 24s-diHC and 24s-HC were dissolved in 30% PEG400 and 5% Tween-80. 7 α 24s-diHC solution was intraperitoneally injected at a dose of 0.15 μ M or 0.75 μ M per day for 6 days a week starting at 3 weeks after hydrodynamic injection. 24s-HC solution was intraperitoneally injected at a dose of 0.75 μ M or 1.5 μ M per day for 6 days a week starting at 3 weeks after hydrodynamic injection. Mice in the control group were injected intraperitoneally with the same amount of the solvent.

Protein extraction, Western blot and cycloheximide (CHX) assay

For total proteins, cells were lysed in IP buffer (1% NP40, 150mM NaCl, 50mM tris PH 7.4, 10% glycerol).

To collect cytoplasmic and nuclear protein fractions, cells were collected with trypsinization and resuspended in Buffer A (10mM HEPES PH 7.9, 10mM KCl, 1.5mM MgCl₂, 0.34M sucrose, 10% glycerol, 1mM dithiothreitol, and protease inhibitors). After adding 0.1% of Triton X-100, cells were lysed on ice and then centrifuged at 1,300g to separate cytoplasmic fractions (supernatant) and nuclear fractions (pellet). Cytoplasmic fractions were further centrifuged at 17,000g and the supernatant was collected as cytoplasmic proteins. Nuclear fractions were washed once by Buffer A and lysed for 30 minutes in Buffer B (3mM EDTA, 0.2 mM EGTA, 1mM dithiothreitol, and protease inhibitors). After centrifuging at 1,700g, the soluble fractions were collected as Soluble nuclear fraction. The insoluble fractions were washed in Buffer B again and resuspended in SDS buffer as Nuclear chromatin-enriched fraction.

Cell lysates were separated by SDS-PAGE Gel and transferred to PVDF membranes. The membranes were incubated with indicated primary antibodies and then secondary antibodies conjugated to horseradish peroxidase for enhanced chemiluminescence detection of the signals

(4A Biotech). These antibodies included Flag-M2 (Sigma, F3165), c-Myc (Abcam, ab32072), Hsp90 (Proteintech, 13171-1-AP), Actin (Sigma, A5441), GAPDH (Proteintech, 10494-1-AP), Histone H3 (Abclonal, WH183266), HRP-linked anti-rabbit IgG antibody (Jackson Immuno Research, lot.129736), HRP-linked anti-mouse IgG antibody (Jackson Immuno Research, lot.129457), and HRP-conjugated AffiniPure Mouse Anti-Rabbit IgG Light Chain (Abclonal, WH118252). For CHX assay, cells were treated with 20ug/ml CHX (Cell signaling technology) and collected at indicated time for western blot assay.

RNA Extraction and RT-qPCR

Total RNA was isolated using Trizol reagent (Invitrogen). cDNA synthesis was performed with 1ug of total RNA using PrimeScript™ RT reagent Kit with gDNA Eraser (Takara). TB Green Premix Ex Taq II (Takara) was used for real time PCR (Bio-rad CFX96 or ABI7500). 18S was used as the reference gene for CYP39A1, CYP17A1, CYP11A1, CYP11B2, MYC, CBX3, CCNB1, CDC25A, CDK4, CKS2, GNL3, NAP1L1, PA2G4, PCNA. All primer sequences are listed in Table S1.

Cell viability, colony formation, apoptosis, 24s-HC and 7 α 24s-diHC treatment

Cell viability was detected by MTT assay (Sangon Biotech). Briefly, Huh7 (1,000 cells/well) or HLF (800 cells/well) was seeded in 96-well plates and cultured for the indicated times till the cell viability measurement. Colony formation was performed using Huh7 and HLF cells. Huh7 (1,000 cells/well) or HLF (800 cells/well) was plated in 6-cm dish and incubated for two weeks. Colonies were stained by crystal violet. Cell apoptosis was examined via a flow cytometry method using Annexin V-FITC/PI kit (Keygen Biotech). For 24s-HC treatment assay, Huh7 or HLF (8,000 cells/well) were seeded in 96-well plates for cell viability assay and Huh7 (1,000 cells/well) or HLF (800 cells/well) were seeded in 6-well plates for colony formation assay. Twenty-four hours after seeding, cells were exposed to different concentration of 24s-HC (MedChemExpress) and 7 α 24s-diHC (Merck). The cell viability was measured after incubating for 12 hours and the colony number was measured after 12 days.

Sex-hormone examination

At 4 weeks after AAV injection, whole blood of C57BL/6 mice was taken from their orbit and serum was collected via centrifugation. The collected serum was used for sex-hormone examination in Human Metabolomics Institute in Shenzhen, China via the liquid chromatography-triple quadrupole mass spectrometry (LC-TQMS).

Statistical Analysis

Class comparison was used for screening for sex-related molecules in Cohort 1. Hierarchical clustering of sex-related molecules was performed by the GENESIS software version 1.7.6 developed by Alexander Sturn (IBMT-TUG, Graz, Austria). Ingenuity pathway analysis (IPA) with

all sex related molecules was performed using their log 2 values of female vs. male to identify the related diseases and functions as well as regulatory networks of these molecules. IPA with CYP39A1-related genes was also performed to explore the common regulators of these genes. One-way ANOVA, two-way ANOVA and student's t-test was used for statistical analysis of comparative data between groups. Log-Rank test was used for statistical analysis of tumor occurrence between groups. All p values were 2-sided, and p value should be less than 0.05 as significant difference.

References:

1. Tao JY, Ji JF, Li XL, et al. Distinct anti-oncogenic effect of various microRNAs in different mouse models of liver cancer. *Oncotarget* 2015;6:6977-88.
2. Mendez-Lucas A, Li XL, Hu JJ, et al. Glucose Catabolism in Liver Tumors Induced by c-MYC Can Be Sustained by Various PKM1/PKM2 Ratios and Pyruvate Kinase Activities. *Cancer Research* 2017;77:4355-64.
3. Ho C, Wang C, Mattu S, et al. AKT (v-akt murine thymoma viral oncogene homolog 1) and N-Ras (neuroblastoma ras viral oncogene homolog) coactivation in the mouse liver promotes rapid carcinogenesis by way of mTOR (mammalian target of rapamycin complex 1), FOXM1 (forkhead box M1)/SKP2, and c-Myc pathways. *Hepatology* 2012;55:833-45.

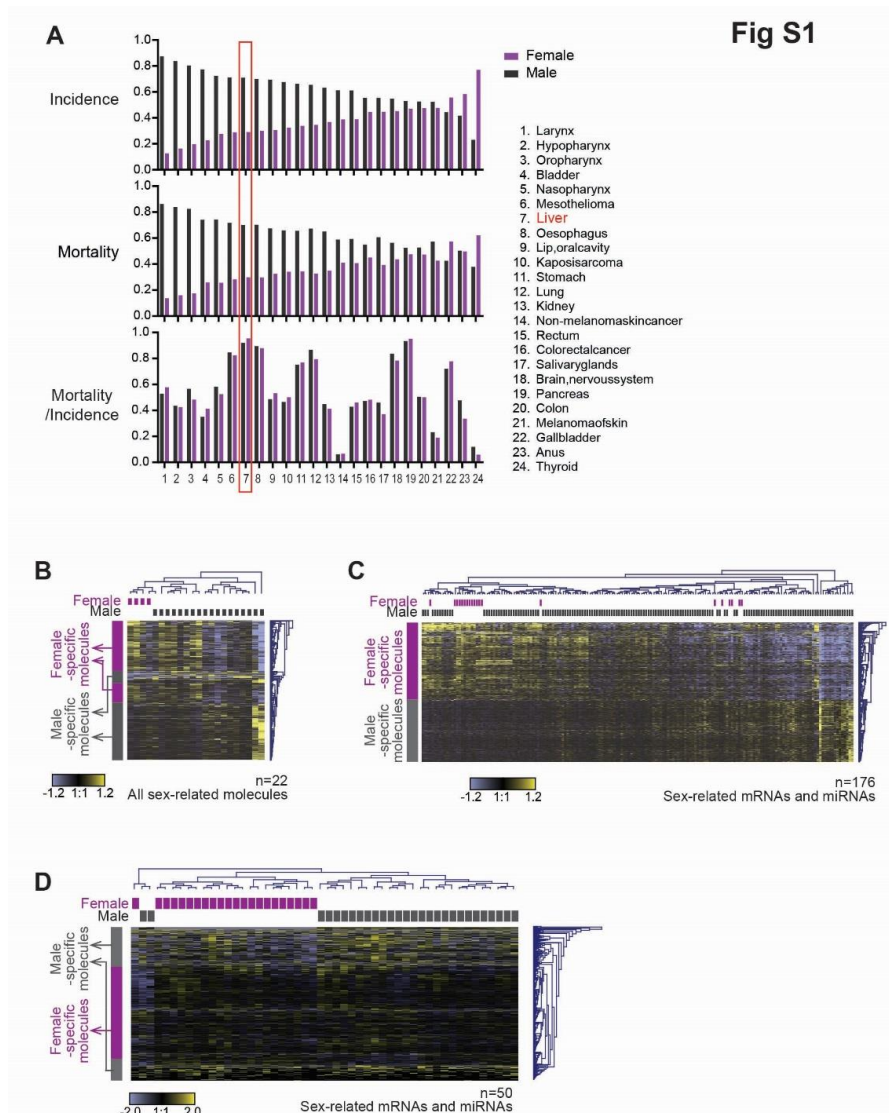


Fig S1. Sex-disparity in hepatocellular carcinoma.

(A) The cancer incidence and mortality rates of men and women. (B) Hierarchical clustering analysis with sex-related molecules in HCC Cohort 1. (C,D) Hierarchical clustering analysis with sex-related miRNAs and genes in HCC Cohort 1 (C) and HCC Cohort 2 (D).

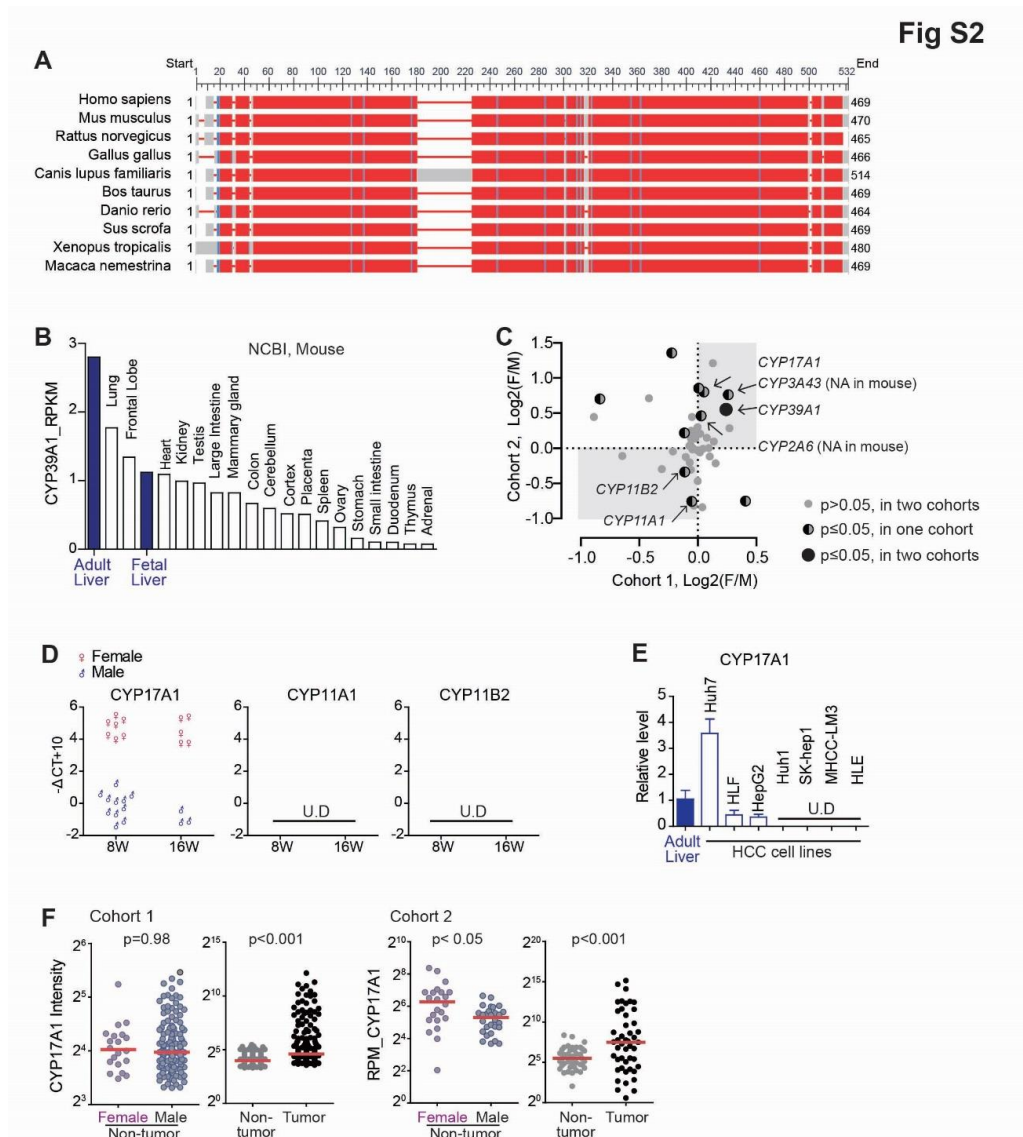


Fig S2. CYP39A1 is a unique female preferentially expressed, liver-specific and tumor-related gene.

(A) CYP39A1 protein sequences were highly conserved among different species. (B) The expression of CYP39A1 in various mouse organs. Original data were downloaded from NCBI. (C) Sex-related CYP genes. Expression levels of CYP family genes were compared between female and male in their non-tumor tissues of Cohorts 1 and 2. (D) CYPs levels in normal liver tissues of C57BL/6 mice. (E) CYP17A1 expression in HCC cell lines and adult liver tissue was measured by qRT-PCR. (F) CYP17A1 levels in female and male non-tumor liver tissues, and in tumor and non-tumors of HCC Cohorts 1 and 2.

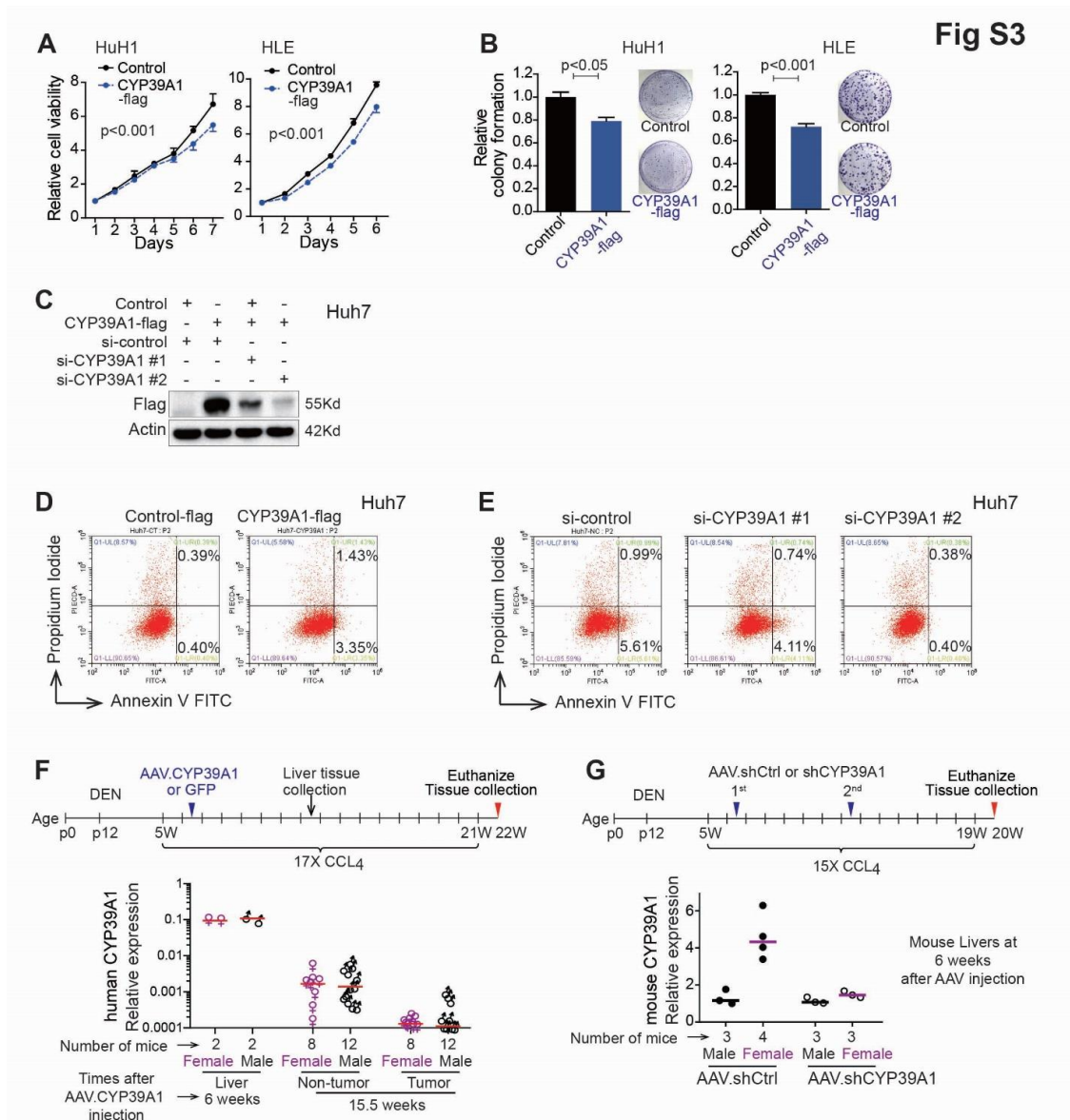


Fig S3. CYP39A1 function in vitro and overall flow of DEN/CCL₄-induced HCC mouse model.

(A) Cell viability was examined in Huh1 and HLE cells transfected with control-flag and CYP39A1-flag. Two-way ANOVA was performed. (B) Colony formation was examined in Huh1 and HLE cells transfected with control-flag and CYP39A1-flag. Student t-test was performed. (C) CYP39A1 level in Huh7 cells transfected with CYP39A1-flag, CYP39A1-flag and siCYP39A1#1, CYP39A1-flag and siCYP39A1#2. (D) Cell apoptosis was examined in Huh7 cells being transfected with control-Flag and CYP39A1-flag. (E) Cell apoptosis was examined in Huh7 cells

being transfected with control siRNAs and CYP39A1 siRNAs. (F) Overall flow of DEN and CCL4 induced orthotopic HCC mouse model treated with AAV particles. Human CYP39A1 expression was measured in liver tissues, non-tumor and tumor tissues of these mice. (G) Overall flow of DEN and CCL4 induced orthotopic HCC mouse model treated with AAV.shCtrl or AAV.shCYP39A1. Mouse CYP39A1 expression was measured in liver tissues of these mice. Number of mice was indicated in panels (F) and (G).

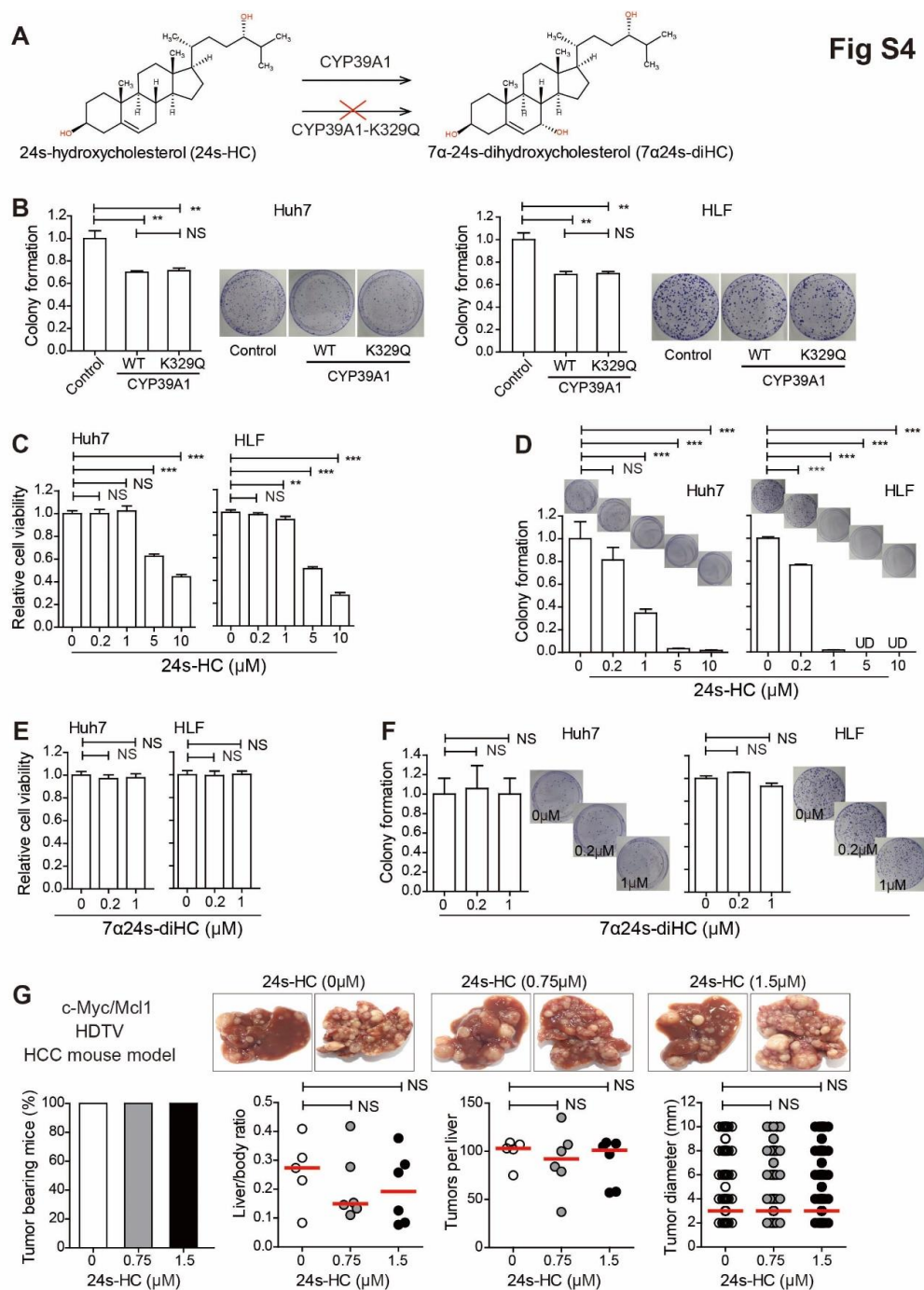


Fig S4

Fig S4. CYP39A1 inhibiting malignancy features of HCC cells was not dependent on its catalytic activity of metabolizing 24s-HC to 7 α 24s-diHC.

(A) CYP39A1 converts 24s-HC to 7 α 24s-diHC, while CYP39A1-K329Q cannot. (B) Colony formation was examined in Huh7 and HLF cells transfected with control, CYP39A1 and

CYP39A1-K329Q. (C) Cell viability of Huh7 and HLF upon exposure to 24s-HC for 12 hours. The reported physiological concentration of 24s-HC is 0.15 μ M (0.03~0.79 μ M). (D) Colony formation of Huh7 and HLF upon exposure to 24s-HC for 12 hours. (E) Cell viability of Huh7 and HLF upon exposure to 7 α 24s-diHC for 12 hours. (F) Colony formation of Huh7 and HLF upon exposure to 7 α 24s-diHC for 12 hours. Unpaired t-test was used. NS, not significant. ***, $p < 0.001$. **, $p < 0.01$. (G) c-Myc/Mcl1 HDTV HCC mouse model was used with 0 μ M, 0.75 μ M and 1.5 μ M 24s-HC treatment (n=5, 6, and 6, respectively). Female mice were used, and representative tumor images were shown. Tumor bearing animals, ratio of liver vs. body, tumors per liver, and diameter were quantified and compared. Unpaired t-test was used. NS, not significant.

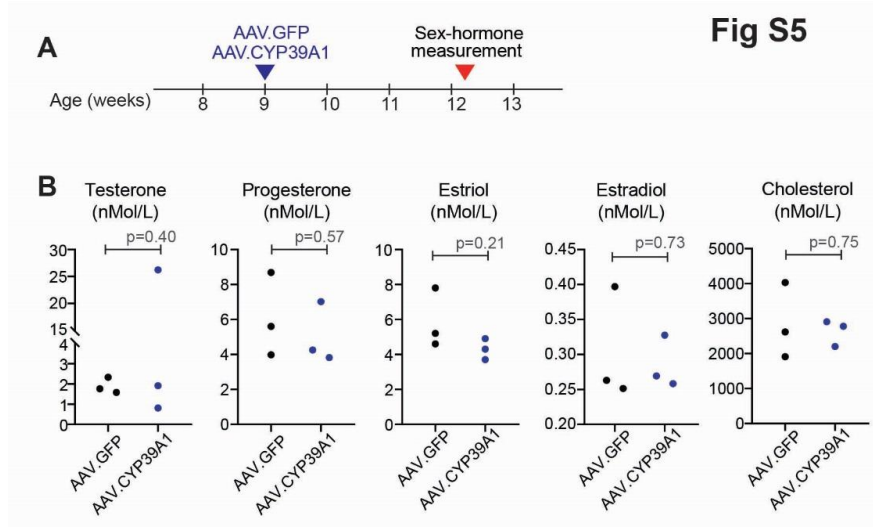


Fig S5. Sex hormone levels in mouse serum.

(A) Time points of AAV virus injection and blood collection for examining sex hormones. (B) The levels of sex hormones between mice with AAV.GFP injection (n=3) and ones with AAV.CYP39A1 injection (n=3). Male mice were used in this assay. Unpaired t-test was performed.

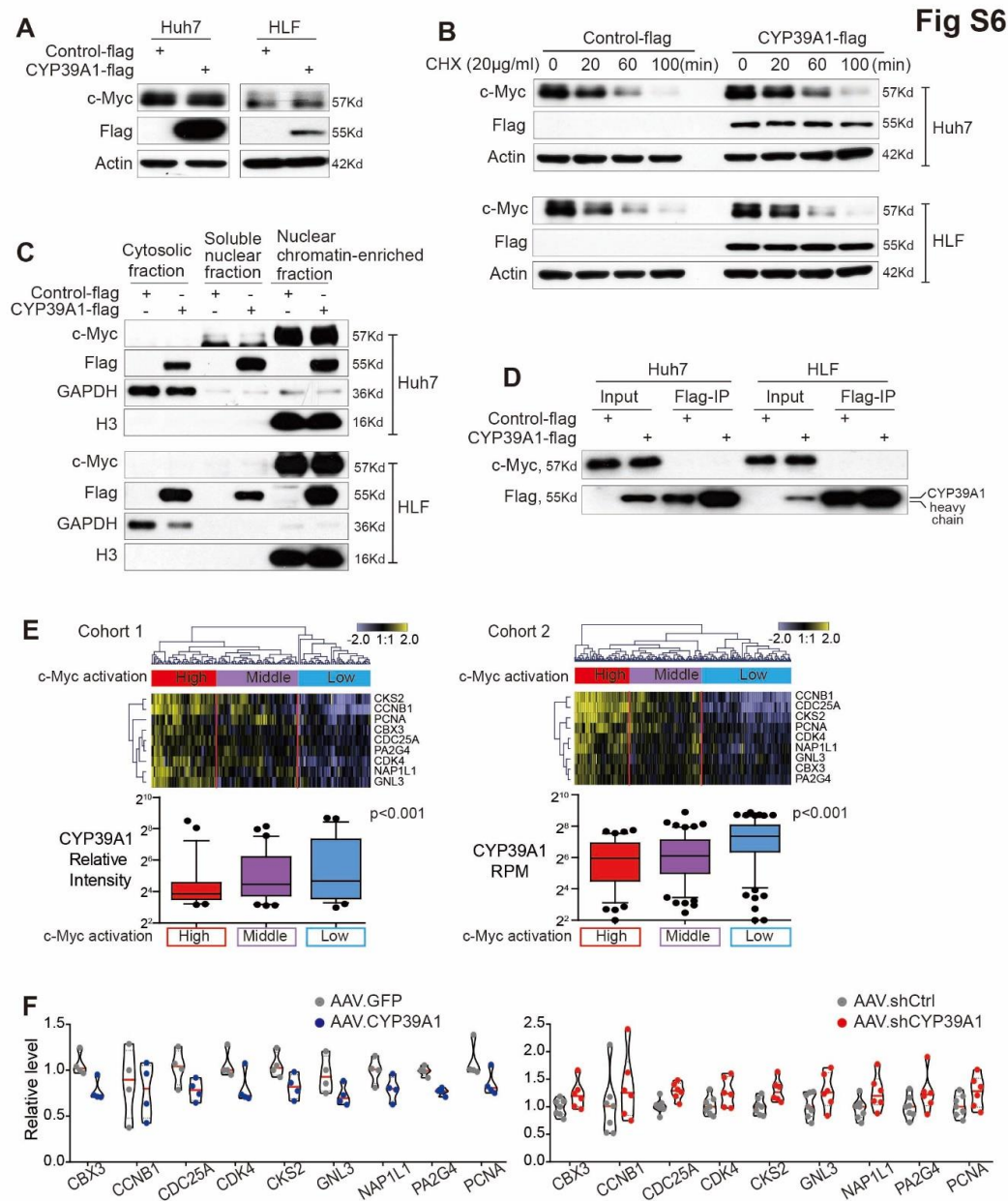


Fig S6. CYP39A1 did not interact with c-Myc or altered c-Myc protein level.

(A) The expression of c-Myc in Huh7 and HLF cells infected with lentivirus CYP39A1-flag. Actin was used as a loading control for western blot. (B) Huh7 and HLF cells were infected with lentivirus CYP39A1-flag and treated with 20ug/ml CHX. The expression of c-Myc was then detected by western blot. (C) Cytosolic and Nuclear c-Myc protein level in control-flag group and CYP39A1-flag group. GAPDH and histone 3 (H3) was used as a loading control for Cytosolic

and Nuclear fractions, respectively. (D) Co-IP between CYP39A1-flag and c-Myc in Huh7 and HLF cells with or without over-expression of CYP39A1-flag. (E) HCC patients in Cohorts 1 and 2 were clustered into three groups by 9 c-Myc target genes. CYP39A1 expression was compared among three groups with different c-Myc activation status. One-way ANOVA was used. (F) c-Myc target gene expression was examined by qRT-PCR at liver tissues were from mice at 6 weeks after AAV.CYP39A1 injection or AAV.shCYP39A1 injection. (AAV.GFP group, 2 female, 2 male; AAV.CYP39A1 group, 2 female, 2 male; AAV.shCtrl group, 4 female, 3 male; AAV.shCYP39A1 group, 3 female, 3 male.)

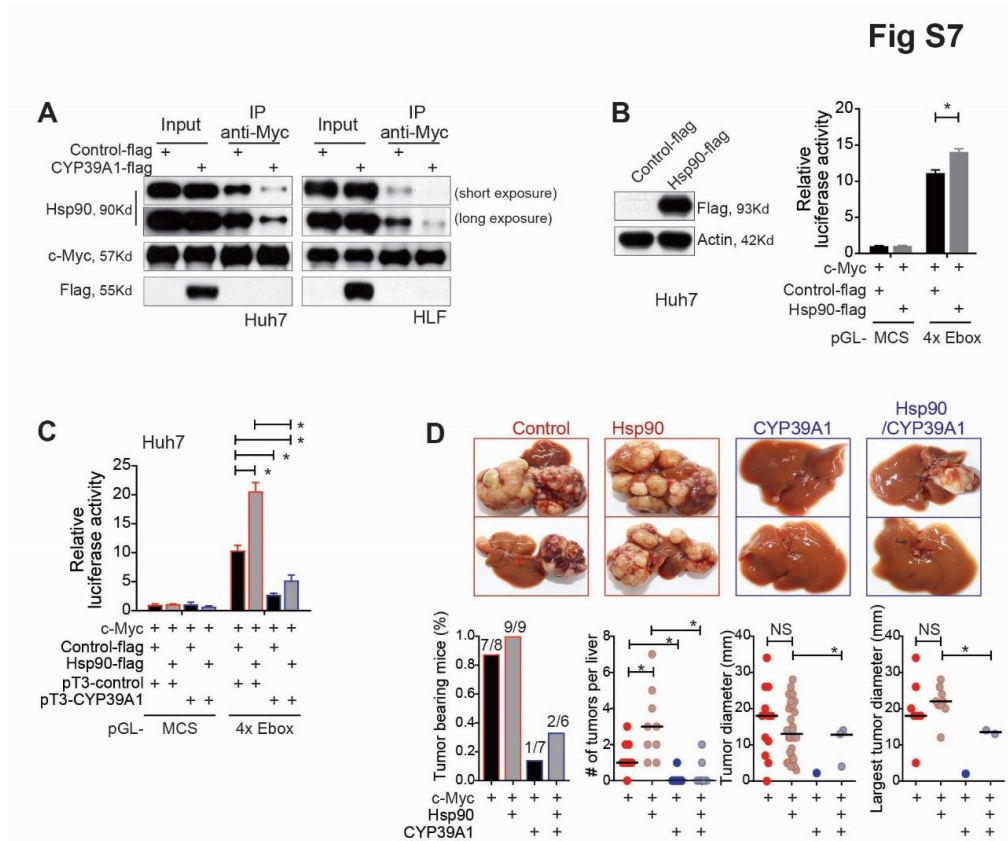


Fig S7. CYP39A1 inhibited the interaction of Hsp90 and c-Myc and impeded the c-Myc/Hsp90 mediated hepatocarcinogenesis.

(A) Co-IP between Hsp90 and c-Myc in Huh7 and HLF cells with or without over-expression of CYP39A1. **(B)** pGL-4xE-box luciferase reporter activity was compared in Huh7 cells transfected with c-Myc and c-Myc with HSP90AA1. Unpaired t-test was used. **(C)** pGL-4xE-box luciferase reporter activity was compared in Huh7 cells transfected with c-Myc, c-Myc with HSP90AA1, c-Myc with CYP39A1, and c-Myc with both HSP90AA1 and CYP39A1. Unpaired t-test was used. **(D)** Representative tumor images from c-Myc group (n=8), c-Myc/Hsp90 group (n=9), c-Myc/CYP39A1 group (n=7), and c-Myc/Hsp90/CYP39A1 group (n=6) at 12 weeks after injection. Tumor bearing animals, ratio of liver vs. body, tumors per liver, and diameter were also quantified and compared. Female mice were used, and Unpaired t-test was performed. NS, not significant. *, p<0.05.

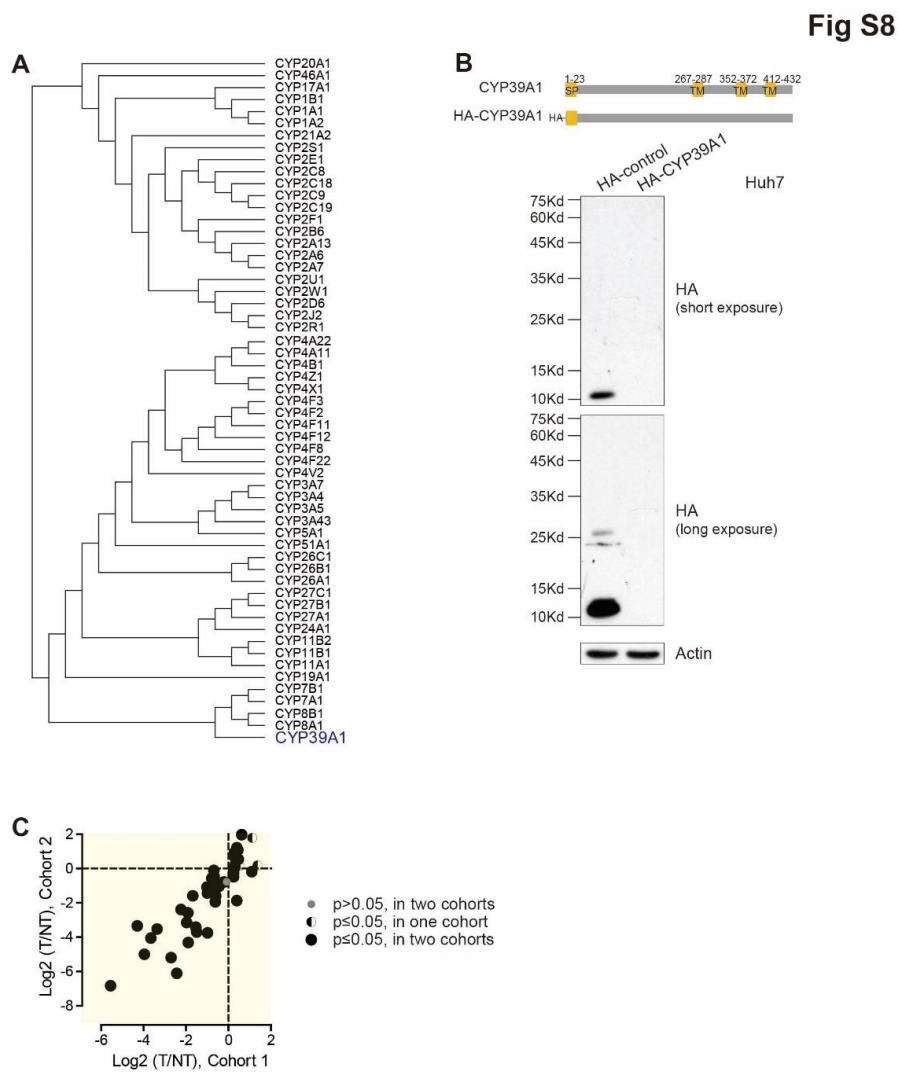


Fig S8. CYP39A1 protein sequence and its expression.

(A) Consensus physicochemical tree of cytochrome families based on their protein sequences, analyzed in MView. **(B)** HA-CYP39A1 expression were examined in Huh7 cells. **(C)** Tumor-related CYP genes. Expression levels of CYP family genes were compared between tumor and non-tumor tissues in Cohorts 1 and 2.

Table S1. Clinical characteristics of patients in HCC Cohort 1 and Cohort 2.

Clinical variable	Cohort 1 (n=184)	Cohort 2 (n=367)	p value ^c
Sex			< 0.001
Female	21	112	
Male	163	235	
Missing data	0	20	
Age			< 0.001
Median	50	61	
Range	21-77	17-88	
AFP (ng/ml)			< 0.001
≤20	54	138	
>20	122	124	
Missing data	8	105	
Race			< 0.001
Asian	184	155	
Caucasian	0	165	
African American	0	16	
American Indian	0	1	
Missing data	0	30	
TNM stage			0.45
I-II	139	241	
III-IV	41	85	
Missing data	4	41	
Tumor size			NA
<3cm	62	NA	
≥3cm	122	NA	
Multi-nodules			NA
No	158	NA	
Yes	26	NA	
Etiology			< 0.001
HBV only	163	71	
HCV only	1	31	
ALD only	0	70	
NAFLD only	0	10	
Mixed etiologies ^a	2	49	
Others ^b	0	6	
None	10	75	
Missing data	8	55	
Albumin			0.10
<4g/dL	67	130	
≥4g/dL	110	154	
Missing data	7	83	
Cirrhosis			< 0.001
No	14	124	
Yes	170	73	
Missing data	0	170	
Survival months			< 0.001
Median (Range)	52.2 (2.0-67.4)	85.1 (0.1-525.0)	

^a, Mixed etiologies refer to two and more HCC risk factors in one case. Cohort 1: HBV+HCV (n=2). Cohort 2: ALD+HBV (n=20), ALD+HCV (n=14), ALD+NAFLD (n=5), HBV+HCV (n=3), HBV+NAFLD (n=1), HCV+Hemochromatosis (n=1), ALD+HBV+HCV (n=3), ALD+HCV+NAFLD (n=1); ALD+HBV+HCV+Hemochromatosis (n=1).

^b, Others contain 5 cases with Hemochromatosis only and 1 case with Alpha-1 antitrypsin deficiency only (Cohort 2).

^c, p values were calculated with the use of the chi-square test, except for Age with the un-paired t test and for Survival time with Log-rank test.

Table S2. Clinical characteristics of patients used for the identification of sex-related genes

Clinical variable	Female	Male G1	Male G2	p value	
				Female vs. Male G1	Female vs. Male G2
Sex				<0.001 ^a	< 0.001 ^a
Female	20	0	0		
Male	0	20	20		
Age				0.76 ^b	0.83 ^b
Median	52.0	50.5	50.5		
Range	27-71	21-77	34-72		
AFP (ng/ml)				0.35 ^a	0.94 ^a
≤20	6	7	5		
>20	12	13	13		
Missing data	2	0	2		
TNM stage				0.74 ^c	0.60 ^c
I	11	9	8		
II	8	9	10		
III-IV	1	2	2		
Tumor size				0.53 ^a	1.00 ^a
<3cm	9	12	8		
≥3cm	11	8	12		
Multi-nodules				1.00 ^a	0.49 ^a
No	18	18	20		
Yes	2	2	0		
HCV-Ab				0.60 ^a	0.52 ^a
Negative	16	17	18		
Positive	1	0	0		
Missing data	3	3	2		
HBV				1.00 ^a	1.00 ^a
Negative	1	0	0		
Positive	19	20	20		
Cirrhosis				1.00 ^a	0.49 ^a
No	2	1	0		
Yes	18	19	20		
Survival months				0.77 ^d	0.82 ^d
Median	55.2	52.2	53.2		
Range	7-67.1	8.0-67.3	3.3-64.5		

^a, Fisher's exact test; ^b, Un-paired t-test; ^c, Chi-square test; ^d, Log-rank test

Table S3. Sex-related genes (n=808), miRNAs (n=6), and metabolites (n=47).

Category	Molecules	Log2, Female vs. Male	p-value
Gene	RPS4Y1	-5.25	2.89E-08
Gene	JARID1D	-2.74	2.54E-06
Gene	DDX3Y	-2.46	6.43E-09
Gene	TSPAN13	-1.60	1.72E-04
Gene	EIF1AY	-1.44	8.88E-07
Gene	CUX2	-0.89	1.65E-03
Gene	CYorf15B	-0.84	9.31E-07
Gene	CYorf14	-0.82	2.16E-06
Gene	PLCXD1	-0.61	1.58E-03
Gene	OXT	-0.51	3.11E-03
Gene	USP9Y	-0.39	2.02E-04
Gene	ROM1	-0.31	1.23E-02
Gene	INA	-0.30	3.65E-02
Gene	DKK4	-0.29	2.85E-02
Gene	CA6	-0.29	2.21E-02
Gene	PLEKHA4	-0.28	1.19E-02
Gene	P2RY6	-0.26	2.63E-03
Gene	ICOS	-0.25	9.95E-04
Gene	SULT4A1	-0.24	4.32E-03
Gene	RP4-724E16.2	-0.24	3.22E-03
Gene	DDX51	-0.24	7.47E-03
Gene	KIR3DL1	-0.24	1.43E-02
Gene	C16orf59	-0.23	2.61E-03
Gene	SRF	-0.23	1.15E-03
Gene	DAZ2	-0.23	4.91E-03
Gene	GPR42	-0.23	1.34E-02
Gene	C14orf122	-0.23	3.51E-02
Gene	FKBP6	-0.22	4.72E-03
Gene	LOC51149	-0.22	3.14E-03
Gene	ST7L	-0.22	1.37E-02
Gene	RAB28	-0.22	5.06E-03
Gene	IL9	-0.21	6.44E-03
Gene	MGC4771	-0.21	1.70E-02
Gene	RTN2	-0.21	5.55E-04
Gene	CYP2W1	-0.21	2.95E-02
Gene	SLC12A3	-0.21	3.11E-04
Gene	PAX9	-0.21	1.79E-03
Gene	DLK2	-0.21	5.94E-03
Gene	SV2B	-0.21	2.19E-02
Gene	LMO1	-0.20	1.27E-02
Gene	LOC732229	-0.20	1.20E-02
Gene	SIX6	-0.20	5.75E-03
Gene	HSF2BP	-0.20	1.95E-02
Gene	SCN2B	-0.19	3.65E-02
Gene	AMN	-0.19	2.03E-02
Gene	DNASE1	-0.19	7.05E-03
Gene	MYH2	-0.19	6.48E-03
Gene	MPPED2	-0.19	1.82E-03
Gene	HOXB8	-0.19	1.95E-02
Gene	PAOX	-0.19	3.27E-02
Gene	DENND3	-0.18	4.54E-02
Gene	LMX1B	-0.18	7.33E-03
Gene	PRKY	-0.18	1.77E-03
Gene	MAST1	-0.18	1.25E-02
Gene	MAB21L1	-0.18	1.93E-02
Gene	GUCY1B2	-0.18	2.48E-02
Gene	IL10	-0.18	3.50E-02
Gene	TEKT2	-0.18	2.17E-02
Gene	CKM	-0.18	2.03E-02

Gene	POU3F4	-0.17	3.47E-03
Gene	GPR37L1	-0.17	2.36E-02
Gene	PGAM2	-0.17	3.10E-02
Gene	MYLK3	-0.17	4.84E-03
Gene	TPM3	-0.17	2.43E-02
Gene	PCBP3	-0.17	2.93E-02
Gene	SEMG2	-0.17	1.24E-02
Gene	CCBP2	-0.17	3.40E-02
Gene	PPFIA3	-0.17	1.91E-04
Gene	ANGPTL7	-0.17	1.38E-03
Gene	PCGF2	-0.17	8.19E-03
Gene	LOC730227	-0.16	4.50E-02
Gene	CTA-126B4.3	-0.16	1.88E-02
Gene	ZNF324B	-0.16	1.76E-03
Gene	TTY15	-0.16	1.31E-02
Gene	DLL3	-0.16	1.08E-03
Gene	MYO3A	-0.16	1.18E-02
Gene	KCNJ14	-0.16	3.60E-02
Gene	SLC6A9	-0.16	1.56E-03
Gene	MAGEL2	-0.16	1.02E-02
Gene	HRASLS2	-0.16	6.71E-03
Gene	LOC645323	-0.16	2.27E-02
Gene	C9orf116	-0.16	3.41E-02
Gene	PCDHB3	-0.16	4.66E-03
Gene	PLCL1	-0.16	2.62E-02
Gene	PDX1	-0.16	1.65E-03
Gene	MAGEA8	-0.16	6.01E-03
Gene	SPTA1	-0.16	3.59E-02
Gene	NAP1L4	-0.16	4.35E-02
Gene	IL3RA	-0.16	3.39E-03
Gene	PRDM13	-0.15	7.20E-03
Gene	PCYT1B	-0.15	2.35E-02
Gene	MEPE	-0.15	1.80E-02
Gene	LOC100129624	-0.15	1.65E-02
Gene	CYP11B2	-0.15	3.17E-02
Gene	ADAMTSL4	-0.15	1.91E-02
Gene	SOX14	-0.15	6.27E-03
Gene	RYR2	-0.15	6.94E-03
Gene	HCG4P6	-0.15	3.10E-03
Gene	DXS542	-0.15	2.67E-02
Gene	EDG5	-0.15	2.58E-02
Gene	TBL1Y	-0.15	2.45E-02
Gene	MAP1A	-0.15	1.27E-02
Gene	ZNF550	-0.15	2.58E-02
Gene	LDB1	-0.15	3.52E-02
Gene	SEMA3F	-0.15	1.71E-02
Gene	MYF6	-0.15	4.59E-02
Gene	ERCC6L	-0.14	5.68E-03
Gene	CHRNA9	-0.14	1.82E-03
Gene	TLX3	-0.14	4.20E-02
Gene	ACTA1	-0.14	1.02E-02
Gene	LOC346329	-0.14	6.20E-03
Gene	FRAP1	-0.14	6.89E-03
Gene	FKSG2	-0.14	5.20E-03
Gene	RP5-886K2.1	-0.14	2.15E-02
Gene	LOC728215	-0.14	3.28E-02
Gene	CDS1	-0.14	3.63E-02
Gene	FGF3	-0.14	2.03E-02
Gene	MMP13	-0.14	2.21E-02
Gene	RET	-0.14	1.14E-04
Gene	AKAP6	-0.14	5.82E-03
Gene	SMPD2	-0.14	9.63E-03

Gene	NPHP4	-0.14	4.31E-02
Gene	SLC4A8	-0.14	3.91E-03
Gene	WDR76	-0.14	3.39E-02
Gene	IVL	-0.14	3.18E-02
Gene	MYT1L	-0.14	2.04E-02
Gene	HIC1	-0.14	3.89E-02
Gene	NACA2	-0.14	3.04E-02
Gene	CABP2	-0.14	1.49E-02
Gene	LOC100131298	-0.14	5.99E-03
Gene	TCL6	-0.13	2.96E-02
Gene	WDR59	-0.13	4.04E-02
Gene	TIMP4	-0.13	4.07E-02
Gene	CD22	-0.13	1.03E-02
Gene	TNP2	-0.13	4.07E-02
Gene	PDE5A	-0.13	5.09E-03
Gene	TPPP	-0.13	4.50E-02
Gene	PCDHA3	-0.13	2.80E-02
Gene	HOXA10	-0.13	1.96E-02
Gene	SLAMF1	-0.13	1.48E-02
Gene	ATP11A	-0.13	1.92E-02
Gene	ANP32C	-0.13	4.52E-02
Gene	TRY6	-0.13	8.76E-03
Gene	POLR2A	-0.13	2.06E-03
Gene	LUZP2	-0.13	1.46E-02
Gene	C3orf52	-0.13	7.80E-03
Gene	NRGN	-0.13	3.88E-02
Gene	FBXO4	-0.13	1.17E-02
Gene	IFNA8	-0.13	9.01E-04
Gene	FGF18	-0.13	4.05E-02
Gene	IL1F5	-0.13	4.39E-03
Gene	MTHFR	-0.13	2.84E-02
Gene	WISP3	-0.13	3.14E-02
Gene	POU2F3	-0.13	1.67E-02
Gene	EYA1	-0.13	3.85E-02
Gene	ZNF16	-0.13	4.47E-02
Gene	SOX3	-0.13	1.13E-02
Gene	HMGA1	-0.13	4.66E-02
Gene	SCAND2	-0.13	3.03E-02
Gene	RNF17	-0.13	7.69E-03
Gene	KLK10	-0.13	2.55E-02
Gene	DEFA5	-0.13	3.25E-02
Gene	UTY	-0.13	1.03E-03
Gene	RP13-401N8.2	-0.13	3.62E-02
Gene	NOX3	-0.13	5.81E-03
Gene	KLHL4	-0.13	2.35E-02
Gene	HTR5A	-0.13	2.78E-02
Gene	SHOX2	-0.13	1.68E-02
Gene	HIF3A	-0.12	4.77E-02
Gene	CNGB1	-0.12	8.53E-03
Gene	INSL6	-0.12	3.41E-02
Gene	FAM12A	-0.12	2.20E-02
Gene	MT4	-0.12	1.15E-02
Gene	NPPC	-0.12	2.41E-03
Gene	HS6ST1	-0.12	1.44E-02
Gene	FLJ12616	-0.12	4.81E-02
Gene	MYH7	-0.12	5.73E-03
Gene	HTR1A	-0.12	1.91E-02
Gene	GLP2R	-0.12	4.39E-02
Gene	MTMR8	-0.12	1.15E-02
Gene	PRDM8	-0.12	1.73E-02
Gene	CACNA1B	-0.12	3.24E-02
Gene	LOC389768	-0.12	3.33E-02

Gene	CCDC28B	-0.12	2.47E-02
Gene	LOC644213	-0.12	1.72E-02
Gene	LOC159110	-0.12	4.61E-02
Gene	PYY	-0.12	1.77E-02
Gene	HCRTR1	-0.12	1.96E-02
Gene	BRF1	-0.12	1.13E-02
Gene	GPC1	-0.12	1.35E-02
Gene	SLC13A1	-0.12	4.33E-02
Gene	DAZL	-0.12	2.54E-04
Gene	HOXD12	-0.12	9.71E-03
Gene	LOC653198	-0.12	6.26E-03
Gene	CAMK1G	-0.12	4.22E-02
Gene	NEIL3	-0.12	8.45E-03
Gene	ABP1	-0.12	3.56E-02
Gene	SAA3P	-0.12	2.31E-02
Gene	SLC6A2	-0.12	4.47E-02
Gene	OTOF	-0.11	3.56E-02
Gene	RHAG	-0.11	2.18E-02
Gene	ULK4	-0.11	2.17E-02
Gene	TFAP2A	-0.11	3.22E-02
Gene	BFSP1	-0.11	1.26E-02
Gene	RS1	-0.11	1.31E-03
Gene	GRIK1	-0.11	7.15E-03
Gene	AGPAT4	-0.11	2.87E-03
Gene	RYR3	-0.11	1.26E-02
Gene	TIGD6	-0.11	4.36E-02
Gene	EDA	-0.11	2.71E-02
Gene	BFSP2	-0.11	4.15E-02
Gene	TUBB4	-0.11	1.41E-02
Gene	NRCAM	-0.11	3.54E-02
Gene	MOBP	-0.11	1.64E-02
Gene	HIST1H3D	-0.11	1.52E-02
Gene	ERBB4	-0.11	4.95E-02
Gene	GSC2	-0.11	1.37E-02
Gene	PSCA	-0.11	3.58E-02
Gene	ZNF155	-0.11	3.84E-02
Gene	HTN3	-0.11	1.56E-02
Gene	C1orf46	-0.11	1.68E-02
Gene	B3GALT5	-0.11	4.70E-03
Gene	KCNIP4	-0.11	6.23E-03
Gene	KLK13	-0.11	4.28E-02
Gene	FOXE1	-0.11	2.60E-02
Gene	MATN3	-0.11	4.20E-02
Gene	ARMC9	-0.11	3.06E-02
Gene	CEACAM7	-0.11	1.64E-02
Gene	TNFSF9	-0.10	2.45E-02
Gene	LOC1720	-0.10	1.18E-02
Gene	TUBB1	-0.10	1.80E-02
Gene	CNGA3	-0.10	3.58E-02
Gene	PPFIA4	-0.10	3.99E-02
Gene	LRP8	-0.10	2.80E-02
Gene	RBP3	-0.10	3.43E-02
Gene	LOC400084	-0.10	2.06E-02
Gene	ATP2C2	-0.10	3.67E-02
Gene	CTAG2	-0.10	3.34E-02
Gene	OR2B2	-0.10	1.71E-02
Gene	KCNAB1	-0.10	3.71E-02
Gene	ATP2A1	-0.10	3.18E-02
Gene	HIST1H1B	-0.10	2.09E-02
Gene	CHRNA7	-0.10	4.85E-02
Gene	PPP1R2P9	-0.10	1.14E-02
Gene	LMTK2	-0.10	1.03E-02

Gene	KRT32	-0.10	3.72E-02
Gene	VPRBP	-0.10	6.01E-03
Gene	RASSF8	-0.10	3.08E-02
Gene	FLJ21511	-0.10	2.13E-02
Gene	SNCA	-0.10	4.36E-02
Gene	TCHH	-0.10	4.51E-02
Gene	SLC26A3	-0.10	2.44E-02
Gene	TBX1	-0.10	2.60E-02
Gene	CSF3	-0.10	3.36E-02
Gene	TNFRSF4	-0.10	3.90E-02
Gene	CIB2	-0.10	1.66E-02
Gene	HTR3A	-0.09	3.82E-02
Gene	INSL3	-0.09	3.55E-02
Gene	FAM130A2	-0.09	1.78E-02
Gene	LL22NC03-75B3.6	-0.09	3.27E-02
Gene	APBB1	-0.09	3.28E-02
Gene	RARB	-0.09	3.57E-02
Gene	GPR110	-0.09	1.85E-02
Gene	MAPK4	-0.09	4.69E-02
Gene	PDE1C	-0.09	1.59E-02
Gene	OR2H2	-0.09	1.94E-02
Gene	TFAP2B	-0.09	2.18E-02
Gene	RGS12	-0.09	1.69E-02
Gene	RICH2	-0.09	4.69E-02
Gene	ELA2	-0.09	3.42E-02
Gene	ZNF480	-0.09	1.36E-02
Gene	FABP7	-0.09	1.84E-02
Gene	KCNQ2	-0.09	2.25E-02
Gene	PCDH1	-0.09	2.69E-02
Gene	ALPI	-0.09	4.68E-02
Gene	PCDHGA11	-0.09	1.96E-02
Gene	MCFD2L	-0.09	2.48E-02
Gene	SIX2	-0.09	4.89E-02
Gene	TAL1	-0.09	4.52E-02
Gene	MPO	-0.08	2.71E-02
Gene	ELA2B	-0.08	4.33E-02
Gene	AMH	-0.08	1.16E-02
Gene	PAPPA	-0.08	2.12E-02
Gene	SLC8A1	-0.08	3.47E-02
Gene	CSH1	-0.08	3.75E-02
Gene	DUSP26	-0.08	4.72E-02
Gene	GJA3	-0.08	2.40E-02
Gene	TSPAN2	-0.08	3.85E-02
Gene	MYH6	-0.08	3.03E-03
Gene	GAP43	-0.08	5.49E-03
Gene	ABCB6	-0.08	8.24E-03
Gene	SSX2	-0.08	1.84E-02
Gene	RAB6B	-0.08	1.80E-02
Gene	TNFAIP6	-0.08	4.41E-02
Gene	CRYGC	-0.08	4.14E-02
Gene	ARHGAP28	-0.08	2.85E-02
Gene	CNPY4	-0.08	4.86E-02
Gene	MC2R	-0.08	2.69E-02
Gene	NHLH2	-0.08	1.05E-02
Gene	SERPINB3	-0.08	4.50E-02
Gene	BCMO1	-0.08	1.01E-02
Gene	MAG	-0.08	3.08E-02
Gene	CCDC132	-0.08	1.00E-02
Gene	SPINLW1	-0.08	2.08E-02
Gene	PLK4	-0.08	2.69E-02
Gene	GH2	-0.08	3.79E-02
Gene	SOX11	-0.08	8.13E-03

Gene	LILRA5	-0.08	1.62E-02
Gene	MFAP5	-0.08	9.22E-03
Gene	HBEGF	-0.08	1.33E-02
Gene	SERPINB13	-0.08	8.66E-03
Gene	TACR1	-0.08	4.11E-02
Gene	TKTL1	-0.08	3.80E-02
Gene	ENTPD2	-0.08	4.92E-02
Gene	SSX4	-0.08	2.76E-02
Gene	PAPOLB	-0.08	4.97E-03
Gene	KRT37	-0.07	1.98E-02
Gene	AANAT	-0.07	1.02E-02
Gene	HOXB9	-0.07	2.32E-02
Gene	MS4A2	-0.07	3.88E-02
Gene	KIAA1661	-0.07	1.53E-02
Gene	OR2W1	-0.07	3.37E-02
Gene	ELA1	-0.07	2.34E-02
Gene	KHDC1	-0.07	2.95E-02
Gene	FOXD4L1	-0.07	2.98E-02
Gene	TMEM151B	-0.07	1.30E-02
Gene	ASTN1	-0.07	3.52E-02
Gene	IL4	-0.07	5.96E-03
Gene	POU4F1	-0.07	2.88E-02
Gene	LOC145899	-0.07	2.67E-02
Gene	CXCR5	-0.07	2.14E-02
Gene	SOX2	-0.07	2.95E-02
Gene	ZNF614	-0.07	2.59E-02
Gene	GP5	-0.07	1.93E-02
Gene	ADCY2	-0.07	1.76E-02
Gene	LHX1	-0.07	5.23E-03
Gene	ACTR8	-0.07	3.76E-02
Gene	SLC7A11	-0.07	4.32E-02
Gene	GPR63	-0.07	2.70E-02
Gene	STC2	-0.07	4.19E-02
Gene	SPAM1	-0.06	3.63E-02
Gene	KIAA1622	-0.06	4.74E-02
Gene	SRD5A3	-0.06	2.62E-02
Gene	AP4S1	-0.06	1.31E-02
Gene	ZNF41	-0.06	4.23E-02
Gene	PTHLH	-0.06	4.62E-02
Gene	VPREB1	-0.06	3.98E-02
Gene	GPR161	-0.06	4.50E-02
Gene	HTR7	-0.06	2.20E-02
Gene	MKRN3	-0.06	2.56E-02
Gene	OR11A1	-0.06	3.89E-02
Gene	PWWP2A	-0.06	1.16E-02
Gene	CLEC16A	-0.06	2.91E-02
Gene	PBOV1	-0.06	2.51E-02
Gene	HOXD3	-0.06	4.95E-02
Gene	GRIA1	-0.05	4.91E-02
Gene	PITX2	-0.05	4.32E-02
Gene	KITLG	-0.04	2.47E-02
Gene	HOXB6	-0.04	4.68E-02
Gene	KCNJ4	-0.04	2.19E-02
Gene	NEK2	-0.04	2.80E-02
Gene	HIST1H2AE	-0.04	3.05E-02
Gene	FCAR	-0.03	4.33E-02
Gene	TPTE	-0.03	2.47E-02
Gene	ZNF250	-0.03	2.82E-02
Gene	ATXN3L	-0.01	4.73E-02
Gene	AQR	0.01	3.54E-02
Gene	ZFR	0.04	1.59E-02
Gene	TOMM34	0.06	4.74E-02

Gene	UQCRB	0.07	2.18E-02
Gene	PWP1	0.07	2.32E-02
Gene	ALG13	0.07	3.12E-02
Gene	SMPD1	0.07	4.34E-02
Gene	CPM	0.08	2.68E-02
Gene	WNK1	0.08	3.40E-02
Gene	ACOX1	0.08	3.78E-02
Gene	MAX	0.08	3.14E-02
Gene	RBBP8	0.09	4.51E-02
Gene	PMS2L3	0.10	4.43E-02
Gene	RBMX	0.10	4.67E-02
Gene	ZBTB1	0.10	4.67E-02
Gene	MEMO1	0.10	3.08E-02
Gene	NCBP2	0.10	3.10E-02
Gene	ATP2B4	0.11	3.10E-02
Gene	ROCK1	0.11	3.51E-02
Gene	PRPF40A	0.11	4.82E-02
Gene	SPAG9	0.11	2.63E-02
Gene	INTS7	0.11	4.12E-03
Gene	SAP18	0.11	4.38E-02
Gene	PSMB2	0.11	1.59E-02
Gene	SMAD4	0.11	6.89E-03
Gene	PDCD4	0.11	2.60E-02
Gene	ARIH1	0.12	7.55E-03
Gene	TWF1	0.12	2.51E-02
Gene	TMEM43	0.12	3.87E-02
Gene	TEX10	0.12	4.08E-02
Gene	CBFB	0.12	3.37E-02
Gene	TRRAP	0.12	4.79E-02
Gene	KIDINS220	0.12	1.81E-02
Gene	GNAQ	0.12	3.03E-03
Gene	SMARCE1	0.12	4.49E-02
Gene	C5orf22	0.13	4.28E-02
Gene	LIMS1	0.13	2.60E-02
Gene	ATP2B1	0.13	1.30E-02
Gene	OGT	0.13	4.94E-02
Gene	CADM1	0.13	2.52E-02
Gene	ELMO2	0.13	4.05E-02
Gene	BICD2	0.13	9.93E-03
Gene	FKSG49	0.13	2.04E-02
Gene	MIA3	0.13	4.75E-02
Gene	ITM2B	0.13	4.89E-02
Gene	SOS2	0.13	5.71E-04
Gene	FETUB	0.13	4.08E-02
Gene	CALM1	0.13	2.51E-02
Gene	H3F3A	0.13	1.90E-02
Gene	KIAA0157	0.13	4.13E-03
Gene	CDK4	0.14	4.55E-02
Gene	SMEK1	0.14	1.54E-03
Gene	MTIF2	0.14	3.57E-02
Gene	ATP6AP2	0.14	2.00E-02
Gene	RAB6IP1	0.14	3.01E-02
Gene	PCBP2	0.14	9.59E-03
Gene	PPFIA1	0.14	5.74E-03
Gene	ERMP1	0.14	8.30E-03
Gene	VPS13A	0.14	9.70E-03
Gene	RAB14	0.14	4.13E-02
Gene	RAB2A	0.15	1.18E-02
Gene	CALCRL	0.15	4.30E-02
Gene	HSPA9	0.15	4.18E-02
Gene	SLC4A4	0.15	4.73E-02
Gene	BMPR2	0.15	3.76E-02

Gene	WAPAL	0.15	2.00E-02
Gene	NUBP1	0.15	4.00E-02
Gene	KIAA0494	0.15	2.76E-02
Gene	H3F3B	0.15	1.54E-02
Gene	BCLAF1	0.15	3.73E-02
Gene	CEACAM1	0.15	3.08E-02
Gene	ARFGEF1	0.15	3.48E-02
Gene	JARID1C	0.15	9.36E-03
Gene	VCP	0.16	2.11E-02
Gene	STX3	0.16	1.13E-02
Gene	GUCY1B3	0.16	1.14E-02
Gene	FEM1C	0.16	3.73E-02
Gene	RAB11A	0.16	3.20E-02
Gene	SLC30A5	0.16	3.82E-02
Gene	EIF4ENIF1	0.16	2.04E-02
Gene	METTL5	0.16	1.88E-02
Gene	STRN4	0.16	6.78E-03
Gene	MBNL1	0.16	1.83E-03
Gene	KRAS	0.16	2.61E-02
Gene	ELF1	0.16	1.67E-02
Gene	LSM14A	0.17	2.75E-02
Gene	RNF10	0.17	2.24E-02
Gene	MAP4K5	0.17	3.57E-02
Gene	FCGR2A	0.17	3.04E-02
Gene	HNRNPC	0.17	5.79E-03
Gene	ECD	0.17	2.84E-02
Gene	HNRNPR	0.17	2.25E-02
Gene	STAU2	0.17	4.24E-02
Gene	CWF19L1	0.17	2.22E-02
Gene	RABGAP1L	0.17	4.64E-02
Gene	ZNF264	0.18	3.29E-02
Gene	ARPP-19	0.18	3.99E-02
Gene	TMEM131	0.18	2.56E-02
Gene	ATP1B1	0.18	2.21E-02
Gene	HNRPA3	0.18	4.95E-02
Gene	TMEM34	0.18	4.46E-02
Gene	MEGF9	0.18	1.43E-02
Gene	AMD1	0.18	1.90E-02
Gene	NAGA	0.18	4.01E-02
Gene	CENTD3	0.18	2.92E-02
Gene	DAG1	0.18	3.17E-03
Gene	RY1	0.18	2.99E-02
Gene	ARFIP1	0.18	3.10E-02
Gene	RPS6	0.18	1.65E-03
Gene	C1orf218	0.19	4.63E-02
Gene	LASS6	0.19	3.35E-02
Gene	ELAVL1	0.19	3.27E-02
Gene	CDK9	0.19	3.07E-02
Gene	DIMT1L	0.19	2.24E-03
Gene	ZFX	0.19	7.20E-04
Gene	SF3B1	0.19	2.21E-02
Gene	WAC	0.20	6.75E-04
Gene	ADNP	0.20	3.69E-03
Gene	ACOT9	0.20	2.43E-02
Gene	SMC1A	0.20	2.16E-02
Gene	IGF2R	0.20	4.13E-02
Gene	PTP4A2	0.20	1.51E-02
Gene	VCL	0.20	4.23E-02
Gene	SMC3	0.21	3.82E-02
Gene	APLP2	0.21	9.24E-03
Gene	ZNF12	0.21	2.69E-02
Gene	NR5A2	0.21	1.99E-02

Gene	UBE2B	0.21	1.15E-02
Gene	SKP1	0.21	3.31E-02
Gene	EID1	0.21	2.94E-02
Gene	SFRS1	0.21	3.19E-02
Gene	AGTR1	0.21	2.48E-02
Gene	RAB1B	0.21	1.31E-02
Gene	ATP13A3	0.21	2.53E-02
Gene	CUL4B	0.21	4.24E-02
Gene	GMDS	0.21	6.12E-03
Gene	POLE3	0.21	4.44E-02
Gene	ZNF24	0.21	3.28E-03
Gene	CCDC91	0.21	2.72E-02
Gene	TXNDC13	0.21	9.87E-03
Gene	WDR1	0.21	4.60E-02
Gene	ARHGAP12	0.21	1.67E-02
Gene	TXN	0.21	3.97E-03
Gene	CTNNA1	0.22	3.61E-03
Gene	SRP72	0.22	4.52E-02
Gene	KIAA0256	0.22	1.94E-02
Gene	EPAS1	0.22	3.07E-02
Gene	C7orf49	0.22	3.42E-02
Gene	PDLIM5	0.22	3.57E-03
Gene	MACF1	0.22	8.00E-03
Gene	LRRC19	0.23	1.18E-02
Gene	COPS7A	0.23	1.84E-02
Gene	CLIC4	0.23	3.78E-03
Gene	SPEN	0.23	3.01E-02
Gene	ENC1	0.23	4.99E-02
Gene	CSNK1A1	0.23	1.30E-03
Gene	EPB41L2	0.23	4.76E-02
Gene	TTC3	0.23	3.19E-02
Gene	COPE	0.23	4.56E-02
Gene	TCEAL1	0.23	4.81E-02
Gene	TKT	0.23	4.97E-02
Gene	HSPA4	0.23	3.15E-02
Gene	KIF5B	0.23	2.17E-02
Gene	NIPBL	0.23	1.84E-03
Gene	COLEC10	0.24	1.44E-02
Gene	TOR1AIP1	0.24	5.99E-03
Gene	AP3B1	0.24	1.49E-02
Gene	PSMF1	0.24	4.61E-04
Gene	TPD52L1	0.24	1.89E-02
Gene	C14orf108	0.24	3.12E-02
Gene	THAP10	0.24	7.85E-03
Gene	WBP11	0.24	1.62E-02
Gene	LSM12	0.24	3.97E-03
Gene	RFC5	0.24	8.42E-04
Gene	TCF21	0.24	2.07E-02
Gene	PSEN1	0.24	2.06E-02
Gene	PTENP1	0.24	4.92E-02
Gene	CTBP1	0.24	2.66E-02
Gene	TM9SF4	0.24	1.07E-02
Gene	MRPS30	0.24	3.55E-02
Gene	ANKRD17	0.24	3.78E-02
Gene	ADD3	0.24	8.46E-03
Gene	FNDC3A	0.24	1.48E-02
Gene	CYP39A1	0.24	1.99E-02
Gene	PAPOLA	0.25	3.59E-02
Gene	DYNLRB1	0.25	8.69E-03
Gene	PITRM1	0.25	1.86E-02
Gene	CTCF	0.25	3.34E-02
Gene	NOTCH2	0.25	4.06E-03

Gene	STS	0.25	3.58E-03
Gene	H2AFV	0.25	1.13E-02
Gene	RDX	0.25	1.99E-02
Gene	FBXL14	0.25	2.65E-02
Gene	ZNF195	0.25	1.37E-02
Gene	DOLK	0.25	2.30E-02
Gene	STAT4	0.25	2.69E-02
Gene	SMARCA1	0.25	7.72E-03
Gene	SCYL2	0.26	5.89E-04
Gene	C20orf19	0.26	2.42E-02
Gene	BUB3	0.26	9.30E-03
Gene	AZIN1	0.26	3.37E-02
Gene	SPIN1	0.26	3.24E-03
Gene	NUP153	0.26	3.65E-02
Gene	ANP32A	0.26	3.70E-02
Gene	PKP4	0.26	2.81E-02
Gene	SUB1	0.26	3.28E-02
Gene	PICALM	0.26	7.63E-03
Gene	CLCN3	0.26	1.43E-02
Gene	C6orf66	0.26	3.65E-02
Gene	SUCLG2	0.26	8.06E-03
Gene	COPS5	0.26	2.20E-02
Gene	UCHL5	0.26	1.82E-02
Gene	CPNE3	0.26	7.25E-03
Gene	PEX19	0.26	3.28E-02
Gene	NARG1	0.26	4.84E-02
Gene	LYPLA1	0.26	4.92E-02
Gene	ALCAM	0.26	2.28E-02
Gene	NBN	0.27	7.28E-03
Gene	PSMD12	0.27	2.88E-02
Gene	CYP3A7	0.27	1.85E-02
Gene	NLK	0.27	4.94E-04
Gene	SNRPB	0.27	1.07E-02
Gene	HSPE1	0.27	2.74E-02
Gene	TRAK2	0.27	1.53E-02
Gene	EGLN1	0.27	1.20E-02
Gene	TIE1	0.27	4.00E-02
Gene	HIPK1	0.27	5.56E-03
Gene	LPHN2	0.27	3.40E-02
Gene	RAB9A	0.27	1.39E-02
Gene	UBE2V1	0.28	3.72E-02
Gene	RNF34	0.28	4.36E-02
Gene	UFD1L	0.28	3.82E-02
Gene	PTPN11	0.28	7.46E-03
Gene	TF	0.28	5.23E-03
Gene	NAIP	0.28	9.65E-03
Gene	TSTA3	0.28	5.64E-03
Gene	SNX4	0.29	1.11E-02
Gene	VASP	0.29	7.63E-03
Gene	TBL1X	0.29	1.55E-02
Gene	PCBP1	0.29	3.23E-02
Gene	USP9X	0.29	1.08E-02
Gene	KIAA1033	0.29	6.67E-03
Gene	SLC22A18	0.29	1.04E-02
Gene	MYH10	0.29	1.61E-03
Gene	POGK	0.29	1.41E-02
Gene	TEX2	0.30	4.18E-03
Gene	ANXA7	0.30	1.67E-02
Gene	IPO7	0.30	6.88E-03
Gene	PREPL	0.30	4.43E-02
Gene	STX17	0.30	4.87E-03
Gene	RCOR1	0.30	1.57E-02

Gene	TRIB2	0.30	4.50E-02
Gene	SGMS1	0.30	1.20E-02
Gene	VEZF1	0.31	1.48E-02
Gene	TRMT11	0.31	4.35E-02
Gene	PGCP	0.31	2.21E-02
Gene	ITGA1	0.31	2.19E-03
Gene	KLHL3	0.31	1.12E-02
Gene	ZNF364	0.31	5.42E-03
Gene	TTRAP	0.31	4.59E-02
Gene	ARF6	0.31	2.44E-02
Gene	NARG2	0.31	2.67E-02
Gene	RNF14	0.31	3.37E-02
Gene	CSNK2A1	0.31	6.90E-04
Gene	MEIS3P1	0.31	2.03E-02
Gene	ARHGAP15	0.31	4.03E-02
Gene	MRPL18	0.31	1.24E-02
Gene	KPNA1	0.31	2.71E-03
Gene	AGPS	0.32	2.15E-02
Gene	RRAS2	0.32	1.16E-02
Gene	RPS6KA3	0.32	8.21E-03
Gene	SPTBN1	0.32	3.67E-05
Gene	TMEM135	0.32	2.39E-02
Gene	PPP4C	0.32	2.27E-02
Gene	STAM	0.32	1.56E-02
Gene	AGA	0.33	8.01E-03
Gene	SEC22B	0.33	9.71E-03
Gene	ETFDH	0.33	4.41E-02
Gene	ITCH	0.33	1.28E-02
Gene	GPR137B	0.33	7.51E-03
Gene	LEPROTL1	0.33	1.65E-02
Gene	DSTN	0.33	1.29E-03
Gene	XPNPEP1	0.33	8.22E-03
Gene	CALD1	0.33	5.40E-04
Gene	CNIH	0.33	3.84E-03
Gene	RPS4X	0.33	2.16E-04
Gene	C6orf62	0.33	6.51E-03
Gene	PCOLCE	0.33	3.16E-02
Gene	ACTR3	0.34	3.91E-03
Gene	GLB1	0.34	4.60E-02
Gene	FAM3C	0.34	2.08E-02
Gene	CLN5	0.34	3.22E-02
Gene	MOCS2	0.34	4.45E-02
Gene	VDAC1	0.34	3.43E-03
Gene	PECR	0.34	2.05E-02
Gene	ZBTB38	0.34	2.00E-02
Gene	LYN	0.35	3.92E-02
Gene	ZNF26	0.35	3.80E-02
Gene	FUSIP1	0.35	1.23E-03
Gene	PRRC1	0.35	4.20E-02
Gene	RP11-74E24.2	0.35	7.90E-03
Gene	PTS	0.35	1.66E-02
Gene	ABCE1	0.36	9.04E-03
Gene	NMD3	0.36	1.46E-02
Gene	ATP6V1A	0.36	1.93E-02
Gene	UBE2D3	0.36	1.07E-02
Gene	ARHGAP5	0.36	2.07E-02
Gene	PAPSS1	0.37	4.38E-02
Gene	DCTN4	0.37	1.32E-03
Gene	CD164	0.37	7.31E-03
Gene	PRKAR1A	0.37	2.79E-02
Gene	CLINT1	0.37	1.80E-03
Gene	PPP3CA	0.37	2.93E-03

Gene	HSPD1	0.37	3.28E-02
Gene	NNT	0.37	1.04E-02
Gene	COL4A3BP	0.37	1.49E-02
Gene	HADHA	0.37	7.05E-03
Gene	UBE2G1	0.38	1.75E-02
Gene	MTUS1	0.38	1.57E-03
Gene	ACSS3	0.38	3.27E-02
Gene	NTAN1	0.38	2.14E-02
Gene	DCN	0.38	4.34E-02
Gene	ADSS	0.38	8.21E-03
Gene	TRAPPC2	0.38	4.02E-03
Gene	EDEM3	0.38	1.09E-02
Gene	GLRX2	0.39	1.07E-02
Gene	LOC643246	0.39	3.44E-02
Gene	RAD21	0.39	2.48E-03
Gene	PJA2	0.39	3.76E-02
Gene	CDK7	0.39	1.47E-02
Gene	ECHDC1	0.40	3.90E-02
Gene	SPRY2	0.40	2.57E-02
Gene	ARF1	0.40	1.39E-03
Gene	TUG1	0.40	3.49E-03
Gene	FAM60A	0.40	3.31E-02
Gene	FBN1	0.41	4.56E-02
Gene	MAP2K1IP1	0.41	4.77E-02
Gene	CHD1	0.41	1.75E-02
Gene	TPRKB	0.41	9.33E-03
Gene	COMMD10	0.41	3.84E-02
Gene	CD46	0.41	3.56E-03
Gene	UGCG	0.41	2.42E-03
Gene	SLC35A5	0.42	6.84E-03
Gene	GNB1	0.42	1.57E-02
Gene	IL15RA	0.42	1.06E-02
Gene	DCTD	0.43	2.93E-02
Gene	SLC3A1	0.43	2.89E-02
Gene	IFIT2	0.43	9.69E-04
Gene	C4orf16	0.43	2.45E-02
Gene	MBNL2	0.43	3.09E-04
Gene	OSBPL8	0.43	1.50E-02
Gene	MRPS15	0.43	2.92E-03
Gene	C1QBP	0.44	4.69E-02
Gene	SPARCL1	0.44	1.81E-02
Gene	CLDND1	0.44	4.27E-03
Gene	ENPEP	0.44	4.17E-02
Gene	SH3BGRL	0.45	2.15E-02
Gene	ARL4C	0.45	1.97E-02
Gene	GTF2B	0.45	3.42E-02
Gene	ARPC3	0.46	7.02E-03
Gene	LOC390183	0.46	1.00E-03
Gene	DDX3X	0.47	9.04E-04
Gene	PPP2R5E	0.47	1.16E-02
Gene	LRRC32	0.48	2.04E-02
Gene	SCARB2	0.48	8.03E-04
Gene	PNPLA4	0.48	1.18E-03
Gene	PFN2	0.49	1.50E-02
Gene	TMEM14B	0.49	4.98E-02
Gene	OSTF1	0.49	2.56E-02
Gene	GK3P	0.49	1.08E-02
Gene	ARL6IP5	0.49	2.40E-04
Gene	CCT2	0.49	2.00E-02
Gene	TMEM106B	0.49	3.62E-03
Gene	HDHD1A	0.50	2.02E-04
Gene	TRAM1	0.50	7.11E-03

Gene	RBM16	0.50	2.28E-02
Gene	TXNDC1	0.50	1.24E-02
Gene	KLRB1	0.51	1.55E-02
Gene	ACYP2	0.51	1.66E-02
Gene	TPM1	0.51	3.61E-02
Gene	YWHAZ	0.52	9.82E-03
Gene	PRKACB	0.52	2.47E-03
Gene	CANX	0.52	9.05E-03
Gene	EIF5A	0.53	2.82E-03
Gene	CNN3	0.53	1.39E-02
Gene	WWC2	0.54	1.82E-03
Gene	GSR	0.54	1.84E-04
Gene	KDELRL1	0.54	3.10E-02
Gene	EML4	0.54	7.51E-03
Gene	RBBP4	0.54	3.10E-02
Gene	IGJ	0.54	1.80E-02
Gene	CDR2	0.54	6.27E-03
Gene	USP25	0.54	2.30E-02
Gene	SYPL1	0.57	2.28E-02
Gene	NRIP1	0.57	2.40E-03
Gene	UTX	0.58	1.72E-06
Gene	ARMC1	0.59	1.06E-02
Gene	VIM	0.59	3.00E-02
Gene	CAV1	0.59	2.70E-02
Gene	EDNRB	0.59	3.41E-02
Gene	OSBPL11	0.60	3.67E-03
Gene	GREM2	0.61	8.28E-03
Gene	ACTR2	0.62	7.35E-04
Gene	BZW1L1	0.62	3.57E-02
Gene	ACSL4	0.62	5.66E-03
Gene	LOC389168	0.62	4.31E-03
Gene	ILF2	0.64	3.14E-02
Gene	MAD1L1	0.64	3.57E-03
Gene	RGS5	0.64	3.17E-02
Gene	S100A10	0.65	9.57E-04
Gene	GYG2	0.66	1.24E-03
Gene	CRIM1	0.68	2.95E-02
Gene	CSTB	0.69	2.30E-03
Gene	SLC17A3	0.69	2.28E-03
Gene	COL5A2	0.70	2.03E-02
Gene	ARSE	0.70	2.35E-03
Gene	LEPR	0.71	2.47E-03
Gene	CLDN1	0.72	6.42E-03
Gene	EIF1AX	0.73	2.52E-06
Gene	PERP	0.75	4.55E-03
Gene	SHBG	0.76	7.23E-03
Gene	CYBA	0.77	3.99E-02
Gene	MYL9	0.78	3.64E-02
Gene	C14orf101	0.78	3.34E-04
Gene	LAMB1	0.78	4.69E-02
Gene	FHL2	0.81	1.05E-02
Gene	GPC3	0.85	4.89E-02
Gene	COL4A1	0.86	2.83E-02
Gene	GSTM3	0.89	4.67E-03
Gene	KCTD12	0.94	4.56E-02
Gene	TIMP1	0.95	4.12E-02
Gene	MGP	0.97	2.87E-02
Gene	YWHAH	0.97	1.65E-03
Gene	PTPLAD1	0.98	2.58E-03
Gene	VIL1	0.99	2.87E-02
Gene	COL6A3	1.03	2.10E-02
Gene	FBLN5	1.07	4.12E-02

Gene	EIF2S3	1.11	8.18E-04
Gene	ENPP2	1.27	1.23E-04
Gene	PZP	2.03	1.30E-02
Gene	PLA2G2A	2.18	2.06E-02
Gene	XIST	5.57	1.72E-07
microRNA	miRNA-342	-0.29	4.00E-02
microRNA	miRNA-99b	0.34	4.00E-02
microRNA	miRNA-10b	0.46	2.00E-02
microRNA	miRNA-26a	0.46	1.00E-02
microRNA	miRNA-125b	0.57	2.00E-02
microRNA	miRNA-325	0.72	5.00E-02
microRNA	miR-321	0.81	1.00E-03
Metabolites (known)	adenylosuccinate	-3.55	1.17E-02
Metabolites (known)	pyroglutamine*	-2.16	5.29E-08
Metabolites (known)	7-beta-hydroxycholesterol	-1.53	5.80E-03
Metabolites (known)	guanosine	-1.24	1.20E-04
Metabolites (known)	deoxycarnitine	-1.00	2.91E-05
Metabolites (known)	tauroolithocholate 3-sulfate	-0.96	2.88E-02
Metabolites (known)	1-palmitoylglycerophosphoinositol*	-0.93	4.93E-03
Metabolites (known)	taurochenodeoxycholate	-0.92	1.49E-03
Metabolites (known)	7-alpha-hydroxycholesterol	-0.88	1.23E-02
Metabolites (known)	1-oleoylglycerophosphoinositol*	-0.83	8.99E-03
Metabolites (known)	taurocholate	-0.70	1.96E-02
Metabolites (known)	N-acetylmethionine	-0.69	1.37E-03
Metabolites (known)	adenosine 3'-monophosphate (3'-AMP)	-0.69	1.93E-03
Metabolites (known)	cholate	-0.67	4.63E-02
Metabolites (known)	glycochenodeoxycholate	-0.65	1.06E-02
Metabolites (known)	1-methylimidazoleacetate	-0.63	5.60E-03
Metabolites (known)	alpha-hydroxyisovalerate	-0.61	2.74E-02
Metabolites (known)	galacturonate	-0.61	2.83E-03
Metabolites (known)	N-acetylaspartate (NAA)	-0.53	4.98E-03
Metabolites (known)	betaine	-0.52	9.25E-04
Metabolites (known)	myristoleate (14:1n5)	-0.44	1.46E-02
Metabolites (known)	2-hydroxypalmitate	-0.42	9.30E-03
Metabolites (known)	myristate (14:0)	-0.30	3.35E-02
Metabolites (known)	pipecolate	-0.27	2.60E-02
Metabolites (known)	spermidine	-0.23	2.81E-02
Metabolites (known)	caproate (6:0)	-0.22	2.18E-02
Metabolites (known)	C-glycosyltryptophan*	-0.16	4.64E-02
Metabolites (known)	2-hydroxystearate	-0.09	3.15E-02
Metabolites (unknown)	Y-11596	-1.53	1.24E-03
Metabolites (unknown)	Y-13557	-1.50	1.03E-02
Metabolites (unknown)	Y-12850	-1.42	3.70E-02
Metabolites (unknown)	Y-13429	-1.13	6.40E-03
Metabolites (unknown)	Y-14658	-0.97	3.39E-03
Metabolites (unknown)	Y-12627	-0.89	1.36E-02
Metabolites (unknown)	Y-12800	-0.87	2.42E-02
Metabolites (unknown)	Y-11282	-0.76	6.10E-03
Metabolites (unknown)	Y-14626	-0.62	2.79E-02
Metabolites (unknown)	Y-14606	-0.52	2.07E-02
Metabolites (unknown)	VGAHAGEYGAEALER*	-0.40	4.22E-02
Metabolites (unknown)	Y-11341	-0.37	3.88E-02
Metabolites (unknown)	Y-13414	-0.33	4.05E-02
Metabolites (unknown)	Y-11245	-0.26	1.88E-02
Metabolites (unknown)	Y-11303	-0.26	4.65E-02
Metabolites (unknown)	Y-12855	-0.24	3.93E-02
Metabolites (unknown)	Y-14139	-0.10	4.34E-02
Metabolites (unknown)	Y-12100	-0.10	4.45E-02
Metabolites (unknown)	Y-11571	0.94	8.87E-03

Table S4. Upstream regulators identified by IPA with all sex-related genes, metabolites, and miRNAs*.

Upstream Regulator	Activation z-score	p-value	Pathway
			ligand-dependent nuclear receptor
ESR1	5.118	8.94E-10	signaling by GPCR, interleukin receptor SHC signaling
			transcription regulator
HNF4A	3.450	6.86E-06	developmental biology, regulation of beta-cell development
SMARCB1	2.000	7.86E-05	transcription ligand-dependent activation of the ESR1/SP pathway, chromatin organization
MEF2C	-2.061	1.54E-04	MAPK signaling pathway, Immune system
			kinase
FLT1	3.153	6.88E-12	PI3K-Akt signaling pathway, signaling by GPCR
MKNK1	2.714	3.53E-04	MAPK signaling pathway, signaling by GPCR
			enzyme
FN1	2.250	3.17E-08	PI3K-Akt signaling pathway, Immune system

*, p-value < 0.001 (Fisher's exact test) and $|z\text{-score}| \geq 2$ were considered as significant enrichment.

ESR1, estrogen receptor 1

HNF4A, hepatocyte nuclear factor 4, alpha

SMARCB1, SWI/SNF related, matrix associated, actin dependent regulator of chromatin, subfamily b, member 1

MEF2C, myocyte enhancer factor 2C

FLT1, fms-related tyrosine kinase 1 (vascular endothelial growth factor/vascular permeability factor receptor)

MKNK1, MAP kinase interacting serine/threonine kinase 1

FN1, fibronectin 1.

Table S5. Associated networks identified by IPA with all sex-related genes, metabolites and miRNAs.

#	Molecules in Network	Score	# of molecule	Top Diseases and Functions
1	ACTR2, ACTR3, ARPC3, BCLAF1, COPS5, COPS7A, CSNK2A1, CUL4B, EFCAB14, FBXL14, Gsk3, H2AFV, HNRNPR, HTR3A, ILF2, MRPS15, NAP1L4, PKP4, PWP1, RAB11A, Ribosomal 40s subunit, RPS4X, RPS4Y1, S100A10, serotonin receptor, SF3B1, SPIN1, SRSF1, SRSF10, STAU2, TMEM43, VPRBP, WDR76, ZBTB1, ZFR	47	32	Cell cycle, Cell morphology, Cellular assembly and organization
2	20s proteasome, ACOT9, AGPAT4, ARIH1, ARL4C, CBFB, CTNNA1, DNASE1, DUB, GSTM3, IL4, KLHL4, MHC CLASS I (family), NPHP4, PCBP1, PCBP3, PCGF2, PJA2, PREPL, PSMB2, PSMD12, RAB2A, RNF115, SNX4, SPTBN1, TMEM131, TSTA3, UBE2D3, Ubiquitin, UCHL5, USP25, USP9X, USP9Y, XPNPEP1, ZNF195	44	31	Post-Translational modification, Tissue development, Developmental disorder
3	AKAP6 , alcohol group acceptor phosphotransferase, ARMC1 , ATPase, Calcineurin A, Calcineurin protein(s), CALM1, CDK7, CDK9 , Ck2, Calmodulin, CAMK1G, DDX3X, DYNLRB1 , Holo RNA polymerase II, ENTPD2, GAP43, KCNQ2, MYH7, NMD3, MACF1, PICALM, PLA2G2A, PPP3CA, RAB14, RAB6B, VCP, RABGAP1L, RFC5, SAP18, STS, TMEM260, TSPAN2, VPS50, WAC	38	28	Energy production, Nucleic acid metabolism, Small molecule biochemistry
4	Akt, ARAP3, CADM1, COL6A3 , Collagen type VI, CSH1/CSH2 , Gata, guanosine, HIF3A, IRS, KIR3DL1, LDB1, LIMS1, LMO1, LMX1B, MAB21L1, mir-26, MS4A2, N-cor, NBN, NHLH2, NRG, OSTF1, PDLIM5, PRDM8, PTP4A2, Rar, RBBP8, SERCA, T3-TR-RXR, TAL1, TBL1X , thyroid hormone receptor, TKT, TTC3	33	26	Cancer, Hematological Disease, Immunological Disease
5	AP-3, AP3B1, ARHGAP28, ATP6AP2, CELA1, CSTB, DOLK , cyclooxygenase, EDA, elastase, ETS, GSR, IFNA8, Il12 receptor, IL36RN, INA, KCNJ4, LEPROTL1, MYLK3, NfκB (complex), NfκB (family), P glycoprotein, PPP4R4, PPP4R3A, RNF34, RS1, SERPINB3, SLC3A1, UBE2, UBE2B, UBE2G1, UBE2V1, TNFAIP6, taurochenodeoxycholate, VPRES1	33	26	Developmental Disorder, Hereditary Disorder, Ophthalmic Disease
6	ADNP, ADSS, ANKRD17, APC (complex), AZIN1, Cbp/p300, FEM1C, FETUB, Fgf, FGF3, FGF18, Fgfr, HOXB6, HOXB9, KIF5B, Mapk, NUBP1, PAOX, PDE5A, PDGF-AA, POGK, PTS, Sos, SOS2, Sox, SOX3, SOX11, SOX14, SPRY2, TCEAL1, TDP2, TLX3, TRAK2, Wnt, ZNF41	33	26	Tissue Morphology, Connective Tissue Disorders, Developmental Disorder
7	AGTR1, AP1AR, C3orf52, C6orf62, DENND3, DENND1B, DENND5A, ELAVL1, GNRH, GTF2B, GTPase, HACD3, Histone h3, IKK (complex), Metalloprotease, MKRN3, MTOR, MTORC1, NADPH oxidase, PEX19, PLCXD1, Pld, POLR2A, POU2F3, PRRC1, RNA polymerase II, RPS6, SCAF8, TFAP2A, THAP10, TM9SF4, WWC2, XIST, YWHAZ, ZNF264	33	26	Hereditary Disorder, Organismal Injury and Abnormalities, Cancer
8	ABCE1, ADCY, ADRB, ALCAM, AMD1, ANXA7, ARF6, BUB3, ATP6V1A, CDK4, CDR2, CPNE3, Creb, GNAQ, HISTONE, histone deacetylase, Histone h4, Mlc, NDUFAF4, NEK2, OGT, OXT, Pak, PDGF BB, PLC, RBBP4, RCOR1, SMARCE1, SPEN, spermidine, SUCLG2, TBL1Y, TRAPPC2, WDR1, ZBTB38	31	25	Cellular Growth and Proliferation, Organismal Development, Developmental Disorder

Eight networks with score > 30 were listed here. Molecules highlighted in Bold are those included in the input list.

Table S6. Disease and functions identified by IPA with all sex-related genes, metabolites and miRNAs

Category	Function Annotation	p-value	z-score
Cancer, z-score < -2			
Cancer, Organismal Injury and Abnormalities	Cancer of secretory structure	5.43E-09	-2.588
Cancer, Organismal Injury and Abnormalities	Cancer	1.12E-14	-2.587
Cell Death and Survival	Cell death of tumor cell lines	4.41E-07	-2.458
Cellular Growth and Proliferation, Cancer, Organismal Injury and Abnormalities, Cellular Development, Immunological Disease, Hematological Disease, Tumor Morphology	Proliferation of lymphoma cells	6.15E-04	-2.219
Cancer, Organismal Injury and Abnormalities, Immunological Disease, Hematological Disease	Lymphocytic cancer	7.18E-04	-2.085
Cancer, Organismal Injury and Abnormalities, Gastrointestinal Disease, Hepatic System Disease	Liver cancer	4.13E-05	-2.073
Cellular Growth and Proliferation, Cancer, Organismal Injury and Abnormalities, Cellular Development, Immunological Disease, Hematological Disease, Tumor Morphology	Proliferation of B cell lymphoma cells	2.49E-04	-2
Cellular Growth and Development, z-score < -2			
Developmental Disorder	Growth Failure	1.64E-05	-2.771
Cellular Growth and Proliferation, Cellular Development, Hematological System Development and Function	Expansion of leukocytes	5.69E-04	-2.172
Cell Cycle	Entry into S phase	7.75E-04	-2.077
Cellular Growth and Proliferation, Cellular Development	Expansion of blood cells	5.10E-04	-2.071
Organismal Injury and Abnormalities, z-score < -2			
Organismal Injury and Abnormalities	Bleeding	3.12E-04	-3.151
Organismal Injury and Abnormalities, Skeletal and Muscular Disorders, Cardiovascular Disease	Dilated cardiomyopathy	4.45E-05	-2.591
Organismal Injury and Abnormalities	Cytosis	1.22E-05	-2.382
Organismal Injury and Abnormalities	Edema	1.92E-04	-2.133
Organismal Survival, z-score < -2			
Organismal Survival	Organismal death	5.35E-19	-2.918
Organismal Survival	Morbidity or mortality	1.20E-18	-2.916
Neurological Disease, z-score < -2			
Neurological Disease	Movement Disorders	1.57E-11	-2.266
Neurological Disease	Neurological signs	2.26E-07	-2
Organismal Injury and Abnormalities, z-score >2			
Organismal Injury and Abnormalities, Ophthalmic Disease	Iris structural abnormality	2.10E-04	2
Organismal Injury and Abnormalities, Hereditary Disorder, Cardiovascular Disease	Familial vascular disease	2.06E-05	2.396
Infectious Diseases, z-score >2			
Infectious Diseases, Organismal Injury and Abnormalities	Infection of embryonic cell lines	4.87E-04	2.232
Infectious Diseases	Viral Infection	1.37E-07	2.95
Infectious Diseases	HIV infection	1.81E-05	2.966
Infectious Diseases	Infection by HIV-1	6.99E-05	3.06
Infectious Diseases	Infection by RNA virus	4.13E-06	3.175
Infectious Diseases	Infection of cells	4.47E-05	3.455

p-value <0.001 (Fisher's exact test) and | z score | ≥ 2 were considered as significant enrichment.

Table S7. The identified regulators of CYP39A1-surrogates via IPA analysis

Regulators	Molecule Type	Activation z-score	- Log (10, p-value)
MYC	transcription regulator	-4.766	12.903
MAP4K4	kinase	-4.359	7.607
gentamicin	chemical drug	-4.269	10.780
MYCN	transcription regulator	-3.925	9.572
nitrofurantoin	chemical drug	-3.909	11.793
TBX2	transcription regulator	-3.742	6.395
ERBB2	kinase	-3.683	10.790
CCND1	transcription regulator	-3.617	6.337
RABL6	other	-3.583	12.102
methapyrilene	chemical drug	-3.422	21.394
PTGER2	g-protein coupled receptor	-3.357	5.273
E2f	group	-3.266	8.470
FOXM1	transcription regulator	-3.05	9.824
staurosporine	chemical - kinase inhibitor	-2.915	2.623
E2F3	transcription regulator	-2.853	7.757
EP400	other	-2.804	5.011
NR0B2	ligand-dependent nuclear receptor	-2.789	4.292
actinomycin D	chemical drug	-2.684	1.963
TNF	cytokine	-2.64	5.559
CSF2	cytokine	-2.613	4.021
Tnf (family)	group	-2.528	3.205
PIM1	kinase	-2.433	1.896
SATB1	transcription regulator	-2.395	1.123
E2F1	transcription regulator	-2.266	10.963
SMOC2	other	-2.236	5.928
HRAS	enzyme	-2.228	4.648
EHHADH	enzyme	-2.219	3.876
HSD17B4	enzyme	-2.219	2.842
GPS2	transcription regulator	-2.219	1.693
chromium	chemical drug	-2.219	1.383
HGF	growth factor	-2.201	5.418
mir-155	microrna	-2.191	0.613
pravastatin	chemical drug	-2.189	1.860
4-nitroquinoline-1-oxide	chemical toxicant	-2.186	4.900
captopril	chemical drug	-2.138	2.226
CD40	transmembrane receptor	-2.129	1.119
ketoconazole	chemical drug	-2.126	6.292
NRIP1	transcription regulator	-2.121	4.228
FOS	transcription regulator	-2.111	5.223
dichlorovinylcysteine	chemical toxicant	-2.091	5.223
ELAVL1	other	-2.061	2.261

GCK	kinase	-2	4.123
PCK1	kinase	-2	3.184
MYBL2	transcription regulator	-2	2.484
ASCL1	transcription regulator	-2	0.638
dexamethasone	chemical drug	6.12	20.376
HNF4A	transcription regulator	6.073	38.439
rosiglitazone	chemical drug	5.131	13.569
PPARGC1A	transcription regulator	5.126	11.417
TP53	transcription regulator	4.807	15.330
HNF1A	transcription regulator	4.62	20.955
phenobarbital	chemical drug	4.517	12.821
pirinixic acid	chemical toxicant	4.373	31.538
PPARG	ligand-dependent nuclear receptor	4.229	13.251
NR1I3	ligand-dependent nuclear receptor	4.107	10.107
PXR ligand-PXR-Retinoic acid-RXR α complex		4.047	14.000
INSR	kinase	4.039	13.740
fenofibrate	chemical drug	3.758	16.790
PPARA	ligand-dependent nuclear receptor	3.173	36.815
GW 4064	chemical toxicant	3.114	11.333
rifampin	chemical drug	3.04	15.708

Table S8. Identified c-Myc interacting proteins in HCC cells transfected with c-Myc control and HCC cells transfected with C-Myc and CYP39A1, which were evidenced and summarized in Literature and Uniprot database.

Symbol	Unique peptides		Validation	Relative unique Peptides [#]	
	Myc group	CYP39A1 & Myc group		Myc group	CYP39A1 & Myc group
MYC	15	12	/	1.00	1.00
HSP90AA1	10	2	(Carystinos et al., 2003)	0.67	0.17
XRCC6	6	4	(Koch et al., 2007)	0.40	0.33
HNRNPU	4	1	(Matsuoka et al., 2009)	0.27	0.08
RUVBL2	3	1	(Li et al., 2010; Liu et al., 2003)	0.20	0.08
TUBB	3	2	(Conacci-Sorrell et al., 2010)	0.20	0.17
GTF2I	2	0	(Roy et al., 1993)	0.13	0.00
RUVBL1	2	0	(Fuchs et al., 2001; Park et al., 2002)	0.13	0.00
HDAC1	1	0	(Liu et al., 2007; Matsuoka et al., 2008)	0.07	0.00
HUWE1	1	0	(Adhikary et al., 2005; Fan et al., 2016)	0.07	0.00
RPL11	1	1	(Dai et al., 2007)	0.07	0.08
MAX	1	1	(Blackwood and Eisenman, 1991; Mac Partlin et al., 2003)	0.07	0.08
MYO1B	11	2	Uniprot	0.73	0.17
HSPA1A	11	9	Uniprot	0.73	0.75
ANXA2	8	0	Uniprot	0.53	0.00
NCL	8	3	Uniprot	0.53	0.25
HNRNPC	7	2	Uniprot	0.47	0.17
YES1	7	5	Uniprot	0.47	0.42
TMPO	7	6	Uniprot	0.47	0.50
EIF4A1	6	0	Uniprot	0.40	0.00
CKAP4	6	1	Uniprot	0.40	0.08
PRDX1	6	2	Uniprot	0.40	0.17
HSPD1	6	6	Uniprot	0.40	0.50
HNRNPK	5	1	Uniprot	0.33	0.08
ALDOA	5	1	Uniprot	0.33	0.08
CCT3	4	0	Uniprot	0.27	0.00
EEF1G	3	0	Uniprot	0.20	0.00
HADHA	3	0	Uniprot	0.20	0.00
YBX1	3	0	Uniprot	0.20	0.00
IQGAP2	3	1	Uniprot	0.20	0.08
RPN1	3	1	Uniprot	0.20	0.08
PRKDC	3	1	Uniprot	0.20	0.08
KPNB1	3	1	Uniprot	0.20	0.08
CCT4	2	0	Uniprot	0.13	0.00
DDX17	2	0	Uniprot	0.13	0.00
HNRNPD	2	0	Uniprot	0.13	0.00
PPP1CA	2	0	Uniprot	0.13	0.00
PSMB5	2	0	Uniprot	0.13	0.00
SDC4	2	0	Uniprot	0.13	0.00
SSBP1	2	0	Uniprot	0.13	0.00
TKT	2	0	Uniprot	0.13	0.00
XRCC5	2	0	Uniprot	0.13	0.00
C15:73SNK2A1	2	1	Uniprot	0.13	0.08
CCT8	2	1	Uniprot	0.13	0.08
IGF2BP1	2	1	Uniprot	0.13	0.08
FBL	2	1	Uniprot	0.13	0.08
HADHB	2	1	Uniprot	0.13	0.08
CSNK2B	1	0	Uniprot	0.07	0.00
ACTG1	1	0	Uniprot	0.07	0.00
ALDH18A1	1	0	Uniprot	0.07	0.00
CCT2	1	0	Uniprot	0.07	0.00
CCT5	1	0	Uniprot	0.07	0.00
CCT6A	1	0	Uniprot	0.07	0.00
CHCHD3	1	0	Uniprot	0.07	0.00
CSE1L	1	0	Uniprot	0.07	0.00
CTNND1	1	0	Uniprot	0.07	0.00
DHX15	1	0	Uniprot	0.07	0.00
GANAB	1	0	Uniprot	0.07	0.00
LGALS1	1	0	Uniprot	0.07	0.00
LRPPRC	1	0	Uniprot	0.07	0.00

OAT	1	0	Uniprot	0.07	0.00
PSMA1	1	0	Uniprot	0.07	0.00
PSMD2	1	0	Uniprot	0.07	0.00
SERP1NH1	1	0	Uniprot	0.07	0.00
SLC25A1	1	0	Uniprot	0.07	0.00
TCP1	1	0	Uniprot	0.07	0.00
TOP1	1	0	Uniprot	0.07	0.00
TRIM21	1	0	Uniprot	0.07	0.00
TRIM28	1	0	Uniprot	0.07	0.00
TXN	1	0	Uniprot	0.07	0.00
XDH	1	0	Uniprot	0.07	0.00
ACTC1	1	1	Uniprot	0.07	0.08
RPL13	1	1	Uniprot	0.07	0.08
SLC25A3	1	1	Uniprot	0.07	0.08
HSPB1	1	1	Uniprot	0.07	0.08
ARF4	1	1	Uniprot	0.07	0.08
PCBP1	1	2	Uniprot	0.07	0.17
ACTB	1	6	Uniprot	0.07	0.50
SLC25A11	0	1	Uniprot	0.00	0.08
HNRNPF	0	2	Uniprot	0.00	0.17
YWHAE	0	2	Uniprot	0.00	0.17
HSPH1	0	3	Uniprot	0.00	0.25
TUBA4A	0	5	Uniprot	0.00	0.42

#, Relative to the number of c-Myc unique peptides in each group.

Table S9. Identified c-Myc interacting proteins in HCC cells transfected with c-Myc and CYP39A1 wild-type or CYP39A1 Δ 369-469, which were evidenced and summarized in Literature and Uniprot database.

Symbol	Unique peptides		Validation	Relative Unique Peptides#	
	c-Myc, CYP39A1 wild-type	c-Myc, CYP39A1 Δ 369-469		c-Myc, CYP39A1 wild-type	c-Myc, CYP39A1 Δ 369-469
MYC	25	25	/	1.00	1.00
HSP90AA1	14	21	(Carystinos et al., 2003)	0.56	0.84
XRCC6	16	21	(Koch et al., 2007)	0.64	0.84
RUVBL1	11	13	(Fuchs et al., 2001; Park et al., 2002)	0.44	0.52
RUVBL2	10	11	(Li et al., 2010; Liu et al., 2003)	0.40	0.44
CCAR2	10	11	(Koch et al., 2007; Menssen et al., 2012)	0.40	0.44
DDB1	0	9	(Choi et al., 2010)	0.00	0.36
ACTL6A	0	8	(Park et al., 2002)	0.00	0.32
HNRNPU	0	8	(Matsuoka et al., 2009)	0.00	0.32
SMARCC1	8	7	(Pal et al., 2003)	0.32	0.28
TUBB	2	3	(Conacci-Sorrell et al., 2010)	0.08	0.12
CKAP4	21	26	Uniprot	0.84	1.04
HSPD1	18	26	Uniprot	0.72	1.04
NCL	16	24	Uniprot	0.64	0.96
LMNA	16	21	Uniprot	0.64	0.84
NOP56	16	21	Uniprot	0.64	0.84
MYBBP1A	13	20	Uniprot	0.52	0.80
XRCC5	16	19	Uniprot	0.64	0.76
HSPA1A	13	18	Uniprot	0.52	0.72
IGF2BP1	12	18	Uniprot	0.48	0.72
CCT2	7	16	Uniprot	0.28	0.64
ALDOA	7	15	Uniprot	0.28	0.60
ANXA2	0	15	Uniprot	0.00	0.60
CCT8	10	15	Uniprot	0.40	0.60
HNRNPK	9	15	Uniprot	0.36	0.60
KPNB1	11	15	Uniprot	0.44	0.60
TOP1	20	15	Uniprot	0.80	0.60
FBL	12	14	Uniprot	0.48	0.56
HNRNPC	14	14	Uniprot	0.56	0.56
SF3B1	7	14	Uniprot	0.28	0.56
TRIM28	7	14	Uniprot	0.28	0.56
CCT6A	0	13	Uniprot	0.00	0.52
GANAB	0	13	Uniprot	0.00	0.52
KPNA2	9	13	Uniprot	0.36	0.52
NUP93	13	13	Uniprot	0.52	0.52
ACTB	9	12	Uniprot	0.36	0.48
LRPPRC	0	12	Uniprot	0.00	0.48
TFAM	0	12	Uniprot	0.00	0.48
TMPO	12	12	Uniprot	0.48	0.48
SMTN	11	11	Uniprot	0.44	0.44
TCP1	0	11	Uniprot	0.00	0.44
YBX1	5	11	Uniprot	0.20	0.44
CCT4	0	10	Uniprot	0.00	0.40
EEF1G	8	10	Uniprot	0.32	0.40
ELAVL1	8	10	Uniprot	0.32	0.40
PES1	0	10	Uniprot	0.00	0.40
PRDX1	9	10	Uniprot	0.36	0.40
SERPINH1	0	10	Uniprot	0.00	0.40
CCT3	10	9	Uniprot	0.40	0.36
HNRNPD	6	9	Uniprot	0.24	0.36
HSPB1	0	9	Uniprot	0.00	0.36
IGF2BP3	0	9	Uniprot	0.00	0.36
LRRC59	0	9	Uniprot	0.00	0.36
SQSTM1	0	9	Uniprot	0.00	0.36
TOP2A	6	9	Uniprot	0.24	0.36
TRIM21	9	9	Uniprot	0.36	0.36
ADAR	0	8	Uniprot	0.00	0.32
CCT5	0	8	Uniprot	0.00	0.32
CSNK2A1	7	8	Uniprot	0.28	0.32
DHX15	0	8	Uniprot	0.00	0.32

HNRNPA0	8	8	Uniprot	0.32	0.32
PRPF6	0	8	Uniprot	0.00	0.32
RPN1	0	8	Uniprot	0.00	0.32
CTNND1	0	7	Uniprot	0.00	0.28
DNAJA2	0	7	Uniprot	0.00	0.28
PSMB5	0	7	Uniprot	0.00	0.28
PSMC2	0	7	Uniprot	0.00	0.28
IGF2BP2	0	6	Uniprot	0.00	0.24
PCBP1	6	6	Uniprot	0.24	0.24
DDX17	8	5	Uniprot	0.32	0.20
SMARCA5	0	5	Uniprot	0.00	0.20
EIF4A1	3	3	Uniprot	0.12	0.12
PPP1CA	4	3	Uniprot	0.16	0.12
ACTC1	2	1	Uniprot	0.08	0.04

#, Relative to the number of c-Myc unique peptides in each group.

Table S10. Primers and Oligos used in this study.

Primers/Oligos Name	Sequence
	Primers for qRT-PCR
Human CYP39A1	F: 5'-CTTCATGGCATTGGAAGC-3' R: 5'-CCTCTAACAGAGCAAACCCACCT-3'
Human CYP17A1	F: 5'-TATGGCCCCATCTATTCGGTT R: 5'-GCGATACCCCTTACGGTTGTTG
Human MYC	F: 5'-GTCAAGAGGCGAACACACAAC-3' R: 5'-TTGGACGGACAGGATGTATGC-3'
Human CBX3	F: 5'-TAGATCGACGTGTAGTGAATGGG-3' R: 5'-TGTCTGTGGACCAATTATTCTT-3'
Human CCNB1	F: 5'-AATAAGGCGAAGATCAACATGGC-3' R: 5'-TTTGTTACCAATGTCCCAAGAG-3'
Human CDC25A	F: 5'-CTCCTCCGAGTCAACAGATTCA-3' R: 5'-CAACAGCTTCTGAGGTAGGGA-3'
Human CDK4	F: 5'-CTGGTGTGAGCATGTAGACC-3' R: 5'-GATCCTTGATCGTTCCGGCTG-3'
Human CKS2	F: 5'-TTCGACGAACACTACGAGTACC-3' R: 5'-AGCCTAGACTCTGTTGGACACC-3'
Human GNL3	F: 5'-AAGCCAAAGTCGGGCAACA-3' R: 5'-GCATCCAAACACCTTAGGACAA-3'
Human NAP1L1	F: 5'-AAGTGCTGACAAAGACATACAGG-3' R: 5'-TTTTCCAATCTATCTGGCACCC-3'
Human PA2G4	F: 5'-CAGGAGCAAATATCGCTGAG-3' R: 5'-GGACCGAAGTACCCTGTTGG-3'
Human PCNA	F: 5'-GCGTGAACCTCACCAGTATGT-3' R: 5'-TCTTCGGCCCTTAGTGAATGAT-3'
Human 18S	F: 5'-GACTCAACACGGGAAACCTC-3' R: 5'-AGCATGCCAGAGTCTCGTTC-3'
Mouse CYP17A1	F: 5'-AGTCAAAGACACCTAATGCCAAG-3' R: 5'-ACGTCTGGGGAGAAACGGT-3'
Mouse CYP11A1	F: 5'-GGATGCGTCGATACTCTTCTCA-3' R: 5'-GGACGATTCGGTCTTTCTTCCA-3'
Mouse CYP11B2	F: 5'-CTGAACCGAAATGTGCTGTCA-3' R: 5'-CCTAGCCGTTCCCCAAAAG-3'
Mouse HSP90AA1	F: 5'-GTGTTATTACGCCACGATG-3' R: 5'-CATTAACTGGGCAATTTCTGC-3'
Mouse CBX3	F: 5'-ACTGGACCGTCGTGTAGTGAA-3' R: 5'-GCCCTTGGTTTGTGACGA-3'
Mouse CCNB1	F: 5'-CTTGCACTGAGTGACGTAGAC-3' R: 5'-CCAGTTGTCGGAGATAAGCATAG-3'
Mouse CDC25A	F: 5'-AGCGTGTATTGTGCTGTTT-3' R: 5'-TCTCTCTCACATATCGGCACA-3'
Mouse CDK4	F: 5'-CATACTGGACAAGCACCTCC-3' R: 5'-GAATGTTCTCTGGCTTCAGGTCC-3'
Mouse CKS2	F: 5'-TCGATGAGCACTACGAGTACC-3' R: 5'-CCATCCTAGACTCTGTTGGACAC-3'
Mouse GNL3	F: 5'-AAAGCGAGTAAACGTATGACCTG-3' R: 5'-AGCACTATTTGGAACACCTGG-3'
Mouse NAP1L1	F: 5'-GTTCTGAGAATGGCGATCTG-3' R: 5'-TTCCCCTTCTCGTCAGCTT-3'
Mouse PA2G4	F: 5'-GCAGGAGCAAATATCGCC-3' R: 5'-ACCAAAGATCGAAGCACCCG-3'
Mouse PCNA	F: 5'-TTGCACGTATATGCCGAGACC-3' R: 5'-GGTGAACAGGCTCATTTCATCTCT-3'
Mouse 18S	F: 5'-GCCGCTAGAGGTGAAATCTT-3' R: 5'-CGTCTTCGAACCTCCGACT-3'
	siRNA target sequence
siCYP39A1 #1	GAAACCGAATGACCTTTGT
siCYP39A1#2	CAGTCACAGTGAATATGCT
siMYC	GGAAACGACGAGAACAGTT
	Forward primer sequence (Enzyme)
p3xflag-CMV-14-CYP39A1	F: 5'-CC ATCGAT GCCACCATGGAACTAATTTCCCAAC-3' (CLAI) R: 5'-CG GGATCCT TATTCTTTGTTTATATTCAATTCGGCA-3' (BAMHI)
p3xflag-CMV-14-HSP90AA1	F: 5'-GG GGTACC ATGCCTGAGGAAACCCAGAC-3' (KPN1) R: 5'-CG GGATCCT GCTACTTCTTCCATGCGTGATGTG-3' (BAMHI)
PCDH-CMV-CYP39A1-3xflag-EF1A-copGFP	F: 5'-CC ATCGAT GCCACCATGGAACTAATTTCCCAAC-3' (CLAI) R: 5'-ATAAGAAT GCGGCCG CCTACTTGTATCGTCATCCTTG-3' (NOTI)
AAV-TBG-CYP39A1	F: 5'-ATAAGAAT GCGGCCG GCCACCATGGAACTAATTTCCCAACAGT-3' (NOTI)

	R: 5'-CG GGATCC TCATATTTCTTTGTTTATTTCAATTCGGCA-3' (BAMHI)
	F: 5'-CG GGATCC ATGCCCCCTCAACGTTAGCTTCA-3' (BAMHI)
PCDA3.0-MYC-C-3XHA	R: 5'-CCG CTCGAG CGCACAAGATTCCGTAGCT-3' (XHOI)
	F: 5'-AGAATCTCCTTCTAATTCAATGGTGTGTTTTGG
p3Xflag-CMV-14-CYP39A1-K329Q	R: 5'-CCAAAACACACCATT GA ATTAGAAGGAGATTCT
p3Xflag-CMV-14-CYP39A1 ^{Δ2-21}	F: 5'-CC ATCGAT GCCACCATGCAGCGGAAGAAATTTGCGTAGA-3' (CLAI)
	R: 5'-CG GGATCC TATTCTTTGTTTATTTCAATTCGGCA-3' (BAMHI)
p3Xflag-CMV-14-CYP39A1 ^{Δ2-145}	F: 5'-CC ATCGAT GCCACCATGCAACTGGAGAATTTAGGCACTCAT-3' (CLAI)
	R: 5'-CG GGATCC TATTCTTTGTTTATTTCAATTCGGCA-3' (BAMHI)
p3Xflag-CMV-14-CYP39A1 ^{Δ291-469}	F: 5'-CC ATCGAT GCCACCATGGAACAAATTTCCCCAACAGT-3' (CLAI)
	R: 5'-CG GGATCC AAGGACGTATGCAAGTGTCC-3' (BAMHI)
p3Xflag-CMV-14-CYP39A1 ^{Δ369-469}	F: 5'-CC ATCGAT GCCACCATGGAACAAATTTCCCCAACAGT-3' (CLAI)
	R: 5'-CG GGATCC AGACAACATCAACAAGTCACCAG-3' (BAMHI)
pEGFP-attL-HSP90AA1	F: 5'-CG GGATCC GCCACCATGCCTGAGGAAACCCAGAC-3' (BAMHI)
	R: 5'-GC TCTAGA TTAGTCTACTTCTTCCATGCGTGATGTG-3' (XBAI)
pEGFP-attL-CYP39A1-K329Q	F: 5'-CC GAGCTC GCCACCATGGAACAAATTTCCCCAACAGT-3' (SACI)
	R: 5'-GC GTCGAC CTACTTGTCATCGTCACTCCTTG-3' (SALI)
pEGFP-attL-CYP39A1 ^{Δ2-21}	F: 5'-CC GAGCTC GCCACCATGGAACAAATTTCCCCAACAGT-3' (SACI)
	R: 5'-GC GTCGAC CTACTTGTCATCGTCACTCCTTG-3' (SALI)
pEGFP-attL-CYP39A1 ^{Δ2-145}	F: 5'-CC GAGCTC GCCACCATGGAACAAATTTCCCCAACAGT-3' (SACI)
	R: 5'-GC GTCGAC CTACTTGTCATCGTCACTCCTTG-3' (SALI)
pEGFP-attL-CYP39A1 ^{Δ291-469}	F: 5'-CC GAGCTC GCCACCATGGAACAAATTTCCCCAACAGT-3' (SACI)
	R: 5'-GC GTCGAC CTACTTGTCATCGTCACTCCTTG-3' (SALI)
pEGFP-attL-CYP39A1 ^{Δ369-469}	F: 5'-CC GAGCTC GCCACCATGGAACAAATTTCCCCAACAGT-3' (SACI)
	R: 5'-GC GTCGAC CTACTTGTCATCGTCACTCCTTG-3' (SALI)
pBIFC-VC155-CYP39A1	F: 5'-CG GAATTC GGAACAAATTTCCCCAACAGTGAT-3' (ECORI)
	R: 5'-GG GGTACC TATTCTTTGTTTATTTCAATTCGGCATTGC-3' (KPN1)
PGL4.20-4X EBOX	F: 5'- TCGAGGAGCACGTG GTGAG CACGTG GTGAG CACGTG GTGAG CACGTG GTGAG CACGTG GTA-3'
	R: 5'- AGCTTACCACGTG CTCACC CACGTG CTCACC CACGTG CTCACC CACGTG CTCACC CACGTG CTCC-3'
AAV-shCYP39A1	F: 5'-GATCG AAGAAGGAATCAATGTGCTT CTCGAG AAGCACATTGATTCCTTCTCTTTTTT -3'
	R: 5'-CTAGAAAAA GAAGAAGGAATCAATGTGCTT CTCGAG AAGCACATTGATTCCTTCTCT -3'
PLKO.1-shHSP90AA1 #1	F: 5'-CCGG GCCCTTCTATTTGTCCACG ACTCGAG TCGTGGGACAAATAGAAGGGC TTTTTG-3'
	R: 5'-AATTCAAAA GCCCTTCTATTTGTCCACG ACTCGAG TCGTGGGACAAATAGAAGGGC -3'
PLKO.1-shHSP90AA1 #2	F: 5'-CCGG GCTGAGGGATGACTTACCTGT CTCGAG ACAGGTAAGTCATCCCTCAGC TTTTTG-3'
	R: 5'-AATTCAAAA GCTGAGGGATGACTTACCTGT CTCGAG ACAGGTAAGTCATCCCTCAGC -3'

Table S11. The detailed usage of plasmids for HDTV mouse models.

Groups	Plasmid amount
pT3-EF1 α -Myc, pT3-EF1 α -CT, pCMV/SB	4 μ g, 12 μ g, 0.64 μ g
pT3-EF1 α -Myc, pT3-EF1 α -CYP39A1, pCMV/SB	4 μ g, 12 μ g, 0.64 μ g
pT3-EF1 α -Myc, pT3-EF1 α -MCL1, pT3-EF1 α -CT, pCMV/SB	4 μ g, 4 μ g, 12 μ g, 0.8 μ g
pT3-EF1 α -Myc, pT3-EF1 α -MCL1, pT3-EF1 α -CYP39A1, pCMV/SB	4 μ g, 4 μ g, 12 μ g, 0.8 μ g
pT3-EF1 α -Myc, pT3-EF1 α -CT, pT3-EF1 α -CT, pCMV/SB	4 μ g, 10 μ g, 12 μ g, 1.04 μ g
pT3-EF1 α -Myc, pT3-EF1 α -HSP90AA1, pT3-EF1 α -CT, pCMV/SB	4 μ g, 10 μ g, 12 μ g, 1.04 μ g
pT3-EF1 α -Myc, pT3-EF1 α -CT, pT3-EF1 α -CYP39A1, pCMV/SB	4 μ g, 10 μ g, 12 μ g, 1.04 μ g
pT3-EF1 α -Myc, pT3-EF1 α -HSP90AA1, pT3-EF1 α -CYP39A1, pCMV/SB	4 μ g, 10 μ g, 12 μ g, 1.04 μ g
pT3-EF1 α -Myc, pT3-EF1 α -MCL1, pT3-EF1 α -HSP90AA1, pT3-EF1 α -CT, pCMV/SB	4 μ g, 4 μ g, 10 μ g, 12 μ g, 1.2 μ g
pT3-EF1 α -Myc, pT3-EF1 α -MCL1, pT3-EF1 α -HSP90AA1, pT3-EF1 α -CYP39A1, pCMV/SB	4 μ g, 4 μ g, 10 μ g, 12 μ g, 1.2 μ g
pT3-EF1 α -Myc, pT3-EF1 α -MCL1, pT3-EF1 α -CT, pCMV/SB	4 μ g, 4 μ g, 12 μ g, 0.8 μ g
pT3-EF1 α -Myc, pT3-EF1 α -MCL1, pT3-EF1 α -CYP39A1, pCMV/SB	4 μ g, 4 μ g, 12 μ g, 0.8 μ g
pT3-EF1 α -Myc, pT3-EF1 α -MCL1, pT3-EF1 α -CYP39A1-K329Q, pCMV/SB	4 μ g, 4 μ g, 12 μ g, 0.8 μ g
pT3-EF1 α -Myc, pT3-EF1 α -MCL1, pT3-EF1 α -CT, pCMV/SB	4 μ g, 4 μ g, 12 μ g, 0.8 μ g
pT3-EF1 α -Myc, pT3-EF1 α -MCL1, pT3-EF1 α -CYP39A1, pCMV/SB	4 μ g, 4 μ g, 12 μ g, 0.8 μ g

